Inositol pyrophosphate specificity of the SPX-dependent polyphosphate polymerase VTC

Authors: Ruta Gerasimaite, [1,4] Igor Pavlovic, [2,4] Samanta Capolicchio,[2] Alexandre Hofer, [2] Andrea Schmidt, [1] Henning J. Jessen,[3,*] Andreas Mayer[1,*]

[1]Department of Biochemistry, University of Lausanne, Chemin de Boveresses 155, 1066 Epalinges, Switzerland

[2]Department of Chemistry, University of Zürich, Winterthurerstrasse 190, 8057 Zürich, Switzerland

[3]Institute of Organic Chemistry, Albert-Ludwigs University of Freiburg, Albertstrasse 21, 79104 Freiburg, Germany

[4] Co-first author

*Correspondence: Andreas.Mayer@unil.ch, Henning.Jessen@oc.uni-freiburg.de

Abstract

The free energy of nucleotide hydrolysis depends on phosphate concentration. Cells regulate cytosolic phosphate levels by orchestrating phosphate acquisition and storage through inositol pyrophosphates (PP-InsP) and SPX domains. Here, we report the synthesis of the novel 5-PPP-$InsP_5$ containing a triphosphate subunit. Using this and a series of synthetic PP-InsP, we examined the ligand specificity of the SPX domain in the PP-InsP-controlled yeast polyphosphate polymerase VTC. SPX decodes the relative positioning of the phosphoric anhydrides, their structure (diphosphate vs triphosphate), and the presence of other phosphates on the inositol ring. Despite the higher potency of 1,5-$(PP)_2$-$InsP_4$, 5-PP-$InsP_5$ is the primary activator of VTC in cells, indicating that its higher concentration compensates for its lower potency. 1,5-$(PP)_2$-$InsP_4$ levels rise and could become relevant under stress conditions. Thus, SPX domains may integrate PP-InsP dependent signaling to adapt cytosolic phosphate concentrations to different metabolic situations.

Phosphate homeostasis is a tightly regulated process in all organisms. The energy for driving endergonic metabolic reactions is often derived from the hydrolysis of P-anhydrides, such as in ATP. Elevated cytosolic concentrations of phosphate (P_i) will reduce the free energy provided by such reactions, which may slow down metabolic processes. Furthermore, phosphate is a limiting macronutrient for plants and micro-organisms, which have therefore developed strategies to store phosphate in forms that can be accessed on demand[1]. One such storage molecule is inorganic polyphosphate (polyP). PolyP contains up to several thousand P-anhydride bonds whose hydrolysis could be used to fuel cellular processes [2,3]. Many other functions of polyP are known [4]. In yeast, the VTC (Vacuolar Transporter Chaperone) complex synthesizes polyP [5]. VTC is a large assembly of proteins (Vtc1-5) that associate in the vacuolar membrane [6,7]. Four of the five VTC proteins contain an SPX domain that has been implicated in P_i-homeostasis[8].

How phosphate availability inside cells is sensed remains largely uncharacterized. Recent evidence suggests that an SPX-dependent signaling pathway for phosphate availability exists, which communicates cytosolic phosphate levels to several proteins that import or export phosphate, store it as polyP, or regulate transcriptional programs [9,10]. Recently, we have shown that SPX domains interact with *myo*-inositol polyphosphates ($InsP_x$, figure 1) [10]. $InsP_x$ constitute a large family of cellular signaling molecules [11]. Up to six phosphate groups can be attached to *myo*-inositol **1**. The inositol pyrophosphates (PP-InsPs, e.g. **4**-**8**) contain additional P-anhydrides in the presence of the phosphate esters[12]. Therefore, they potentially contain more than six phosphates, such as 5-PP-$InsP_5$ and 1,5-$(PP)_2$-$InsP_4$ [13]. Less densely phosphorylated inositol pyrophosphates have been described with free OH groups, e.g. **8**, and also a species containing a triphosphate (5-PPP-$InsP_5$) is known [14].

Notably, the most abundant inositol pyrophosphate 5-PP-$InsP_5$ stimulates polyP synthesis of the VTC complex by binding to the SPX domain at around 500 nM concentration [10]. This is in line with the fact that yeast strains deficient in *KCS1* (also known as *IP6K, Figure 1*), the kinase required for synthesis of 5-PP-$InsP_5$, do not accumulate polyP [19,20]. This link is weakened because the lack of KCS1 changes the expression of hundreds of other genes and could

therefore impair polyP synthesis also indirectly [21]. In addition, an inositol phosphate kinase 1 (*IPK1*) deficient yeast strain retains the ability to accumulate polyP [20]. This strain cannot produce $InsP_6$, and is also deficient in 5-PP-$InsP_5$ and 1,5-$(PP)_2$-$InsP_4$. However, *ipk1*Δ cells accumulate 5-PP-$InsP_4$, which contains a free 2-OH group [22]. It is unknown whether this reflects a direct effect of 5-PP-$InsP_4$ on the SPX-dependent VTC complex.

Recently, we have reported the chemical synthesis of all six possible X-PP-$InsP_5$ and two X,Y-$(PP)_2$-$InsP_4$ [15-17,23]. To study the effect of 5-PP-$InsP_4$, we repeated its chemical synthesis [24]. The chemical synthesis of an inositol containing a triphosphate group has never been reported. However, the mammalian IP6Ks are known to also synthesize triphosphates, such as in 5-PPP-$InsP_5$ (an $InsP_8$ constitutional isomer), at least in vitro [14]. We were interested in developing synthetic approaches to target such densely phosphorylated compounds and to compare the effectiveness of triphosphate and diphosphate groups in the stimulation of the VTC complex.

The synthesis (figure 2, **A**) commenced with *myo*-inositol **1** that was protected as the *ortho*-benzoate, followed by *para*-methoxybenzyl (PMB) protection and a regioselective reductive cleavage of the orthoester to yield acetal **9** [15-17]. The OH-group was then phosphitylated with a P-amidite and oxidized to **10**. The P-amidite was used to introduce a phosphate bearing two allyloxycarbonyl (alloc) groups connected via a benzyl adapter to the P-atom (figure 2, **B**). This novel allocB group is akin to the levulinic acid derived LevB group described recently [17]. The benzyl adapter strategy extends the application of acyl protecting groups to phosphate protection and therefore potentially facilitates the development of alternative mild and orthogonal methods that were previously not accessible. Next, all alcohol protecting groups where removed and pentaol **11** was phosphorylated using P(III) chemistry and oxidation to give hexakisphosphate **12**. The allocB groups in **12** were then selectively removed using $PdCl_2$. This is an almost quantitative process, which requires transallylation, presumably to MeOH, followed by decarboxylation (figure 2, **B**). This process leads to an Umpolung from an acceptor (carbonate) to a donor (OH), and is followed by fragmentation of the benzyl adapter to a quinone methide, which is again intercepted by MeOH.

Phosphate **13** can then be transformed into the diphosphate **14** [25]. The allocB group is resistant to cleavage if installed on a diphosphate moiety. Therefore, another orthogonal protecting group was required. To remain orthogonal to the Fm groups, the extension was performed with yet another new P-amidite bearing *tert*-butoxycarbonyl (Boc) protecting groups and a benzyl adapter (BocB, figure 2, **B**). Generation of the protected P-anhydride in **14** proceeded in 60% isolated yield and acid treatment released the free diphosphate **15**. Finally, the triphosphate was obtained by installing an Fm-protected phosphate delivering **16** with 12 Fm protecting groups. All protecting groups where removed with piperidine generating the piperidinium salt of 5-PPP-$InsP_8$ **7** which was precipitated from diethylether in good quality as judged by ^{31}P NMR and polyacrylamide gel electrophoresis (PAGE) resolution followed by staining (Figure S1). The counterions where then exchanged to Na^+ by precipitation from methanol.

The described procedure enables the first synthesis of 5-PPP-$InsP_5$ **7** based on an iterative P-anhydride synthesis using the two novel phosphate protecting groups allocB and BocB. The successful application of iterative and selective P-anhydride synthesis to a highly congested and complex *myo*-inositol scaffold underscores the potential of the P(III)-P(V) coupling strategy in natural product synthesis.

Next, we tested the ability of all different synthetic inositol pyrophosphates to stimulate an SPX-domain-controlled process, such as polyP synthesis by the VTC complex of isolated vacuoles [26]. In this system, the VTC complex is devoid of surrounding cytosol and sources of PP-InsPs, resulting in a very low, basal polyP synthesis activity. Addition of 5-PP-$InsP_5$ stimulates apparent polyP synthesis activity 10 to 50-fold [10]. Whereas $InsP_6$ hardly influenced the reaction, all analyzed PP-InsPs stimulated polyP accumulation to a similar maximal rate. Only 4-PP-$InsP_4$ and PPP-$InsP_5$ showed lower efficacy, inducing 40-70% lower maximal activity (Fig. 3A,B). In contrast, the EC_{50} varied over three orders of magnitude (Fig. 3C). Among the PP-InsP isomers, the two isomers that have been found in living cells (1-PP-$InsP_5$ and 5-PP-$InsP_5$) were the most potent and stimulated VTC with an EC_{50} of 350-500 nM. 2-PP-$InsP_5$, 4-PP-$InsP_5$ and 6-PP-$InsP_5$ displayed up to 10-fold higher EC_{50}.

1,5-$(PP)_2$-$InsP_4$, which is also found in yeast, displayed ~20-fold lower EC_{50} than 5-PP-$InsP_5$. Also the "non-natural" enantiomer 3,5-$(PP)_2$-$InsP_4$, although 5 times less potent than 1,5-$(PP)_2$-$InsP_4$, still showed a roughly 5-fold lower EC_{50} than 5-PP-$InsP_5$.

A peculiar property of PP-InsPs is their exceptionally high charge density [27], and $(PP)_2$-$InsP_4$ isomers might be more potent than PP-$InsP_5$ isomers simply due to the fact that they accumulate more charged phosphate groups. In this case, one should expect similar potency for the $(PP)_2$-$InsP_4$ constitutional isomer 5-PPP-$InsP_5$ in our activity assays. This was, however, not observed. The EC_{50} of 5-PPP-$InsP_5$ was very close to that of 5-PP-$InsP_5$ and the maximal apparent rate of synthesis that it induced was 70% lower.

We also tested the effect of the naturally occurring 5-PP-$InsP_4$ with a free OH group in the 2-position. This isomer does normally not accumulate to appreciable levels in logarithmically growing cells, but it becomes the major PP-InsP isomer in *ipk1*Δ cells [22]. *ipk1*Δ cells cannot phosphorylate $InsP_5$ to $InsP_6$ and also lack 5-PP-$InsP_5$ and 1,5-$(PP)_2$-$InsP_4$, yet they do accumulate polyP *in vivo*. In *ipk1Δ*, a promiscuous activity of Kcs1 converts $InsP_5$ to 5-PP-$InsP_4$ [22,28], which might be able to activate VTC in the absence of other PP-InsPs. In this scenario, the phosphate group in the 2-position, which is missing in 5-PP-$InsP_4$, might be dispensable for activation. This would be inconsistent with the coordination of this phosphate group by several highly conserved residues in the PP-InsP binding site (Fig. 3D) of the SPX domain, which suggests that the group is important [10]. Therefore, we assayed stimulation of VTC by 5-PP-$InsP_4$ *in vitro*. While 5-PP-$InsP_4$ could induce a similar maximal rate as 5-PP-$InsP_5$, its EC_{50} was 20 times higher, pointing towards a role of the 2-phosphate group. The accumulation of polyP in an *ipk1*Δ strain can still be understood, as the concentration of 5-PP-$InsP_4$ in *ipk1*Δ cells is ~10-fold higher than that of 5-PP-$InsP_5$ in wildtype yeast [22], which compensates for the lower EC_{50} of 5-PP-$InsP_4$.

The results from these *in vitro* activation assays can, to some degree, be blended with the test of mutants in the PP-InsP synthesis pathways to

establish which of the activators are physiologically relevant. First, we sought to verify that the lack of polyP in *kcs1Δ* cells was indeed due to reduced VTC activity and not only a secondary effect of the large transcriptional reprogramming in *kcs1Δ* cells [21]. Vacuoles from *kcs1Δ* cells contained VTC levels comparable to wildtype. They also showed a similar apparent polyP synthesis activity as wildtype when 5-PP-$InsP_5$ was supplied (Fig. 4A, B). Similar observations were made in mutants affecting the earlier steps of the PP-InsP pathway, such as phospholipase C (*plc1Δ*), which catalyzes the hydrolysis of $PI(4,5)P_2$ to diacylglycerol and $InsP_3$, and $InsP_3$-kinase (*arg82Δ*), which generates $InsP_4$ and $InsP_5$ (Fig. 4C). In order to test for potential secondary effects in a living *kcs1*Δ cell, we replaced VTC by a constitutively active variant that bears the point mutations $vtc3^{K126A}$/$vtc4^{K129A}$ in its SPX domains and provides polyP synthesis activity comparable to activated wildtype VTC [10]. This mutant fully restored polyP accumulation in *kcs1Δ* cells (Fig. 4D). Thus, polyP synthesis by VTC is limited by the activation of its SPX domains in *kcs1Δ* cells. This allows us to use polyP accumulation as a bona fide readout for the action of PP-InsPs on SPX domains *in vivo*.

Four PP-InsPs have been found in wildtype yeast: 1-PP-$InsP_5$, 5-PP-$InsP_5$, 5-PP-$InsP_4$**,** and 1,5-$(PP)_2$-$InsP_4$. Given its lower potency and the fact that 5-PP-$InsP_4$ does not accumulate to appreciable levels, it appears as a weak candidate for a regulator of steady-state polyP levels in logarithmically growing cells [22]. Loss of 5-PP-$InsP_5$ and 1,5-$(PP)_2$-$InsP_4$ by deleting *KCS1* impairs polyP accumulation, suggesting that these compounds are relevant for activation *in vivo*. Loss of VIP1, which produces 1-PP-$InsP_5$ and 1,5-$(PP)_2$-$InsP_4$, does not abolish polyP accumulation (Fig. 4E) [20]. However, since 1-PP-$InsP_5$ constitutes only 5-10% of total PP-InsPs pool, its role in regulation of the VTC complex is likely masked by the more abundant 5-PP-$InsP_5$. In order to test a potential role of 1-PP-$InsP_5$ further, we analyzed polyP content in *kcs1*Δ *ddp1Δ* cells. The lack of the diphosphoinositol phosphohydrolase Ddp1 allows 1-PP-$InsP_5$ to accumulate to levels exceeding those of 5-PP-$InsP_5$ in wildtype cells [29]. Yet *kcs1*Δ *ddp1Δ* cells did not accumulate polyP, suggesting that 1-PP-$InsP_5$ is not sufficient to activate VTC *in vivo* (Fig. 4E). We can also

eliminate 1,5-$(PP)_2$-$InsP_4$, because its absence in a *vip1Δ* mutant does not impair polyP accumulation. The collective *in vivo* and *in vitro* evidence thus points to 5-PP-$InsP_5$ as a physiologically relevant stimulator of the SPX-dependent VTC complex.

In the present work, we elucidate the structural requirements of inositol pyrophosphates for regulating SPX domains of the VTC complex. We compare several X-PP-$InsP_5$, 5-PP-$InsP_4$, 1,5-$(PP)_2$-$InsP_4$, and 3,5-$(PP)_2$-$InsP_4$. This unique collection of data enables us to delineate the ideal arrangement of pyrophosphates and phosphates required to stimulate the VTC complex. In addition, we report for the first time a chemical synthesis of 5-PPP-$InsP_5$ containing a triphosphate subunit based on an iterative phosphorylation approach and evaluate its ability to stimulate the VTC complex. We find that the most effective stimulator of polyP synthesis is 1,5-$(PP)_2$-$InsP_4$. 5-PP-$InsP_5$ can assume its major role *in vivo* because, although it is 10- to 20-fold less potent than 1,5-$(PP)_2$-$InsP_4$, it is much more abundant, also in mammalian cells [22,30]. We underline that this conclusion is based on standard growth conditions, under which other PP-InsPs may not accumulate to sufficiently high levels to provide a stimulus. Significant fluctuations of 1,5-$(PP)_2$-$InsP_8$ under stress conditions are documented [31,32]. 1,5-$(PP)_2$-$InsP_4$ and other PP-InsPs that can activate VTC *in vitro* might therefore serve as critical signals in response to several stimuli or stressors. We hence suppose that SPX domains integrate inputs through a variety of PP-InsPs that are produced in response to different cellular or environmental conditions, in order to optimize cellular phosphate homeostasis.

Methods

Quantification of polyP in vivo

PolyP was isolated by phenol extraction [20]. 2-2.5 OD_{600} of cells were collected by centrifugation and resuspended in 300 µl buffer (10 mM Tris, pH 7.4, 0.1 M LiCl, 10 mM EDTA, 0.5% SDS). The suspension was mixed with an equal volume of phenol (pH 5.2), ~250 µl of glass beads were added, cells

were lysed by shaking for 5 min (4-8°C). Samples were centrifuged for 10 min. (4°C). 250 µl of aqueous phase was collected and extracted with 250 µl chloroform. PolyP was precipitated by mixing 200 µl of aqueous phase with 500 µl ethanol. The pellet was washed with 75% ethanol, dried and dissolved in 100 µl 10 mM Tris·HCl pH 7.4 0.5 mM EDTA (1h at 4°C with shaking). 5 µl of the polyP sample were digested with recombinant scPpx1 in 100 µl of reaction buffer containing 5 mM Tris·HCl pH 7.0, 1.5 mM $MgCl_2$ and 0.4 µg/ml recombinant scPpx1 for 1.5-3h (37°C). Control samples were incubated without scPpx1. 10 µl of this reaction was diluted with 90 µl water (96-well plate) and released phosphate was measured by adding 150 µl malachite-green reagent (absorbance at 595 nm) [5]. To ensure that the values were in the linear range, a calibration curve with 0-100 µM NaH_2PO_4 was prepared in the same plate. To quantify phosphate released from polyP, the background readings obtained from the samples without scPpx1 were subtracted from the corresponding "with scPpx1" values. The results were normalized to the wildtype and are presented as mean of biological triplicates ± SD.

Measuring polyP Synthesis & Chemical Synthesis

Details can be found in the supporting information.

Associated Content

Supporting Information Available: This material is available free of charge *via* the Internet.

Author Information

Corresponding authors:
email: Andreas.Mayer@unil.ch
email: henning.jessen@oc.uni-freiburg.de
ORCID:
HJ: ORCID: 0000-0002-1025-9484
AM: ORCID: 0000-0001-6131-313X

Author Contributions:

RG, IP contributed equally.

Acknowledgments

We thank Y. Desfougères and A. Saiardi for strains. This work was supported by the SNSF (AM: CRSII5_170925 and 310030B_163477; HJ: PP00P2_157607) and the ERC (AM: 233458).

References

1 Elser, J. J. (2012) Phosphorus: a limiting nutrient for humanity? *Curr. opin. biotechnol. 23*, 833-838.

2 Livermore, T. M., Chubb, J. R. & Saiardi, A. (2016) Developmental accumulation of inorganic polyphosphate affects germination and energetic metabolism in Dictyostelium discoideum. *Proc. Natl. Acad. Sci. USA 113*, 996-1001.

3 Nocek, B., Kochinyan, S., Proudfoot, M., Brown, G., Evcokimova, E., Osipiuk, J., Edwards, A. M., Savchenko, A., Joachimiak, A. & Yakunin, A. F. (2008) Polyphosphate-dependent synthesis of ATP and ADP by the family-2 polyphosphate kinases in bacteria. *Proc. Natl. Acad. Sci. USA 105*, 17730-17735.

4 Rao, N. N., Gomez-Garcia, M. R. & Kornberg, A. (2009) Inorganic polyphosphate: essential for growth and survival. *Annu. Rev. Biochem. 78*, 605-647.

5 Hothorn, M., Neumann, H., Lenherr E. D., Wehner, M., Rybin V., Hassa P. O., Uttenweiler, A., Reinhardt, M., Schmidt, A., Seiler, J., Ladurner, A. G., Herrmann, C., Scheffzek, K. & Mayer, A. (2009) Catalytic core of a membrane-associated eukaryotic polyphosphate polymerase. *Science 324*, 513-516.

6 Desfougeres, Y., Gerasimaite, R. U., Jessen, H. J. & Mayer, A. (2016) Vtc5, a Novel Subunit of the Vacuolar Transporter Chaperone Complex, Regulates Polyphosphate Synthesis and Phosphate Homeostasis in Yeast. *J. Biol. Chem. 291*, 22262-22275.

7 Müller, O., Neumann, H., Bayer, M. J. & Mayer, A. (2003) Role of the Vtc proteins in V-ATPase stability and membrane trafficking. *J. Cell. Sci. 116*, 1107-1115.

8 Secco, D., Wang, C., Arpat, B. A., Wang, Z., Poirier, Y., Tyerman, S. D., Wu, P. Shou, H., & Whelan, J. (2012) The emerging importance of the SPX domain-containing proteins in phosphate homeostasis. *New phytol. 193*, 842-851.

9 Lee, Y. S., Mulugu, S., York, J. D. & O'Shea, E. K. (2007) Regulation of a cyclin-CDK-CDK inhibitor complex by inositol pyrophosphates. *Science 316*, 109-112.

10 Wild, R. Gerasimaite, R., Jung, J.-Y., Truffault, V., Pavlovic, I., Schmidt, A., Saiardi, A., Jessen, H. J., Poirier, Y., Hothorn, M. &

Mayer, A. (2016) Control of eukaryotic phosphate homeostasis by inositol polyphosphate sensor domains. *Science 352*, 986-990.

11 Irvine, R. F. & Schell, M. J. (2001) Back in the water: the return of the inositol phosphates. *Nat. rev. Mol. cell biol. 2*, 327-338.

12 Menniti, F. S., Miller, R. N., Putney, J. W. & Shears, S. B. (1993) Turnover of Inositol Polyphosphate Pyrophosphates in Pancreatoma Cells. *J. Biol. Chem. 268*, 3850-3856.

13 Wilson, M. S., Livermore, T. M. & Saiardi, A. (2013) Inositol pyrophosphates: between signalling and metabolism. *Biochem. J. 452*, 369-379.

14 Draskovic, P., Saiardi, A., Bhandari, R., Burton, A., Ilc, G., Kovacevic, M., Snyder, S. H. & Podobnik, M. (2008) Inositol hexakisphosphate kinase products contain diphosphate and triphosphate groups. *Chem. Biol. 15*, 274-286.

15 Capolicchio, S., Thakor, D. T., Linden, A. & Jessen, H. J. (2013) Synthesis of Unsymmetric Diphospho-Inositol Polyphosphates. *Angew. Chem. Int. Ed. 52*, 6912-6916.

16 Capolicchio, S., Wang, H. C., Thakor, D. T., Shears, S. B. & Jessen, H. J. (2014) Synthesis of Densely Phosphorylated Bis-1,5-Diphospho-myo-Inositol Tetrakisphosphate and its Enantiomer by Bidirectional P-Anhydride Formation. *Angew. Chem. Int. Ed. 53*, 9508-9511.

17 Pavlovic, I., Thakor, D. T., Vargas, J. R., McKinlay, C., Hauke, S., Anstaett, P., Camuna, R. C., Bigler, L., Gasser, G., Schultz, C. Wender, P. A. & Jessen, H. J. (2016) Cellular delivery and photochemical release of a caged inositol-pyrophosphate induces PH-domain translocation in cellulo. *Nat. Commun. 7*, 10622.

18 Thomas, M. P., Mills, S. J. & Potter, B. V. (2016) The "Other" Inositols and Their Phosphates: Synthesis, Biology, and Medicine (with Recent Advances in myo-Inositol Chemistry). *Angew. Chem. Int. Ed. 55*, 1614-1650.

19 Auesukaree, C., Tochio, H., Shirakawa, M., Kaneko, Y. & Harashima, S. (2005) Plc1p, Arg82p, and Kcs1p, enzymes involved in inositol pyrophosphate synthesis, are essential for phosphate regulation and polyphosphate accumulation in Saccharomyces cerevisiae. *J. Biol. Chem. 280*, 25127-25133.

20 Lonetti, A., Szijgyarto, Z., Bosch, D., Loss, O., Azevedo, C. & Saiardi, A. (2011) Identification of an evolutionarily conserved family of inorganic polyphosphate endopolyphosphatases. *J. Biol. Chem. 286*, 31966-31974.

21 Lev, S., Li, C., Desmarini, D., Saiardi, A., Fewings, N. L., Schibeci, S. D., Sharma, R., Sorrell, T. C. & Djordjevic J. T. (2015) Fungal Inositol Pyrophosphate IP7 Is Crucial for Metabolic Adaptation to the Host Environment and Pathogenicity. *mBio 6*, e00531-00515.

22 Saiardi, A., Sciambi, C., McCaffery, J. M., Wendland, B. & Snyder, S. H. (2002) Inositol pyrophosphates regulate endocytic trafficking. *Proc. Natl. Acad. Sci. USA 99*, 14206-14211.

23 Pavlovic, I., Thakor, D. T. & Jessen, H. J. (2016) Synthesis of 2-diphospho-myo-inositol 1,3,4,5,6-pentakisphosphate and a photocaged analogue. *Org. Biomol. Chem. 14*, 5559-5562.

24 Wang, H. C., Godage, H. Y., Riley, A. M., Weaver, J. D., Shears, S. B. & Potter, B. V. (2014) Synthetic Inositol Phosphate Analogs Reveal that PPIP5K2 Has a Surface-Mounted Substrate Capture Site that Is a Target for Drug Discovery. *Chem. Biol. 21*, 689-699.

25 Cremosnik, G. S., Hofer, A. & Jessen, H. J. (2014) Iterative Synthesis of Nucleoside Oligophosphates with Phosphoramidites. *Angew. Chem. Int. Ed. 53*, 286-289.

26 Gerasimaite, R., Sharma, S., Desfougeres, Y., Schmidt, A. & Mayer, A. (2014) Coupled synthesis and translocation restrains polyphosphate to acidocalcisome-like vacuoles and prevents its toxicity. *J. cell sci*. 127, 5093-5104.

27 Wang, H., Falck, J. R., Hall, T. M. & Shears, S. B. (2011) Structural basis for an inositol pyrophosphate kinase surmounting phosphate crowding. *Nat. chem. biol. 8*, 111-116.

28 Saiardi, A., Caffrey, J. J., Snyder, S. H. & Shears, S. B. (2000) The inositol hexakisphosphate kinase family. Catalytic flexibility and function in yeast vacuole biogenesis. *J. Biol. Chem. 275*, 24686-24692.

29 York, S. J., Armbruster, B. N., Greenwell, P., Petes, T. D. & York, J. D. (2005) Inositol diphosphate signaling regulates telomere length. *J. Biol. Chem. 280*, 4264-4269.

30 Wundenberg, T. & Mayr, G. W. (2012) Synthesis and biological actions of diphosphoinositol phosphates (inositol pyrophosphates), regulators of cell homeostasis. *Biol. chem. 393*, 979-998.

31 Choi, J. H., Williams, J., Cho, J., Falck, J. R. & Shears, S. B. (2007) Purification, sequencing, and molecular identification of a mammalian PP-InsP5 kinase that is activated when cells are exposed to hyperosmotic stress. *J. Biol. Chem. 282*, 30763-30775.

32 Pesesse, X., Choi, K., Zhang, T. & Shears, S. B. (2004) Signaling by higher inositol polyphosphates. Synthesis of bisdiphosphoinositol tetrakisphosphate ("InsP8") is selectively activated by hyperosmotic stress. *J. Biol. Chem. 279*, 43378-43381.

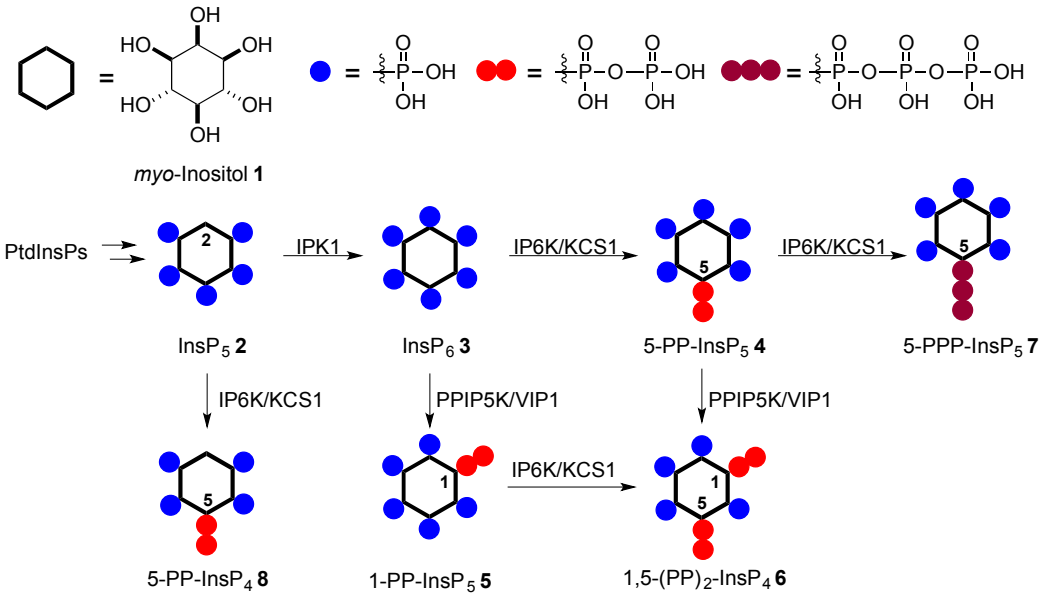

Figure 1. Biosynthesis of inositol pyrophosphates. IPK1: inositol pentakisphosphate 2-kinase; IP6K: inositol hexakisphosphate 5-kinase; PPIP5K, diphosphoinositol pentakisphosphate 1-kinase.

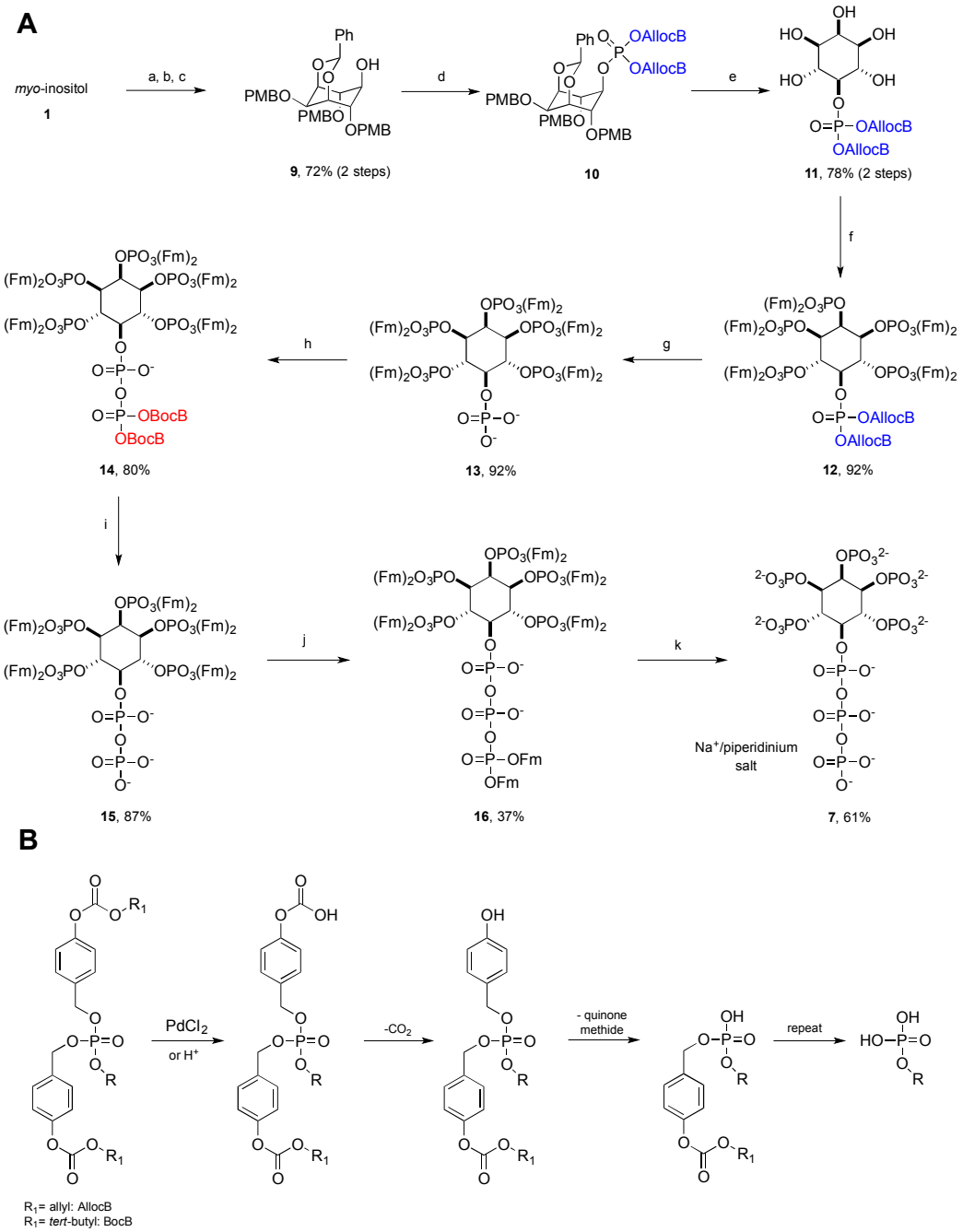

Figure 2. A) Synthesis of 5-PPP-InsP_5 **7**; **B)** Structure and cleavage mechanism of the AllocB and BocB protecting groups. a-c: $PhC(OMe)_3$, CSA, DMSO; NaH, PMB-Cl, DMF; DIBAL-H, CH_2Cl_2, 67% over three steps. d) Bis-AllocB P-amidite, DCI, MeCN, then *t*BuOOH; e) TFA in DCM, 78% over two steps. f) Bis-Fm P-amidite, DCI, THF/MeCN, then *m*CPBA, 92%. g) $PdCl_2$, MeOH, CH_2Cl_2, 92%. h) Bis-BocB P-amidite, DCI, CH_2Cl_2, then *m*CPBA, 60%. i) TFA, CH_2Cl_2, 87%. j) Bis-Fm P-amidite, DCI, CH_2Cl_2, then *m*CPBA, 37%. k) Piperidine, DMF, then NaI in MeOH, 61%. Abbreviations: alloc:

allyloxycarbonyl, boc: *tert*-butyloxycarbonyl, CSA: camphor sulfonic acid, DIBAL-H: di*iso*butylaluminium hydride, DCI: 4,5-dicyanoimidazole, DMSO: dimethylsulfoxide, DMF: dimethylformamide, PMB: para-methoxybenzyl, Fm: 9-fluorenylmethyl, *m*CPBA: *meta*-chloroperbenzoic acid, TFA: trifluoro acetic acid.

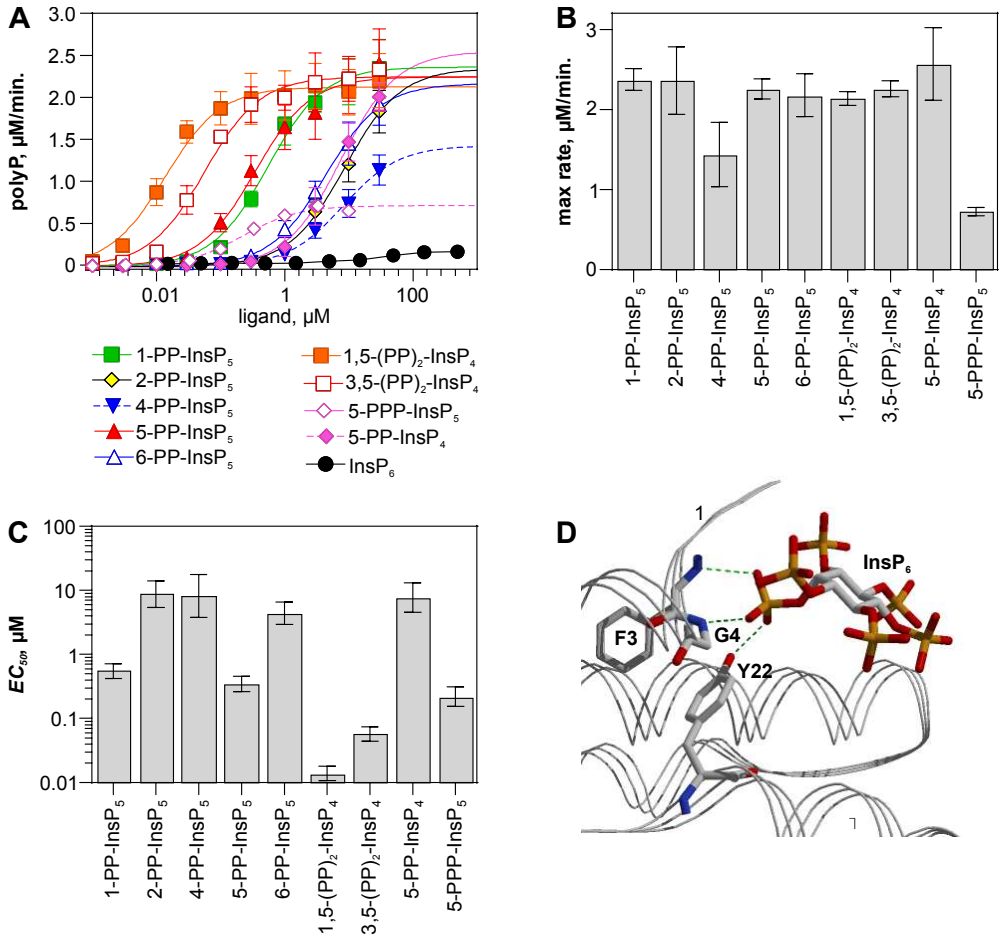

Figure 3. Stimulation of VTC activity on isolated vacuoles by InsPs.

A) Titration of InsPs. Isolated vacuoles were incubated in polyP synthesis assays in the presence of increasing concentrations of the indicated InsPs. Synthesized polyP was quantified. The data was fitted to a three parameter dose response curve and the derived parameters, maximal rate and EC_{50}, are shown in **B** and **C**, respectively. n=3. Error bars show the standard deviation.

D) Coordination of the 2-phosphate of $InsP_6$ by the SPX domain from CtVtc4 (pdb code *5ijp*). The 2-phosphate makes H-bonds with main chain atoms of F3 and G4 from the α1 helix and with the side chain of Y22 from the α2 helix. Only H-bonds to the 2-phosphate are shown (green dashed lines).

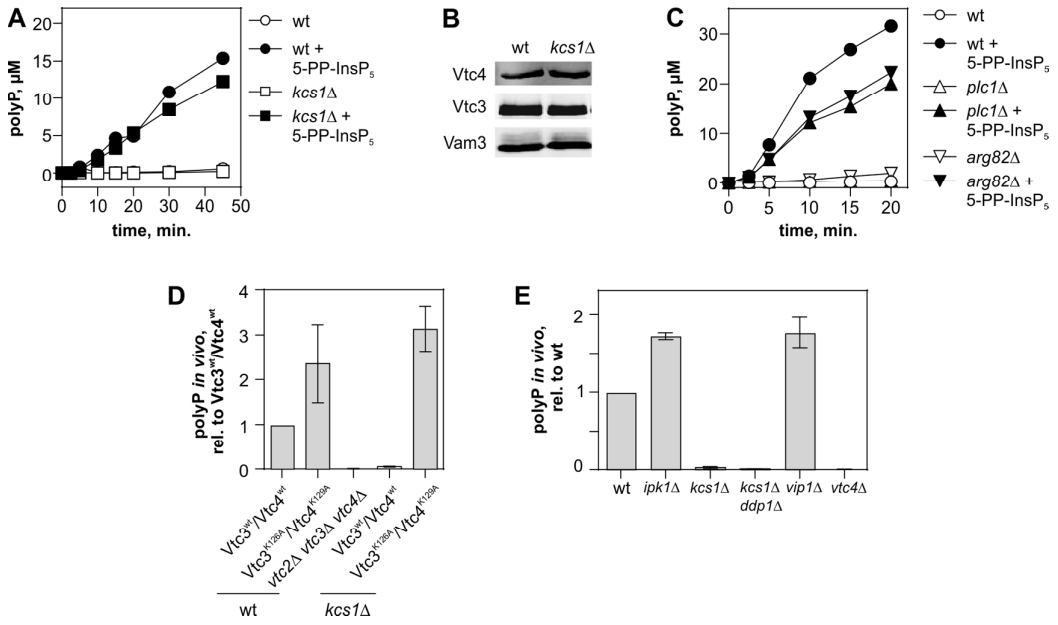

Figure 4. The yeast polyP synthesis machinery is correctly assembled but not active in the absence of PP-InsPs. **A)** Time-course of polyP synthesis by vacuoles isolated from wildtype (BJ3505) and *kcs1Δ* strains. The vacuoles were incubated in polyP synthesis reactions in the presence or absence of 0.5 µM 5-PP-InsP$_5$. **B)** Levels of catalytic (Vtc4) and regulatory (Vtc3) subunits on wildtype and *kcs1Δ* vacuoles from A, as determined by SDS-PAGE and Western blotting. The vacuolar SNARE protein Vam3 is shown as a loading control. **C)** Time-course of polyP synthesis by vacuoles isolated from wildtype (BY4741) and *arg82Δ* and *plc1Δ* strains, measured as in A. **D)** Rescue of polyP accumulation in *kcs1Δ* cells by constitutively active SPX domains. *vtc3Δ vtc4Δ* and *vtc3Δ vtc4Δ kcs1Δ* mutants were complemented with integrating plasmids expressing the indicated alleles of VTC3 and VTC4, coding for wildtype or constitutively active SPX domains. The cells were grown logarithmically in SC medium and polyP content was determined. n=3; **E)** PolyP accumulation in vivo is not rescued by overproduction of 1-PP-InsP$_5$. The indicated strains were logarithmically grown in SC medium and polyP was determined. n=3. Error bars show the standard deviation.

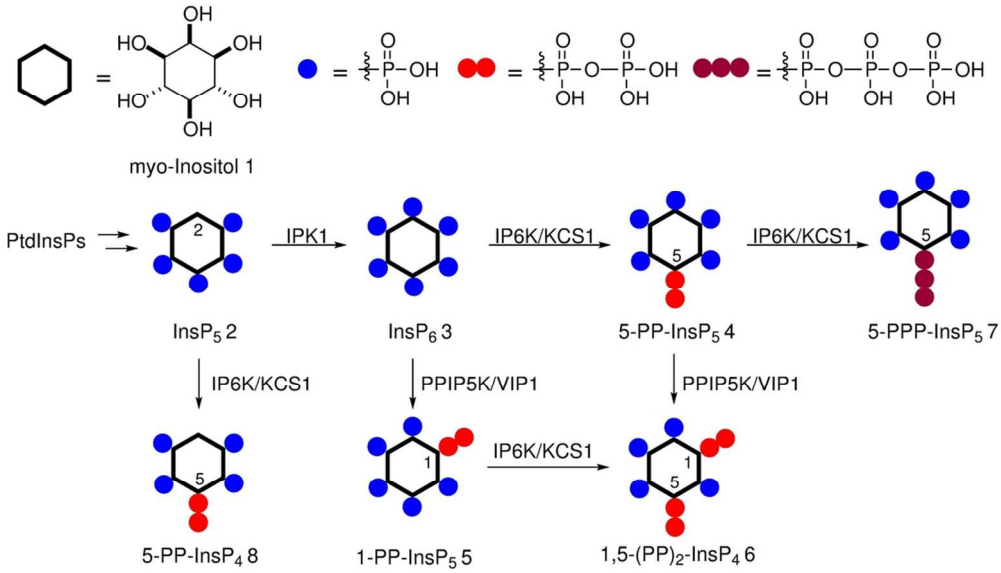

Figure 1. Biosynthesis of inositol pyrophosphates. IPK1: inositol pentakisphosphate 2-kinase; IP6K: inositol hexakisphosphate 5-kinase; PPIP5K, diphosphoinositol pentakisphosphate 1-kinase.

101x58mm (300 x 300 DPI)

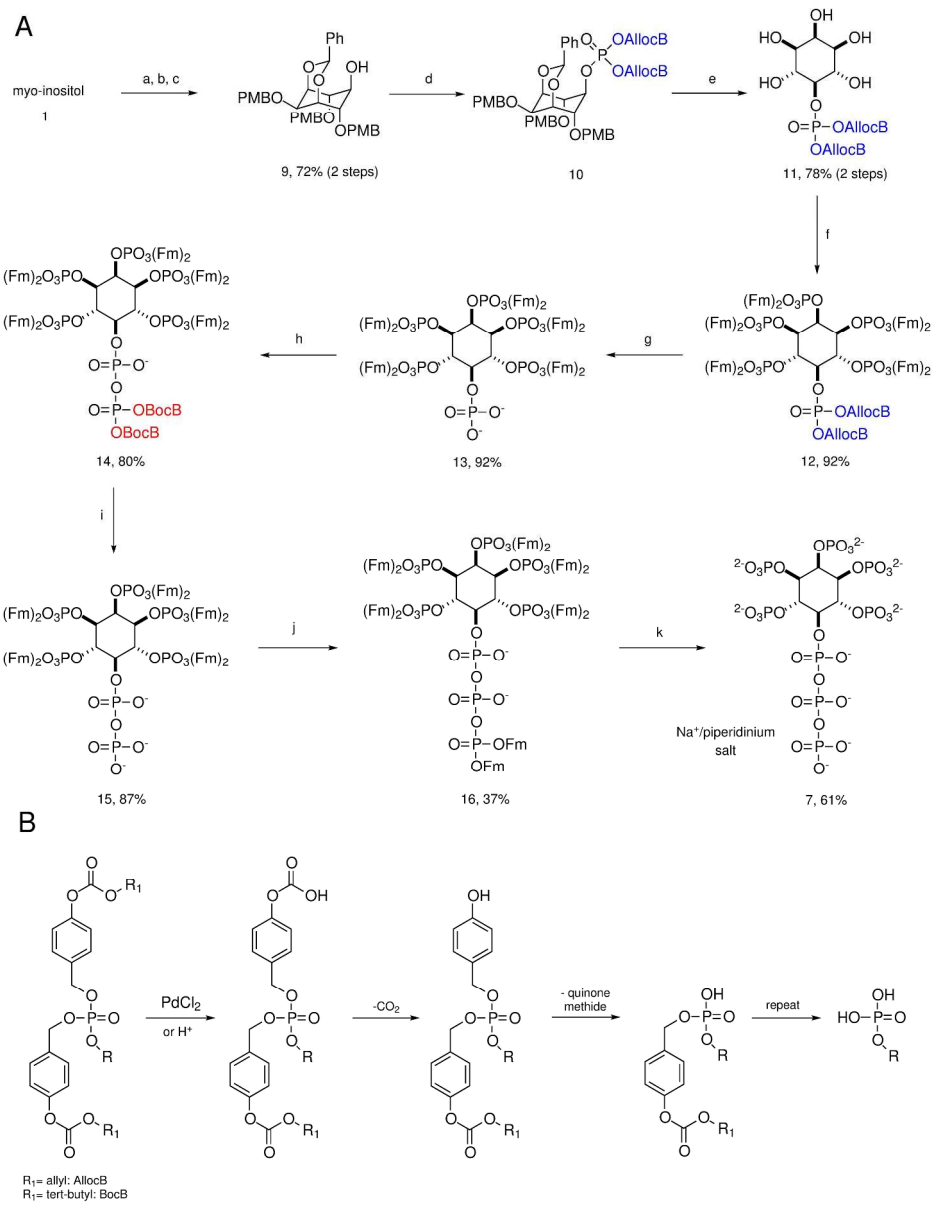

Figure 2. A) Synthesis of 5-PPP-InsP5 7; B) Structure and cleavage mechanism of the AllocB and BocB protecting groups. a-c: PhC(OMe)3, CSA, DMSO; NaH, PMB-Cl, DMF; DIBAL-H, CH2Cl2, 67% over three steps. d) Bis-AllocB P-amidite, DCI, MeCN, then tBuOOH; e) TFA in DCM, 78% over two steps. f) Bis-Fm P-amidite, DCI, THF/MeCN, then mCPBA, 92%. g) PdCl2, MeOH, CH2Cl2, 92%. h) Bis-BocB P-amidite, DCI, CH2Cl2, then mCPBA, 60%. i) TFA, CH2Cl2, 87%. j) Bis-Fm P-amidite, DCI, CH2Cl2, then mCPBA, 37%. k) Piperidine, DMF, then NaI in MeOH, 61%. Abbreviations: alloc: allyloxycarbonyl, boc: tert-butyloxycarbonyl, CSA: camphor sulfonic acid, DIBAL-H: diisobutylaluminium hydride, DCI: 4,5-dicyanoimidazole, DMSO: dimethylsulfoxide, DMF: dimethylformamide, PMB: para-methoxybenzyl, Fm: 9-fluorenylmethyl, mCPBA: meta-chloroperbenzoic acid, TFA: trifluoro acetic acid.

273x350mm (300 x 300 DPI)

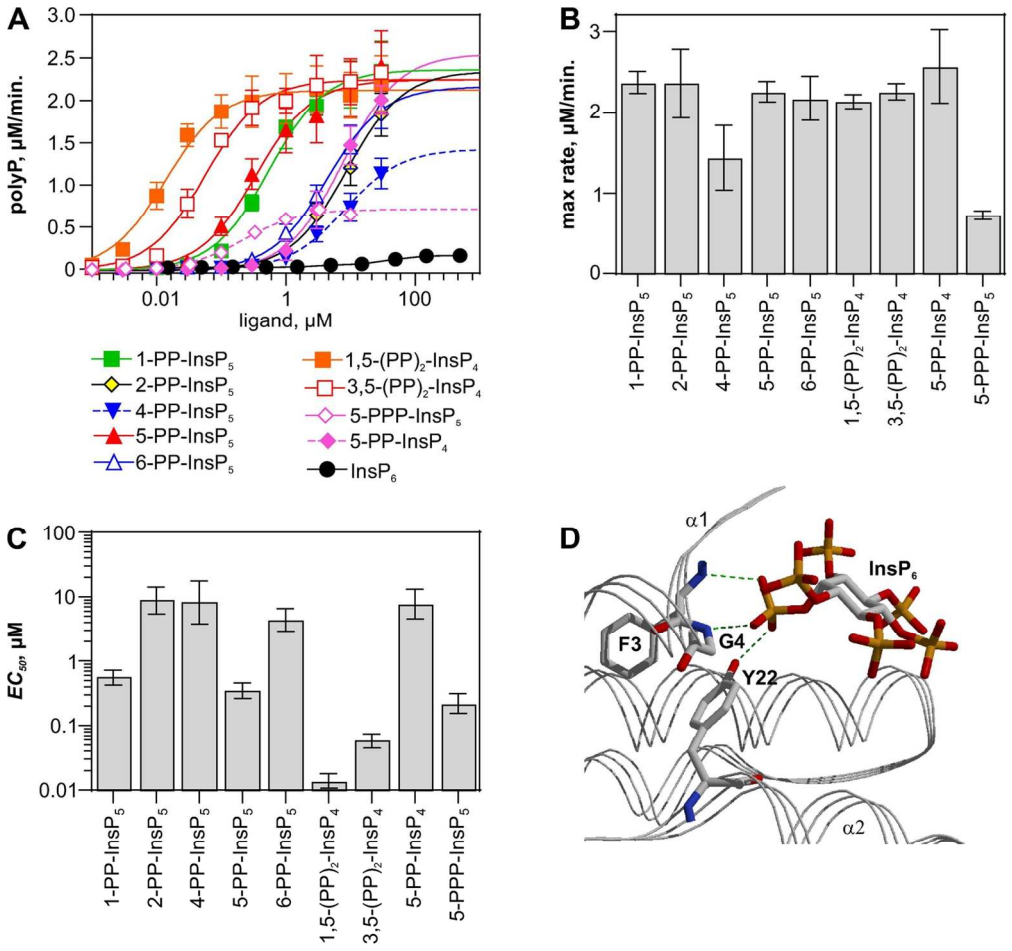

Figure 3. Stimulation of VTC activity on isolated vacuoles by InsPs.
A) Titration of InsPs. Isolated vacuoles were incubated in polyP synthesis assays in the presence of increasing concentrations of the indicated InsPs. Synthesized polyP was quantified. The data was fitted to a three parameter dose response curve and the derived parameters, maximal rate and EC50, are shown in B and C, respectively. n=3. Error bars show the standard deviation.
D) Coordination of the 2-phosphate of InsP6 by the SPX domain from CtVtc4 (pdb code 5ijp). The 2-phosphate makes H-bonds with main chain atoms of F3 and G4 from the α1 helix and with the side chain of Y22 from the α2 helix. Only H-bonds to the 2-phosphate are shown (green dashed lines).

130x122mm (300 x 300 DPI)

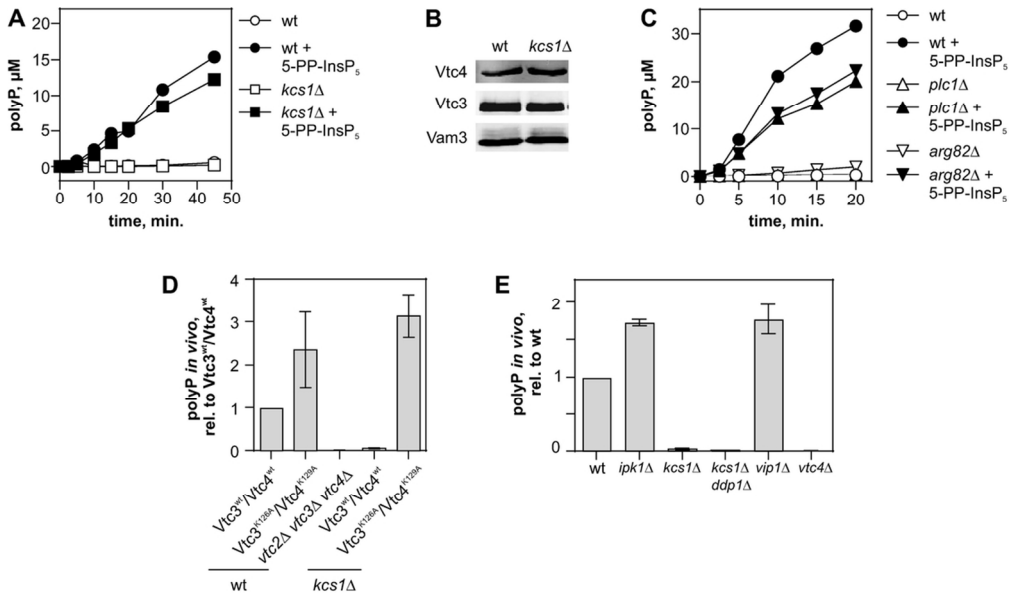

Figure 4. The yeast polyP synthesis machinery is correctly assembled but not active in the absence of PP-InsPs.

A) Time-course of polyP synthesis by vacuoles isolated from wildtype (BJ3505) and kcs1Δ strains. The vacuoles were incubated in polyP synthesis reactions in the presence or absence of 0.5 µM 5-PP-InsP5. B) Levels of catalytic (Vtc4) and regulatory (Vtc3) subunits on wildtype and kcs1Δ vacuoles from A, as determined by SDS-PAGE and Western blotting. The vacuolar SNARE protein Vam3 is shown as a loading control. C) Time-course of polyP synthesis by vacuoles isolated from wildtype (BY4741) and arg82Δ and plc1Δ strains, measured as in A. D) Rescue of polyP accumulation in kcs1Δ cells by constitutively active SPX domains. vtc3Δ vtc4Δ and vtc3Δ vtc4Δ kcs1Δ mutants were complemented with integrating plasmids expressing the indicated alleles of VTC3 and VTC4, coding for wildtype or constitutively active SPX domains. The cells were grown logarithmically in SC medium and polyP content was determined. n=3; E) PolyP accumulation in vivo is not rescued by overproduction of 1-PP-InsP5. The indicated strains were logarithmically grown in SC medium and polyP was determined. n=3. Error bars show the standard deviation.

102x59mm (300 x 300 DPI)

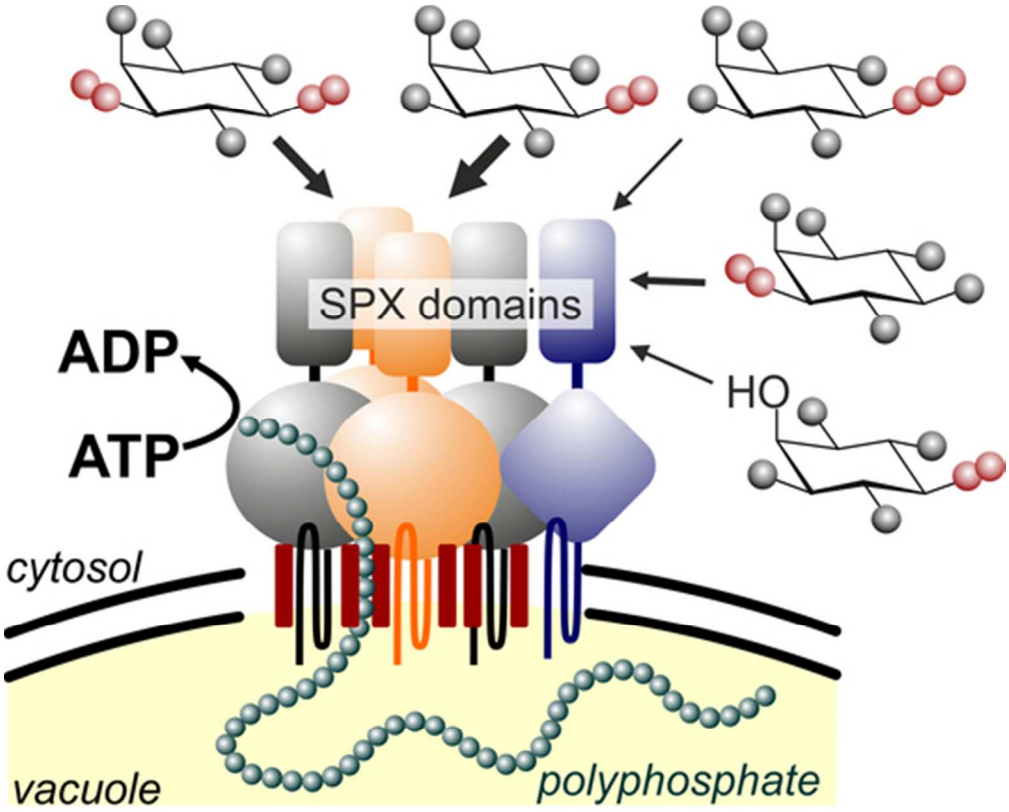

SPX domains of yeast polyP polymerase integrate signaling by differnt inositol pyrophosphate isomers

TOC

45x42mm (300 x 300 DPI)

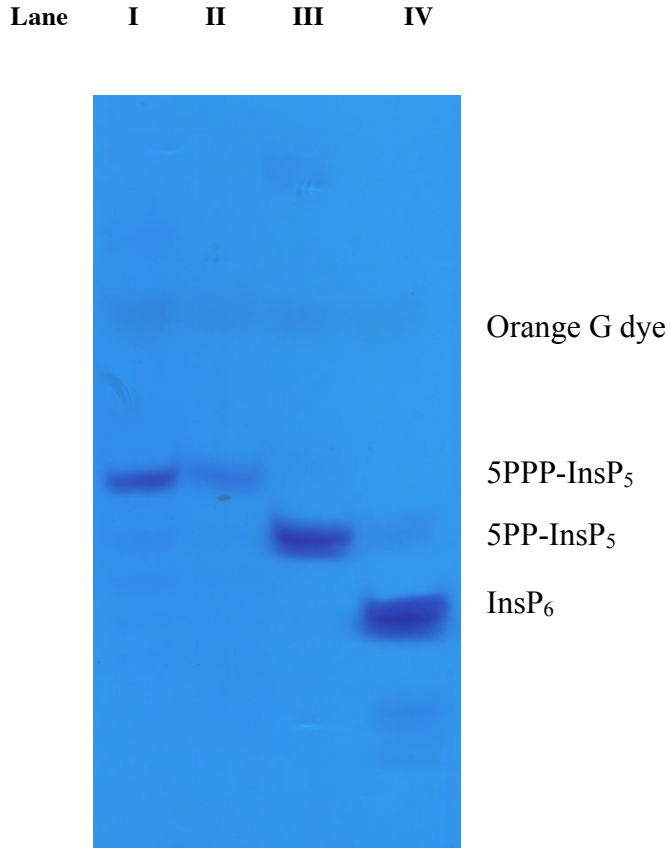

Figure S1. PAGE analysis (purity check) of synthetic 5PPP-$InsP_5$ **7**. The gel was stained with toluidine blue. Lanes I and II: two concentrations (high, low) of 5-PPP-$InsP_5$ **7**. Lane III: control 5PP-$InsP_5$; lane IV: control $InsP_6$.

Yeast strains

Table S1. Yeast strains used in this study

Strain	**Genotype**	**Source / Reference**
BY4742	MATα his3Δ1 leu2Δ0 lys2Δ0 ura3Δ0	[1]
BY4742 *vtc4*Δ	vtc4::kanMX	Euroscarf
BY4742 *plc1*Δ	plc1::URA3	(Andreas Uttenweiler)
BY4742 *vtc2*Δ *vtc3*Δ *vtc4*Δ $Vtc3^{wt}/Vtc4^{wt}$	BY4742 vtc2::LEU2 vtc3::NatNT2 vtc4::kanMX VTC3::URA3 VTC4::HIS3	[2]
BY4742 *vtc2*Δ *vtc3*Δ *vtc4*Δ $Vtc3^{K126A}/Vtc4^{K129A}$	BY4742 vtc2::LEU2 vtc3::NatNT2 $VTC3^{K126A}$::URA3 $VTC4^{K129A}$::HIS3	[2]
BY4742 *vtc2*Δ *vtc3*Δ *vtc4*Δ *kcs1*Δ	BY4742 vtc2::LEU2 vtc3::NatNT2 vtc4::kanMX kcs1::HphNT1	this study
BY4742 *vtc2*Δ *vtc3*Δ *vtc4*Δ *kcs1*Δ $Vtc3^{wt}/Vtc4^{wt}$	BY4742 vtc2::LEU2 vtc3::NatNT2 vtc4::kanMX kcs1::HphNT1 VTC3::URA3 VTC4::HIS3	this study
BY4742 *vtc2*Δ *vtc3*Δ *vtc4*Δ *kcs1*Δ $Vtc3^{K126A}/Vtc4^{K129A}$	BY4742 vtc2::LEU2 vtc3::NatNT2 vtc4::kanMX kcs1::HphNT1 $VTC3^{K126A}$::URA3 $VTC4^{K129A}$::HIS3	this study
BY4741	MATα his3Δ200 leu2Δ0 lys2Δ0 met15Δ0 trp1Δ63 ura3Δ0	Euroscarf
BY4741 *kcs1*Δ	kcs1::kanMX	
BY4741 *arg82*Δ	arg82::NatNT2	this study
BY4741 *ipk1*Δ	ipk1::kanMX	[3]
BY4741 *vip1*Δ	vip1::kanMX	[3]
BY4741 *kcs1*Δ *ddp1*Δ	kcs1::kanMX ddp1::NatNT2	this study
BJ3505	MATa pep4::HIS3 prb1- Δ1.6R lys2-208 trp-Δ101 ura3-52 gal2 can	[4]
BJ3505 *kcs1*Δ	BJ3505 kcs1::kanMX	this study

[1] C. B. Brachmann, A. Davies, G. J. Cost, E. Caputo, J. Li, P. Hieter, J. D. Boeke, *Yeast* **1998**, *14*, 115-132.

[2] R. Wild, R. Gerasimaite, J. Y. Jung, V. Truffault, I. Pavlovic, A. Schmidt, A. Saiardi, H. J. Jessen, Y. Poirier, M. Hothorn, A. Mayer, *Science* **2016**, *352*, 986-990.

[3] D. D. Shoemaker, D. A. Lashkari, D. Morris, M. Mittmann, R. W. Davis, *Nature genetics* **1996**, *14*, 450-456.

[4] E. W. Jones, G. S. Zubenko, R. R. Parker, *Genetics* **1982**, *102*, 665-677.

Experimental Procedures

Polyacrylamide Gel Electrophoresis (PAGE) was carried out by employing 24cm long; 18cm wide glass plates, 1.0mm wide spacers and a 15-lane comb were used for loading the samples. The purity of synthetic material was analyzed by PAGE (35% Acrylamide- bis acrylamide) and staining with a fluorescent dye (toludine blue) according to a published procedure (Pisani F, Livermore T, Rose G, Chubb JR, Gaspari M, et al. PLoS ONE, 2014, 9(1): e85533. doi: 10.1371/journal.pone.0085533.). Orange G dye has been added to track progression of the electrophoresis.

Reactions were carried out using oven-dried glassware under an atmosphere of dry N2 and magnetically stirred, unless noted otherwise. Air- and moisture-sensitive liquids and solutions were transferred via syringe or stainless steel canula.

Reagents were purchased from commercial suppliers (Acros, Aldrich, Fluka, TCI) and used without further purification, unless noted otherwise.

Solvents (methylene chloride, diethyl ether, tetrahydrofuran, acetonitrile, toluene) for reactions were purified by filtration and dried by passage over activated anhydrous neutral A-2 alumina (MBraun solvent purification system) under an atmosphere of dry nitrogen. Analytical grade solvents were used as received for extractions and chromatographic purifications.

Deuterated solvents were obtained from Armar Chemicals, Switzerland, in the indicated purity grade.

Thin Layer Chromatography were used for monitoring reactions and carried out using Merck silica gel 60 F254 plates, visualized with UV light or developed either with phosphormolybdic acid solution or with potassium permanganate solution followed by heating

Flash Chromatography was performed using Fluka silica gel 60 (230-400 Mesh) at a pressure of ca. 0.3 bar. Eluents and Rf are indicated.
Lyophilizations were performed on a Christ Freeze Dryer Alpha 1-2 LD+.

^{1}H-NMR spectra were recorded on Bruker 400 MHz spectrometers or Bruker 500 MHz spectrometers (equipped with a cryo platform) at 298K in the indicated deuterated solvent. Data are reported as follow: chemical shift (δ, ppm), multiplicity (s, singlet; d, doublet; t, triplet; q, quartet; m, multiplet or not resolved signal; br, broad signal), coupling constant(s) (*J*, Hz), integration. All signals were referenced to the internal solvent signal as standard ($CDCl_3$, δ 7.26; CD_3OD, δ 3.31; DMSO-d_6, δ 2.50).

^{13}C-NMR spectra were recorded with ^{1}H-decoupling on Bruker 101 MHz or Bruker 125 MHz spectrometers (equipped with a cryo platform) at 298K in the indicated deuterated solvent. All signals were referenced to the internal solvent signal as standard ($CDCl_3$, δ 77.0; CD_3OD, δ 49.0; DMSO-d_6, δ 39.5).

^{31}P-NMR spectra were recorded with proton coupling and 1H-decoupling on Bruker 162 MHz or Bruker 202 MHz spectrometers (equipped with a cryo platform) at 298K in the indicated deuterated solvent. All signals were referenced to an internal standard (PPP)

IR spectra were recorded on a JASCO FT-IR-4100 spectrometer and data are reported in terms of frequency of absorption (cm^{-1}).

Mass spectra were recorded by the Mass spectroscopy Service of UZH on Finnigan MAT95 MS, Bruker EsquireLC MS , Bruker maXis QTof HR MS and Finnigan TSQ700 MS machines.

Measuring polyP synthesis by isolated vacuoles

For vacuole isolation, the cells were grown in 1 l YPD media at 30°C overnight, harvested at OD_{600} of 0.8-1.9 and vacuoles were isolated as described previously (R. Gerasimaite, S. Sharma, Y. Desfougeres, A. Schmidt, A. Mayer, *J. Cell Sci*. **2014**, *127*, 5093-5104). Vacuole concentration was determined by Bradford assay using BSA as a standard and is reported as concentration of total vacuolar protein. PolyP synthesis by isolated vacuoles was assessed as previously described (R. Gerasimaite, S. Sharma, Y. Desfougeres, A. Schmidt, A. Mayer, *J. Cell Sci*. **2014**, *127*, 5093-5104). Briefly, to follow the time-course of the reaction, 0.005 mg/ml vacuoles were incubated in reaction buffer (10 mM PIPES/KOH pH 6.8, 150 mM KCl, 0.5 mM $MnCl_2$, 200 mM sorbitol) containing an ATP-regenerating system (ATP-RS: 1 mM ATP-$MgCl_2$, 40 mM creatine phosphate and 0.25 mg/ml creatine kinase) at 27°C in the presence or absence of 0.5 μM 5-PP-$InsP_5$. At the indicated time points, 80 μl aliquots were mixed with 160 μl of stop solution (10 mM PIPES/KOH pH 6.8, 150 mM KCl, 200 mM sorbitol, 12 mM EDTA, 0.15% Triton X-100 and 15 μM DAPI) in a black 96-well plate. The samples were allowed to equilibrate for 15 min in the dark. Then, fluorescence of the polyP-DAPI complex was measured using λ_{ex} = 415 nm, λ_{em} = 550 nm (cutoff = 530 nm) at 27°C. PolyP concentration was determined by using 30 μM polyP-60 as a standard (kind gift of T. Shiba, Regenetiss Inc.). The experiments were repeated with three independent vacuole preparations and are represented as mean ± standard deviation.

For determining EC_{50}, the aforementioned reaction mixtures were prepared with serial dilutions of the ligands. The reactions were started by adding the vacuoles to 0.005 mg/ml, incubated at 27°C for 10 min, stopped as above and synthesized polyP was quantified. The obtained data was fitted into three-parameter dose response curve, derived parameters (EC_{50} and maximal rate) are reported with confidence intervals (95%).

Synthesis of 9

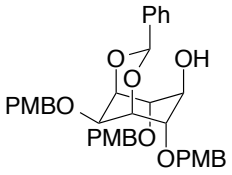

The compound was synthesized as described before in three steps starting from *myo*-inositol **1**. Analytical data were identical with the values reported in the literature.
Capolicchio, S., Thakor, D. T., Linden, A. & Jessen, H. J. Synthesis of unsymmetric diphospho-inositol polyphosphate. Angew Chem Int Ed **52**, 6912-6916, (2013)

Synthesis of allyl (4-formylphenyl) carbonate

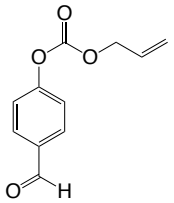

11.8 g (98.2 mmol, 1.20 eq.) of allyl chloroformate was slowly added to a solution of 10 g (81.8 mmol, 1.00 eq.) 4-hydroxybenzaldehyde and Et_3N (13.6 mL) in Et_2O (130 mL) at 0ºC. The mixture was stirred for 2 h at r.t. until TLC showed full conversion. Hexane and Et_2O (1:1, 300 mL) were added to the mixture, and the white precipitate was filtered. The filtrate was washed with a aq. soln. of $NaHCO_3$ (sat. 2 X 300 mL) and H_2O (2 X 300 mL) and the organic layer was dried over Mg_2SO_4. After evaporation, the pure product was obtained as a pale yellow oil of allyl (4-formylphenyl) carbonate (16.9 g, 81.0 mmol, 99 %).

TLC (Hex: EtOAc; 3:2): $\mathbf{R_f}$ = 0.73; **^{1}H-NMR** (500 MHz, DMSO-d_6): δ 10.01 (s, 1H), 8.00 (d, *J* = 8.6 Hz, 2H), 7.50 (d, *J* = 8.6 Hz, 2H), 6.13 - 5.93 (m, 1H), 5.42 (dq, *J* = 17.3, 1.6 Hz, 1H), 5.32 (dq, *J* = 10.5, 1.3 Hz, 1H), 4.76 (dt, *J* = 5.6, 1.4 Hz, 2H); **^{13}C-NMR** (126 MHz, DMSO-d_6): δ 191.9, 154.9, 152.1, 134.1, 131.6, 131.2, 122.1, 119.1, 69.0, 40.0, 39.9, 39.8, 39.8, 39.7, 39.6, 39.5, 39.4, 39.3, 39.2, 39.0; **IR** (neat, cm^{-1}) 3405.5, 2924.7, 1763.9, 1605.4, 1508.2, 1366.1, 1198.2, 1145.4, 1017.4, 844.7; **HRMS** (ESI) $[M+CH_3OH+Na]^+$ calcd for $C_{12}H_{14}NaO_5$, 261.0739; found, 261.0732

Synthesis of *tert*-butyl (4-formylphenyl) carbonate

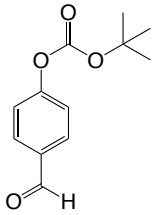

The compound was synthesized as described before in patent WO2014/174064 A1, 2014, page 56, by M. Perez, I. Rilatt, M. Lamothe, Pierre Fabre Medicament.
4-hydroxybenzaldehyde 3.00 g (24.6 mmol, 1.0 eq.) was dissolved in DCM (30 mL) in the presence of DMAP 0.300 g (2.46 mmol, 0.100 eq.) and di-*tert*-butyl dicarbonate 5.35 g (24.6 mmol, 1.00 eq.) and stirred for 1 hour at room temperature. When TLC showed full conversion, the solution was diluted with H_2O (200 mL) and extracted with DCM (3 x 100 mL). The organic phases were combined, dried over $MgSO_4$, filtered and concentrated under reduced pressure to yield pure compound *tert*-butyl (4-formylphenyl) carbonate as a white solid (5.24 g, 23.6 mmol, 96 %). Analytical data were identical with the values reported in the literature.
A. Schechter, D. Goldrich, J. R. Chapman, B. M. Uberheide, D. Lim; *Synth. Comm.* **2015**, 45, 643-650.

General procedure 1: Reduction of 4-substituted benzaldehydes

A 4-substituted benzaldehyde (1.00 eq.) was dissolved in analytical grade *i*-prOH (12.0 eq.). Al(O*i*-Pr)$_3$ (1.00 eq.) was added to the solution. The mixture was stirred at r.t. for 22 h until TLC showed no remaining starting modified benzaldehyde. Water was added and the mixture was extracted with Et_2O. The org. layer was washed with H_2O (3 x) and dried over Mg_2SO_4. Evaporation of the solvent delivered a crude product which was purified by chromatography (SiO_2, EtOAc:pentane, 4:1) to afford modified benzyl alcohols as yellowish oils.

Synthesis of allyl (4-(hydroxymethyl)phenyl) carbonate

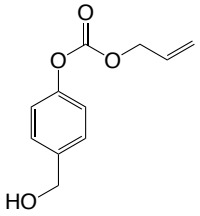

The product was synthetized according to the general procedure 1. 10.2 g (49.7 mmol, 1.00 eq) of allyl (4-formylphenyl) carbonate, 35.8 g (0.596 mol, 12.0 eq.) of *i*-prOH, 13.2 g (64.6 mmol, 1.00 eq.) of Al(O*i*-Pr)$_3$. Yield: 9.04 g, 43.4 mmol, 87 %

TLC (EtOAc:Hexane, 2:3 v/v): $\mathbf{R_f}$ = 0.36; **^{1}H-NMR** (500 MHz, DMSO-d_6): δ 7.36 (d, *J* = 7.5 Hz, 2H), 7.18 (d, *J* = 7.5 Hz, 2H), 6.10 - 5.90 (m, 1H), 5.40 (dq, *J* = 17.4, 1.6 Hz, 1H), 5.31 (dq, *J* = 10.5, 1.4 Hz, 1H), 5.22 (t, *J* = 5.7 Hz, 1H), 4.72 (dd, *J* = 5.2, 1.9 Hz, 2H), 4.50 (d, *J* = 5.7 Hz, 2H); **^{13}C-NMR** (126 MHz, DMSO-d_6): δ 153.4, 149.9, 140.9, 132.3, 128.0, 121.3, 119.3, 69.1, 62.8; **IR** (neat, cm^{-1}): 2926.2, 2354.4, 1754.1, 1694.0, 1611.6, 1414.7, 1352.1, 1292.4, 1215.3, 1144.1, 743.9, 654.1; **HRMS** (ESI) $[M+Na]^+$ calcd for $C_{11}H_{12}NaO_4$, 231.0628; found, 231.0628

Synthesis of *tert*-butyl (4-(hydroxymethyl)phenyl) carbonate

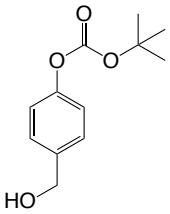

The product was synthetized according to the general procedure 1. 1 g (4.50 mmol, 1.00 eq) of *tert*-butyl (4-formylphenyl) carbonate, 3.24 g (54.1 mmol, 12.0 eq.) of *i*-prOH, 1.01 g (4.50 mmol, 1.00 eq.) of Al(O*i*-Pr)$_3$. Yield: 0.969 g, 4.32 mmol, 96 %

TLC (EtOAc:Hexane, 2:3 v/v): $\mathbf{R_f}$ = 0.41; **^{1}H-NMR** (500 MHz, $CDCl_3$): δ 7.38 (d, *J* = 8.4 Hz, 2H), 7.18 (d, *J* = 8.6 Hz, 2H), 4.69 (s, 2H), 1.76 (s, 1H), 1.58 (s, 9H); **^{13}C-NMR** (126 MHz, $CDCl_3$): δ 151.9, 150.6, 138.4, 127.9, 121.3, 83.5, 77.3, 77.2, 77.0, 76.7, 64.7, 60.4, 27.7, 14.2; **IR** (neat, cm^{-1}): 2936.2, 2352.1, 1744.3, 1695.1, 1612.5, 1444.7, 1352.1, 1232.1, 1146.3, 756.2; **HRMS** (ESI) $[M+Na]^+$ calcd for $C_{12}H_{16}NaO_4$, 247.0941; found, 247.0940

General procedure 2: Synthesis of phosphoramidites

The modified benzyl alcohol (2.10 eq.) was dissolved in dry THF and cooled in an ice bath. Et_3N (2.20 eq.) was slowly added. After 1 hour, (dichlorophosphanyl)bis(propan-2-yl)amine (1.00 eq.) was added. Reaction progress was followed by ^{31}P NMR spectroscopy. After 1.2 to 2 hours, dry Et_2O was added in order to completely precipitate the formed salt. The precipitate was removed by filtration and the solvent was evaporated under reduced pressure. The phosphoramidites were obtained as a yellowish oil.

Synthesis of Bis-AllocB P-amidite

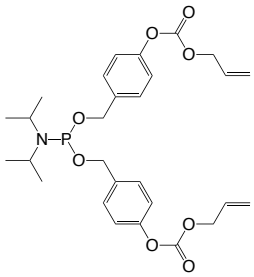

Bis-AllocB P-amidite was synthetized according to general procedure 2. 6.69 g (32.1 mmol, 2.10 eq.) of benzyl alcohol, 3.41 g (33.7 mmol, 2.20 eq.) Et_3N, 3.10 g (15.3 mmol, 1.00 eq.) (dichlorophosphanyl)bis(propan-2-yl)amine, THF (125 mL), Et_2O (80 mL). Yield: 8.25 g, 5.15 mmol, 99%

TLC (EtOAc:Hexane, 1:4 v/v): $\mathbf{R_f}$ = 0.45; **^{1}H-NMR** (400 MHz, $CDCl_3$): δ 7.33 (d, *J* = 8.6 Hz, 4H), 7.12 (d, *J* = 8.5 Hz, 4H), 5.98 (ddt, *J* = 17.2, 10.4, 5.8 Hz, 2H), 5.41 (dd, *J* = 17.3, 1.5 Hz, 2H), 5.31 (dd, *J* = 10.5, 1.2 Hz, 2H), 4.76 – 4.68 (m, 6H), 4.68 (s, 1H), 4.66 (s, 1H), 3.74 – 3.60 (m, 2H), 1.18 (d, *J* = 6.8 Hz, 12H); **^{13}C-NMR** (101 MHz, $CDCl_3$) δ 153.7, 150.5, 137.6, 131.4, 128.2, 121.6, 121.0, 119.7, 110.2, 77.5, 77.4, 77.2, 76.9, 69.3, 66.1, 65.1, 64.9, 43.4, 43.3, 24.9, 24.8, 15.5; **^{31}P{1H}-NMR** (162 MHz, $CDCl_3$): δ 149.01; **^{31}P-NMR** (162 MHz, $CDCl_3$): δ 149.00 (h, *J* = 8.7 Hz); **IR** (neat, cm^{-1}): 2962.5, 1465.2,1180.2, 1047.3, 760.8, 720.1, 433.3; **HRMS** (ESI) $[M+Na]^+$ calcd for $C_{28}H_{36}NNaO_8P$, 568.2071; found, 568.2078.

Synthesis of Bis-BocB P-amidite

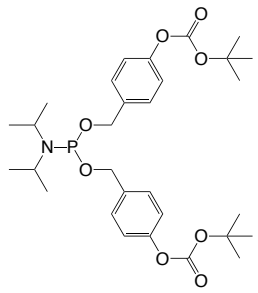

Bis-BocB P-amidite was synthetized according to general procedure 2. 1.90 g (8.47 mmol, 2.10 eq.) of modified benzyl alcohol, 0.896 g (8.87 mmol, 2.20 eq.) Et_3N, 0.816 g (4.03 mmol, 1.00 eq.) (dichlorophosphanyl)bis(propan-2-yl)amine, THF (20 mL), Et_2O (10 mL). Yield: 2.27 g, 3.94 mmol, 98%

TLC (EtOAc:Hexane, 1:4 v/v): $\mathbf{R_f}$ = 0.50; **^{1}H-NMR** (400 MHz, $CDCl_3$): 7.38 (d, *J* = 8.4 Hz, 4H), 7.16 (d, *J* = 8.4 Hz, 4H), 4.85 – 4.68 (m, 4H), 3.81 – 3.62 (m, 2H), 1.59 (s, 9H), 1.23 (d, *J* = 6.8 Hz, 12H); **^{13}C-NMR** (126 MHz, $CDCl_3$) δ 151.87, 150.30, 137.02, 136.96, 127.93, 120.99, 83.34, 64.91, 64.77, 43.24, 43.14, 27.71, 24.65, 24.59; **^{31}P{1H}-NMR** (162 MHz, $CDCl_3$): δ 149.25; **^{31}P-NMR** (162 MHz, $CDCl_3$): δ 149.24 (h, *J* = 8.76, 7.96 Hz); **IR** (neat, cm^{-1}): 2972.8, 1501.3, 1047.3, 997.1, 734.0, 489.3; **HRMS** (ESI) $[M+Na]^+$ calcd for $C_{30}H_{44}NNaO_8P$, 600.2697; found, 600.2694.

Synthesis of 11

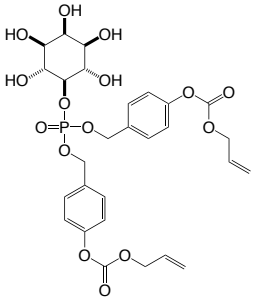

A) 1.97 g (3.13 mmol, 1.00 eq.) **9** and 2.05 g (3.75 mmol, 1.20 eq) AllocB-PA were dissolved in dry MeCN (8 mL). 480 mg (4.07 mmol, 1.30 eq) of DCI was added and mixture was stirred for 15 minutes at room temperature. Progress of the reaction was monitored by ^{31}P NMR spectroscopy. Oxidation was achieved by addition of 1.72 mL (15.7 mmol, 5.00 eq, solution in nonane) *t*-BuOOH. The solvent was evaporated and the obtained crude oil was directly used in the next step.
B) The intermediate was dissolved in DCM (100 mL) and 5% of TFA (5 ml) and stirred for 45 min at room temperature (color change to red). The reaction was monitored by TLC and ^{31}P NMR. After completion of the reaction, the solution was concentrated *in vacuo* and a precipitate was formed upon addition of Et_2O. Filtration gave the pure product as a white solid **11** (1.88 g, 2.94 mmol, 78 % yield).
TLC (CH_2Cl_2:MeOH, 8:1 v/v): $\mathbf{R_f}$ = 0.27; **^{1}H-NMR** (500 MHz, DMSO-d_6): δ 7.46 (d, *J* = 8.2 Hz, 4H), 7.24 (d, *J* = 8.3 Hz, 4H), 6.01 (ddt, *J* = 16.4, 10.9, 5.6 Hz, 2H), 5.41 (dt, *J* = 17.1, 1.5 Hz, 2H), 5.32 (d, *J* = 10.5 Hz, 2H), 5.12 (d, *J* = 6.9 Hz, 3H), 5.06 – 4.94 (m, 1H), 4.74 (d, *J* = 5.6 Hz, 4H), 4.03 (q, *J* = 9.2 Hz, 1H), 3.75 (d, *J* = 2.6 Hz, 1H), 3.65 (t, *J* = 9.5 Hz, 2H), 3.26 (dd, *J* = 9.7, 2.7 Hz, 2H); **^{13}C-NMR** (126 MHz, DMSO-d_6): δ 152.7, 150.4, 134.7 (d, *J* = 8.1 Hz), 131.7, 129.1, 121.1, 118.9, 83.4 (d, *J* = 7.2 Hz), 72.4, 71.5, 71.3 (d, *J* = 2.7 Hz), 68.7, 67.4 (d, *J* = 5.1 Hz), 30.9, 28.5, 22.0, 13.9; **^{31}P{1 H}-NMR** (162 MHz, DMSO-d_6): δ -0.46 (s); **^{31}P-NMR** (162 MHz, DMSO-d_6): δ -0.45 (h, *J* = 7.7 Hz); **IR** (neat, cm-1) 3335.9, 2944.1, 1758.6, 1725.6, 1686.1, 1371.5, 1169.1, 1132.4, 1019.2, 738.4; **HRMS** (ESI) $[M+Na]^+$ calcd for $C_{28}H_{33}NaO_{15}P$, 663.1449; found, 663.1452.

Synthesis of 12

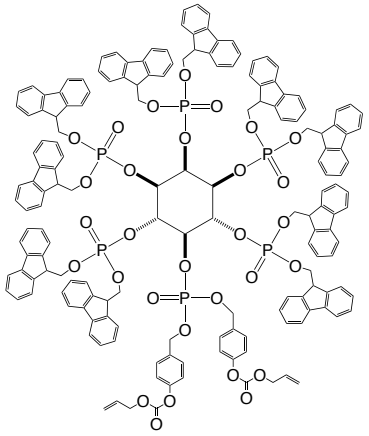

100 mg (0.156 mmol, 1.00 eq.) of inositol monophosphate **11** and 0.851 g (1.56 mmol, 10.0 eq.) of bis 9-fluorenylmethyl phosphoramidite (Fm-PA) were coevaporated with dry MeCN (2 mL). The residue was dissolved in dry THF (4 mL). To this solution, 276 mg (2.43 mmol, 15.0 eq.) of DCI were added. Progress of the reaction was monitored by ^{31}P-NMR. After completion of the reaction (30-45 min), oxidation was achieved by slow (!) addition of 378 mg (1.56 mmol, 10.0 eq.) mCPBA (70% moistened with water) at 0ºC. The mixture was concentrated *in vacuo* and the product was precipitated by addition of MeOH (2 x 5 ml) yielding 405 mg of **12** as a white sticky solid (0.143 mmol, 92%).
TLC (EtOAc:Hexane, 3:2 v/v): $\mathbf{R_f}$ = 0.35; **^{1}H-NMR** (400 MHz, $CDCl_3$): δ 7.96 (s, 3H), 7.84 (s, 3H), 7.73 – 7.62 (m, 1H), 7.61 – 7.39 (m, 24H), 7.37 (s, 4H), 7.33 – 7.27 (m, 5H), 7.28 – 7.09 (m, 21H), 7.09 (s, 4H), 7.04 – 6.89 (m, 20H), 6.86 (s, 3H), 5.94 (ddt, *J* = 16.6, 10.9, 5.4 Hz, 1H), 5.76 (d, *J* = 9.7 Hz, 1H), 5.38 (dd, *J* = 17.2, 3.9 Hz, 2H), 5.28 (dd, *J* = 10.8, 3.9 Hz, 2H), 5.25 – 5.09 (m, 2H), 4.97 – 4.86 (m, 2H), 4.68 (q, *J* = 8.2, 4.8 Hz, 6H), 4.63 – 4.50 (m, 3H), 4.46 – 4.34 (m, 2H), 4.35 – 4.24 (m,

8H), 4.08 – 3.82 (m, 7H), 3.82 – 3.69 (m, 3H), 2.88 (dd, *J* = 16.8, 4.0 Hz, 1H); **^{13}C-NMR** (101 MHz, $CDCl_3$): δ 169.2, 151.5, 143.8 - 143.2 (m), 141.8 - 141.6 (m), 134.9, 133.7, 132.2, 131.7, 130.6, 130.2, 129.8, 128.7 - 127.4 (m), 126.2 - 125.7 (m), 121.5, 120.4 - 120.0 (m), 74.0, 70.7, 69.6, 48.4, 22.9; **^{31}P{1 H}-NMR** (162 MHz, $CDCl_3$) δ 0.50 (s), 0.03 (s), -0.53 (s), -1.85 (s); **^{31}P-NMR** (162 MHz, $CDCl_3$): δ 0.62 – 0.37 (m), 0.07 – -0.09 (m), -0.42 – -0.61 (m), -1.71 – -1.95 (m); **IR** (neat, cm-1) 2923.3, 2823.5, 2352.1, 2351.9, 1739.3, 1446.2, 1229.4, 1040.1, 983.6; **HRMS** (ESI) $[M+2Na]^{2+}$ calcd for $C_{168}H_{138}Na_2O_{30}P_6$, 1433.8758; found, 1433.8775.

Synthesis of 13

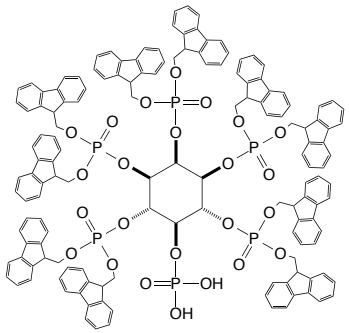

100 mg (35.5 μmol, 1.00 eq.) of hexakisphosphate **12** were dissolved in a mixture of dry CH_2Cl_2 (3 mL) and MeOH (2 mL). 1 mg of $PdCl_2$ (5.65 μmol, 0.160 eq.) was added. The reaction mixture was stirred overnight at room temperature under N_2. Progress was monitored by ^{31}P-NMR spectroscopy. The reaction mixture was concentrated *in vacuo* and the residue was dissolved in EtOAc (5 mL). $PdCl_2$ was removed by filtration over celite and cotton. The filtrate was concentrated *in vacuo* and the product was precipitated by addition of MeOH. The crude material **13** was obtained as a sticky white solid (80 mg, 92%) and it was used directly in the next step.
TLC (CH_2Cl_2:MeOH; 10:1): $\mathbf{R_f}$ = 0.4; **^{31}P{1 H}-NMR** (203 MHz, $CDCl_3$): δ -1.73 (s), -1.36 (s), -1.95 (s); **^{31}P-NMR** (203 MHz, $CDCl_3$): δ 1.73 (d, *J* = 17.1 Hz), -1.12 – -1.54 (m), -1.80 – -2.10 (m); **HRMS** (ESI) $[M]^-$ calcd for $C_{146}H_{118}O_{24}P_6$, 2440.6439; found, 2440.6458.

Synthesis of 14

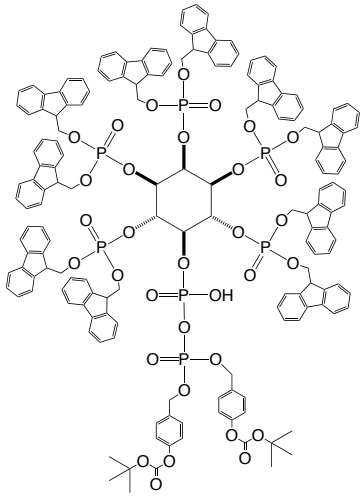

30.0 mg (12.3 μmol, 1.00 eq.) of crude hexakisphosphate **13** were dissolved in dry CH_2Cl_2 (2 mL). Bis-BocB phosphoramidite (BocB-PA) 14.2 mg (24.6 μmol, 2.00 eq) were added and the mixture was coevaporated with MeCN (2x). The dry mixture was dissolved in CH_2Cl_2 (2 mL) and DCI 3.00 mg (24.6 μmol, 2.00 eq.) was added. The mixture was stirred for 15 minutes. Progress of the reaction was monitored by ^{31}P-NMR spectroscopy. After completion of the reaction, oxidation was achieved by slow (!) addition of 6.00 mg (24.6 μmol, 2.00 eq) *m*CPBA (70% moistened with water).
The reaction mixture was concentrated and MeOH (3 ml) was added. A white precipitate was formed and it was isolated by centrifugation. The solvent was removed and the precipitate was purified by

column chromatography (CH_2Cl_2:MeOH; 10:0.1 to CH_2Cl_2:MeOH; 10:0.5), yielding 21.4 mg **14** as a white sticky solid (7.29 µmol, 60%).

TLC (CH_2Cl_2:MeOH; 10:1): $\mathbf{R_f}$ = 0.60; **^{1}H-NMR** (500 MHz, $CDCl_3$): δ 7.72 – 7.63 (m, 3H), 7.62 – 7.30 (m, 26H), 7.25 (d, *J* = 7.7 Hz, 6H), 7.20 – 6.94 (m, 27H), 6.92 – 6.67 (m, 21H), 6.66 – 6.52 (m, 5H), 5.71 (d, *J* = 8.9 Hz, 1H), 5.17 – 5.01 (m, 4H), 4.88 – 4.73 (m, 5H), 4.33 (s, 7H), 4.15 – 3.55 (m, 23H), 1.58 (s, 18H); **^{13}C-NMR** (126 MHz, $CDCl_3$): δ 151.4, 150.7, 143.2, 142.8, 141.3, 141.0, 132.2, 128.6, 127.7 - 126.7 (m), 125.5, 125.2, 120.9, 83.1, 77.3, 77.2, 77.0, 76.7, 75.9, 73.2, 69.7, 69.2, 53.4, 50.9, 47.5, 29.7, 27.7, 27.7; **^{31}P{1 H}-NMR** (203 MHz, $CDCl_3$): δ -0.18 (s), -1.54 (s), -2.88 (s), -9.79 (s), -10.78 (s); **^{31}P-NMR** (203 MHz, $CDCl_3$): δ 0.81 – -0.81 (m), -0.03 – -1.80 (m), -2.35 – -3.28 (m), -9.56 – -10.00 (m), -10.49 – -11.04 (m); **IR** (neat, cm-1) 3036.1, 2944.2, 2438.3, 1728.3, 1614.2, 1451.5, 1284.3, 1036.1, 992.7; **HRMS** (ESI) $[M]^-$ calcd for $C_{170}H_{147}NO_{33}P_7$, 2932.7988; found, 2932.7973.

Synthesis of 15

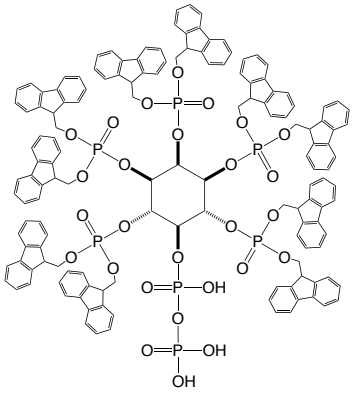

20.0 mg (6.82 µmol, 1.00 eq.) of protected 5-PP-IP_5 **14** were dissolved in dry CH_2Cl_2 (2 mL). TFA 4.20 µL (54.6 µmol, 8.00 eq.) was added. (!) A larger amount of TFA causes partial or complete cleavage of the phosphoric anhydride (!). The mixture was stirred for 20 hours. Progress of the reaction was monitored by ^{31}P-NMR. After completion, the reaction mixture was concentrated *in vacuo* and MeOH (3 ml) was added. A colorless precipitate was formed and it was isolated by centrifugation yielding the crude material **15** as a yellowish sticky solid: 15.0 mg (5.95 µmol, 87%).

TLC (CH_2Cl_2:MeOH; 10:1): $\mathbf{R_f}$ = 0.30; **^{31}P{1 H}-NMR** (162 MHz, $CDCl_3$): δ -1.62 (s), -2.85 (s), -9.13 (s), -11.74(s); **^{31}P-NMR** (203 MHz, $CDCl_3$): δ -0.74 – -2.29 (m), -2.54 – -3.80 (m), -8.82 – -10.38 (m), -11.40 – -13.32 (m); **HRMS** (ESI) $[M]^{2-}$ calcd for $C_{146}H_{119}O_{27}P_7$, 1259.7995; found, 1259.7278.

Synthesis of 16

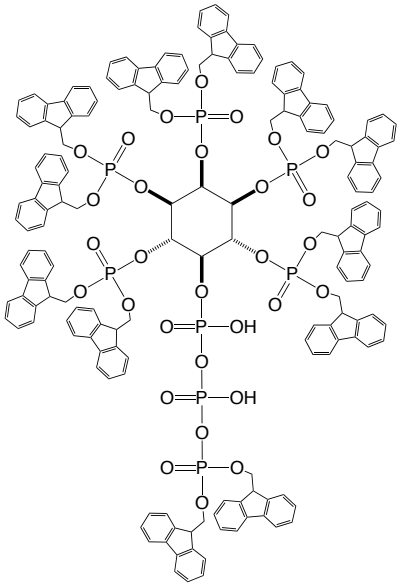

15.0 mg (5.95 µmol, 1.00 eq.) of crude **15** were dissolved in dry CH_2Cl_2 (2 mL). 7.00 mg 9-fluorenylmethyl phosphoramidite (Fm-PA) (11.9 µmol, 2.00 eq) were added and the mixture was coevaporated twice with MeCN (2x). The dry mixture was dissolved in CH_2Cl_2 (2 mL) and 2.81 mg DCI (23.8 µmol, 4.00 eq.) were added. The reaction was stirred for 45 minutes. Progress of the reaction was monitored by ^{31}P-NMR spectroscopy. After completion of the reaction, oxidation was achieved by slow (!) addition of 2.92 mg (11.9 µmol, 2.00 eq) *m*CPBA (70% moistened with water).
The reaction mixture was concentrated and MeOH (3 ml) was added. A colorless precipitate was formed which was isolated by centrifugation. The solvent was removed and the precipitate was purified by column chromatography (CH_2Cl_2:MeOH; 10:0.1 to CH_2Cl_2:MeOH; 10:0.5), yielding 6.50 mg **16** as a yellowish sticky solid (2.19 µmol, 37%).

TLC (CH_2Cl_2:MeOH; 10:1): $\mathbf{R_f}$ = 0.60; **^{1}H-NMR** (500 MHz, $CDCl_3$): δ 7.85 – 7.31 (m, 42H), 7.27 – 6.62 (m, 54H), 4.71 – 3.52 (m, 42H);**^{13}C-NMR** (126 MHz, $CDCl_3$): δ 162.6, 141.1, 127.6, 127.1, 126.9, 125.3, 120.0, 119.7, 92.9, 80.8, 77.3 - 76.8 (m), 74.5, 73.9, 69.9, 50.8, 50.8, 47.7, 36.5, 31.5, 31.5, 29.7, 29.7, 25.8, 19.1; **^{31}P{1 H}-NMR** (203 MHz, $CDCl_3$): δ 2.14 – -7.21 (m), -8.99 – -17.15 (m), -18.81 – -28.28 (m); **^{31}P-NMR** (203 MHz, $CDCl_3$): δ 0.84 – -6.86 (m), -8.51 – -16.68 (m), -19.28 – -28.75 (m); **IR** (neat, cm-1) 3030.8, 2964.2, 1652.1, 1531.6, 1449.4, 1254.4, 1078.1, 898.3; **HRMS** (ESI) $[M]^{2-}$ calcd for $C_{174}H_{138}O_{30}P_8$, 1477.8609; found, 1477.8626.

Synthesis of 7

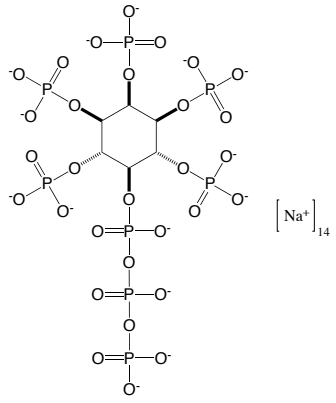

6.50 mg (2.19 µmol, 1.00 eq.) of **16** were dissolved in DMF (1.5 mL) and piperidine (0.250 ml) was added. The solution was stirred 1 hour at room temperature. After completion of the deprotection, the solution was concentrated and the product precipitated with Et_2O (5 mL). The precipitate was isolated by centrifugation. The precipitate was dissolved in MeOH and crystallized by addition of Et_2O. The

centrifugation process was repeated and yellowish crystals were obtained that were dried *in vacuo*. The piperidinium counter ions were exchanged to sodium by addition of excess NaI to a methanolic solution of **7**. After 30 minutes of stirring, the sodium salt of **7** precipitated. This procedure removed the majority of piperidinium counterions, but a small amount of piperidinium resonances was still observed in the proton NMR. The salt was isolated by centrifugation and dried yielding 1.51 mg of **11** (6.98 μmol, 61%).

^{1}H-NMR (400 MHz, D_2O): δ 4.85 (dd, *J* = 14.5, 6.4 Hz, 1H), 4.53 (dd, *J* = 18.9, 8.6 Hz, 2H), 4.33 (dd, *J* = 17.9, 8.7 Hz, 1H), 4.22 (dd, *J* = 11.2, 7.3 Hz, 2H), 3.17 (piperidine), 1.78 (piperidine) 1.67 (piperidine); **^{13}C-NMR** (126 MHz, D_2O): δ 77.6, 76.0, 75.7, 73.3, 48.9 (MeOH), 36.90 (piperidine), 31.38 (piperidine), 22.22 (piperidine); **^{31}P{1 H}-NMR** (162 MHz, D_2O): δ ^{31}P NMR (203 MHz, Deuterium Oxide) δ 2.39 – 1.27 (m), 0.92 – -0.42 (m), -5.40 (s), -10.30 (s), -18.33 – -19.67 (m); **^{31}P-NMR** (203 MHz, D_2O): δ 2.33 – 1.20 (m), 0.88 – -0.56 (m), -4.94 – -6.06 (m), -9.81 – -11.19 (m), -18.20 – -20.01 (m); **IR** (neat, cm-1): 3461.3, 3431.4, 2996.1, 2941.3, 1673.6, 1636.9, 1111.1, 953.8; **HRMS** (ESI) $[M+K]^{3-}$ calcd for $C_6H_{16}KO_{30}P_8$, 284.9094; found, 284.9075.

1H

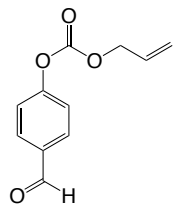

10.01
8.01
7.99
7.51
7.49
6.05
6.04
6.03
6.03
6.02
6.02
6.01
6.01
6.00
5.99
5.98
5.97
5.44
5.44
5.44
5.44
5.41
5.41
5.40
5.40
5.34
5.33
5.33
5.33
5.32
5.31
5.31
5.31
4.77
4.77
4.76
4.76
4.75
4.75
A (s) 10.01
B (d) 8.00
C (d) 7.50
D (m) 6.01
E (dq) 5.42
F (dq) 5.32
G (dt) 4.76
1.00
2.03
2.00
0.97
1.01
1.01
1.99
12.5
12.0
11.5
11.0
10.5
10.0
9.5
9.0
8.5
8.0
7.5
7.0
6.5
6.0
5.5
5.0
4.5
4.0
3.5
3.0
2.5
2.0
1.5
1.0
0.5
0.0
-0.5
f1 (ppm)

13C

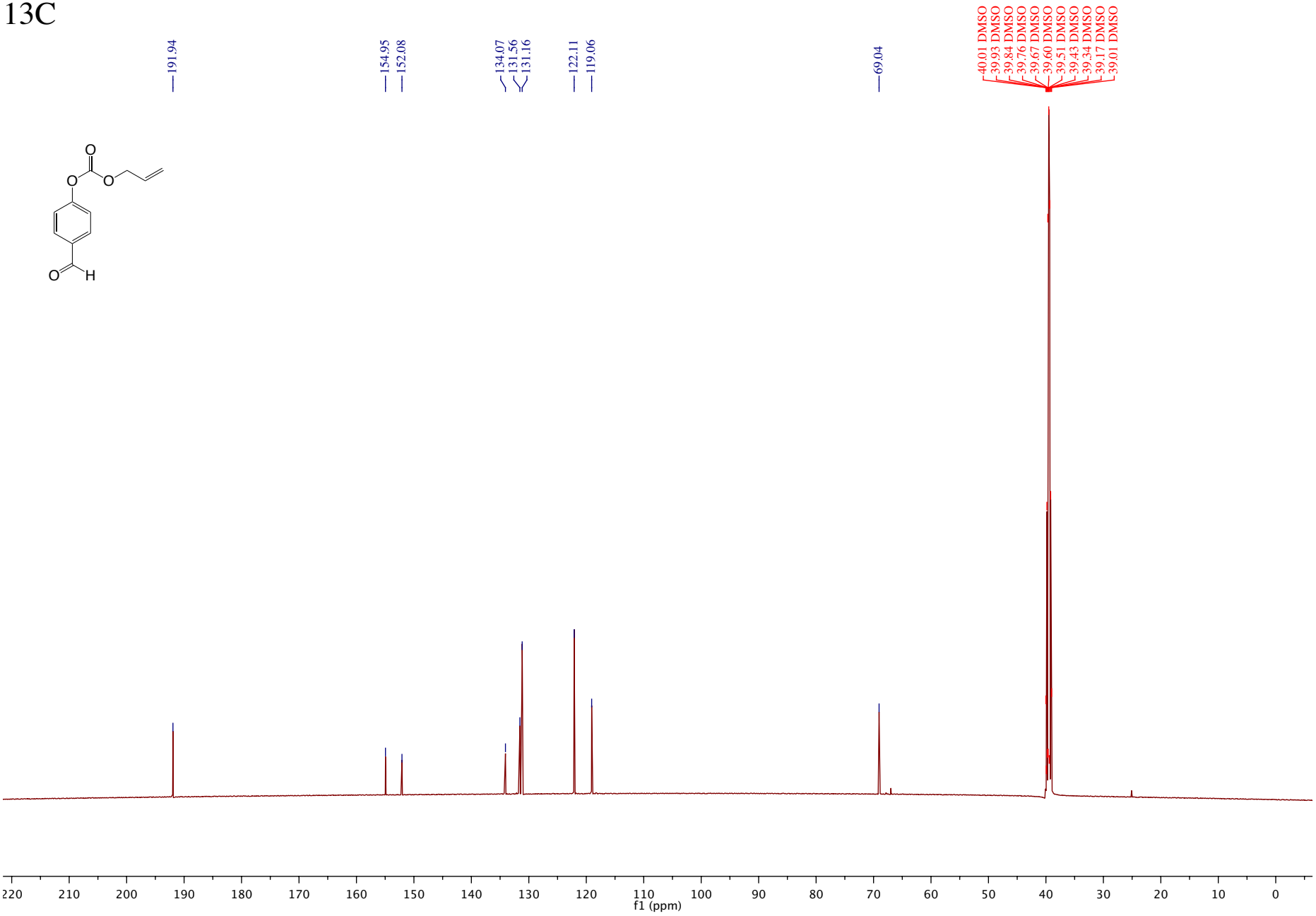
191.94
154.95
152.08
134.07
131.56
131.16
122.11
119.06
69.04
40.01 DMSO
39.93 DMSO
39.84 DMSO
39.76 DMSO
39.67 DMSO
39.60 DMSO
39.51 DMSO
39.43 DMSO
39.34 DMSO
39.17 DMSO
39.01 DMSO
O
O
O
O
H
220
210
200
190
180
170
160
150
140
130
120
110
100
90
80
70
60
50
40
30
20
10
0
f1 (ppm)

D:\Data\Service\Data\siQEx2191 03/04/16 15:32:46 Sample: RC13
Client: Pavlovic (+)-HR-ESI-MS Solvent: MeOH

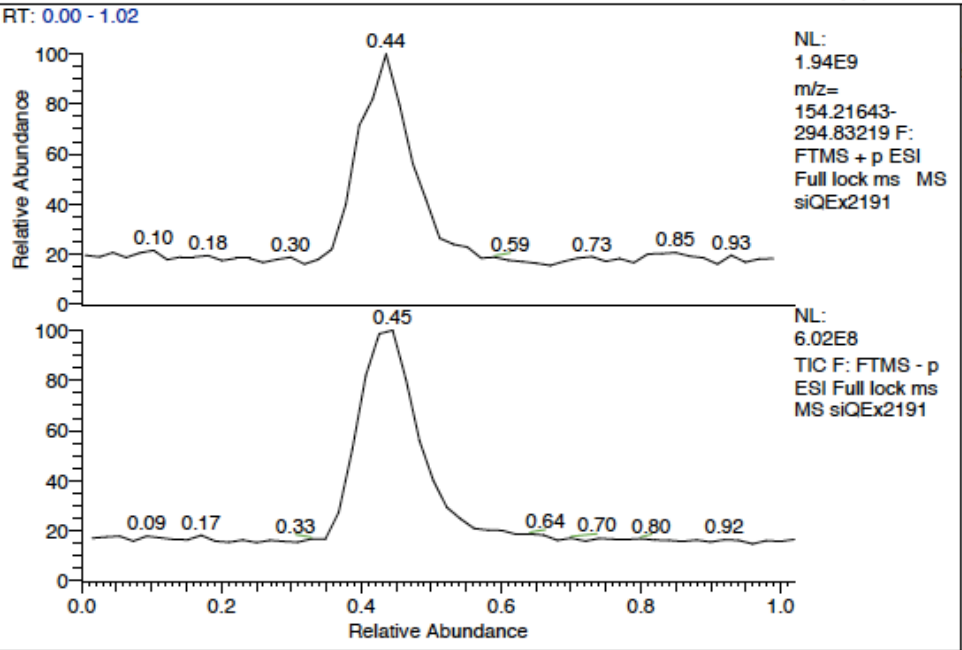

siQEx2191#37-53 RT: 0.36-0.51 AV: 9
SB: 25 0.07-0.29 , 0.70-0.98
T: FTMS + p ESI Full lock ms [50.00-750.00]
m/z= 217.19618-281.49643

m/z	Intensity	Relative	Theo. Mass	Delta (ppm)	RDB equiv.	Composition
221.08088	64860396.0	19.83	221.08084	0.20	6.5	$C_{12}H_{13}O_4$
			221.07843	11.08	3.5	$C_{10}H_{14}O_4Na$
261.07327	327073248.0	100.00	261.07334	-0.27	5.5	$C_{12}H_{14}O_5Na$
			261.07575	-9.48	8.5	$C_{14}H_{13}O_5$
			261.06988	13.01	17.5	$C_{21}H_9$
262.07662	43021120.0	13.15	262.07770	-4.14	17.0	$C_{21}H_{10}$
			262.07530	5.04	14.0	$C_{19}H_{11}Na$
277.04722	56076736.0	17.15	277.04713	0.33	10.5	$C_{15}H_{10}O_4Na$
			277.04954	-8.35	13.5	$C_{17}H_9O_4$

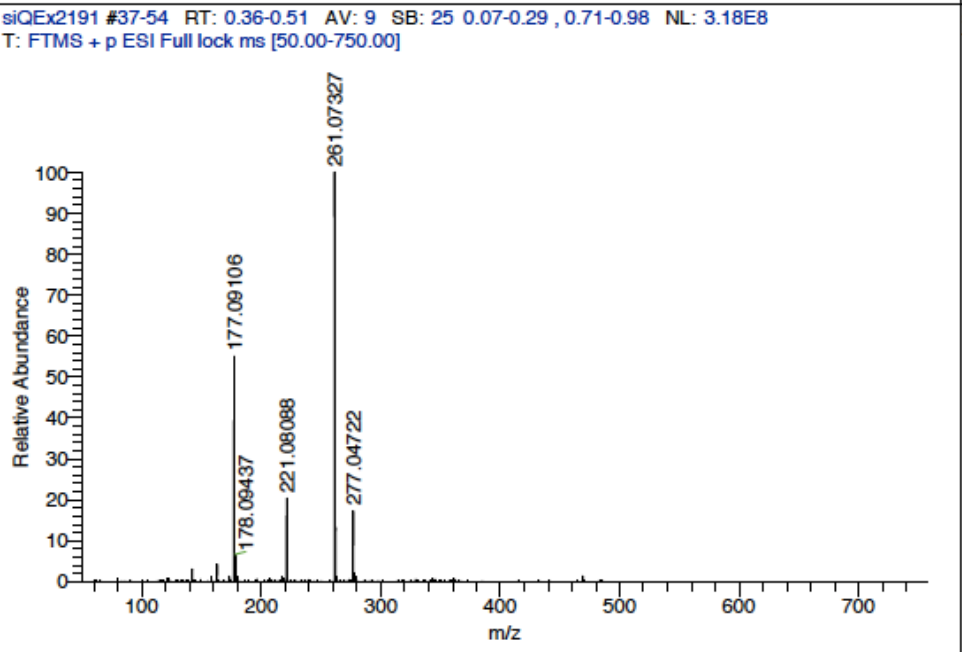

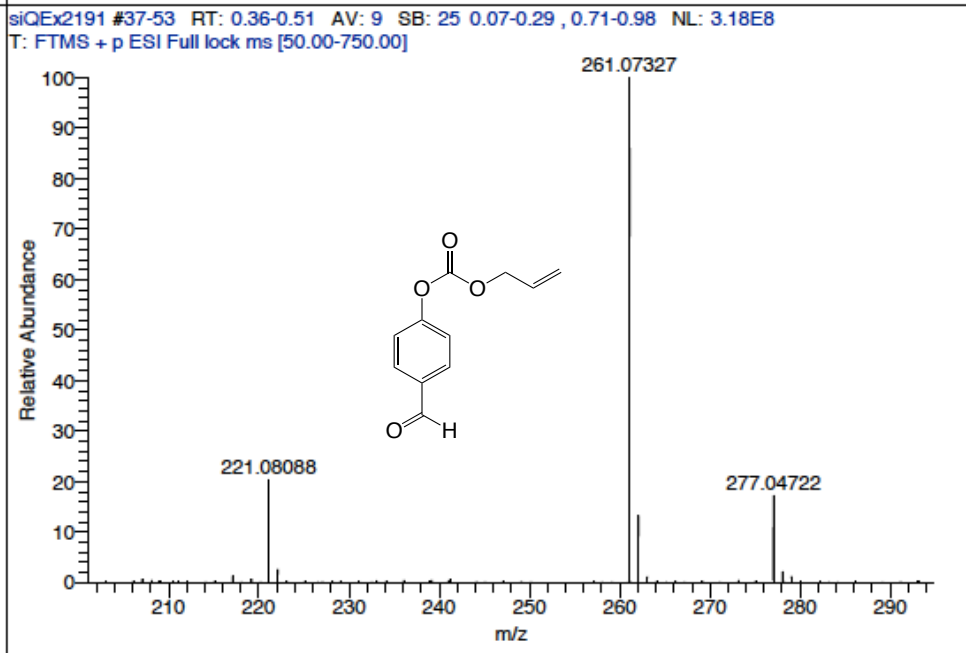

1H

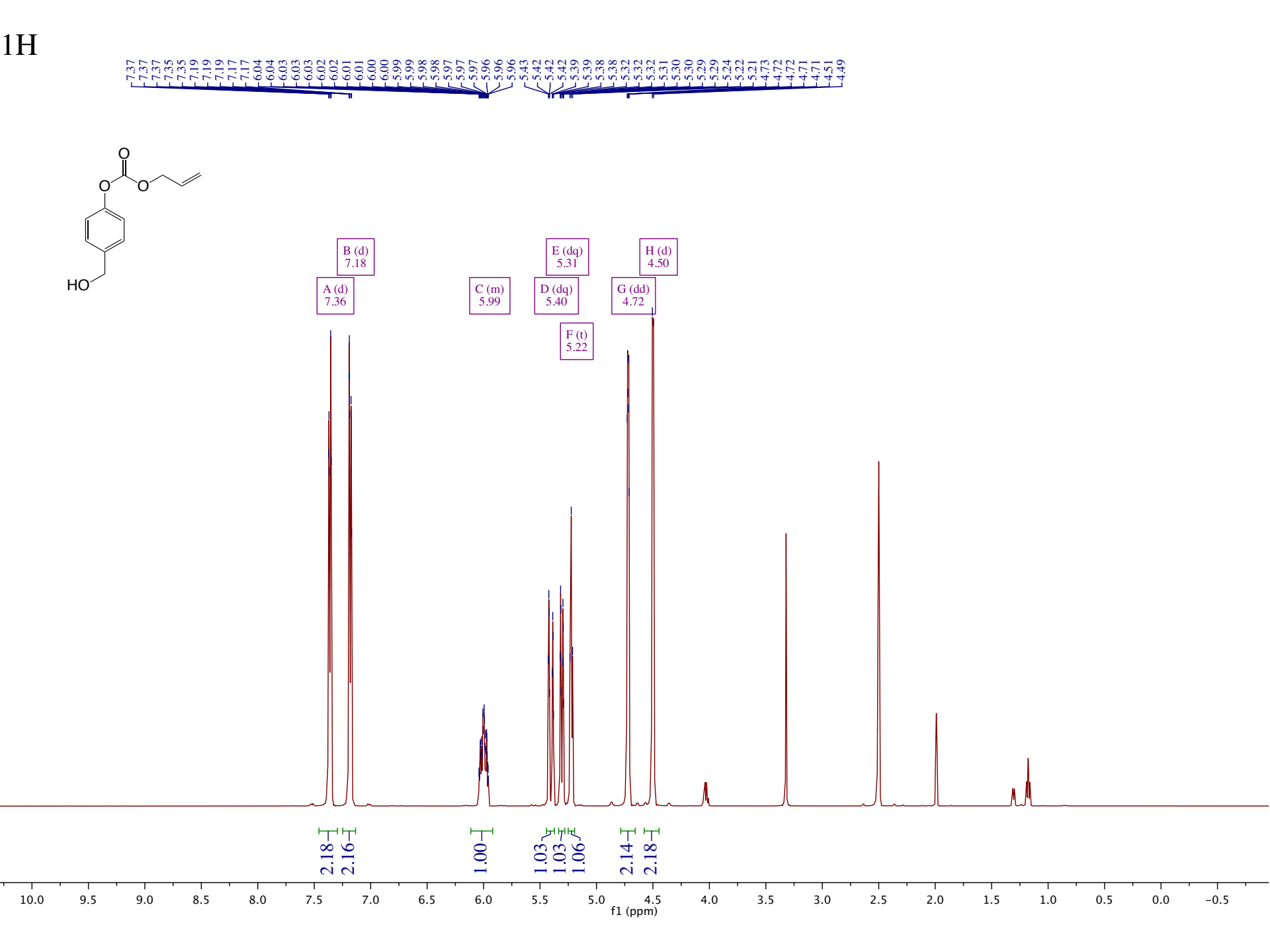
7.37 7.37 7.37 7.35 7.35 7.19 7.19 7.19 7.17 7.17 6.04 6.04 6.03 6.03 6.03 6.02 6.02 6.01 6.01 6.00 6.00 5.99 5.99 5.98 5.98 5.97 5.97 5.97 5.96 5.96 5.96 5.43 5.42 5.42 5.42 5.39 5.39 5.38 5.38 5.32 5.32 5.32 5.31 5.30 5.30 5.29 5.29 5.24 5.22 5.21 4.73 4.72 4.72 4.71 4.71 4.51 4.49
O
O
O
HO
A (d) 7.36
B (d) 7.18
C (m) 5.99
D (dq) 5.40
E (dq) 5.31
F (t) 5.22
G (dd) 4.72
H (d) 4.50
2.18
2.16
1.00
1.03
1.03
1.06
2.14
2.18
10.0 9.5 9.0 8.5 8.0 7.5 7.0 6.5 6.0 5.5 5.0 4.5 4.0 3.5 3.0 2.5 2.0 1.5 1.0 0.5 0.0 -0.5
f1 (ppm)

13C

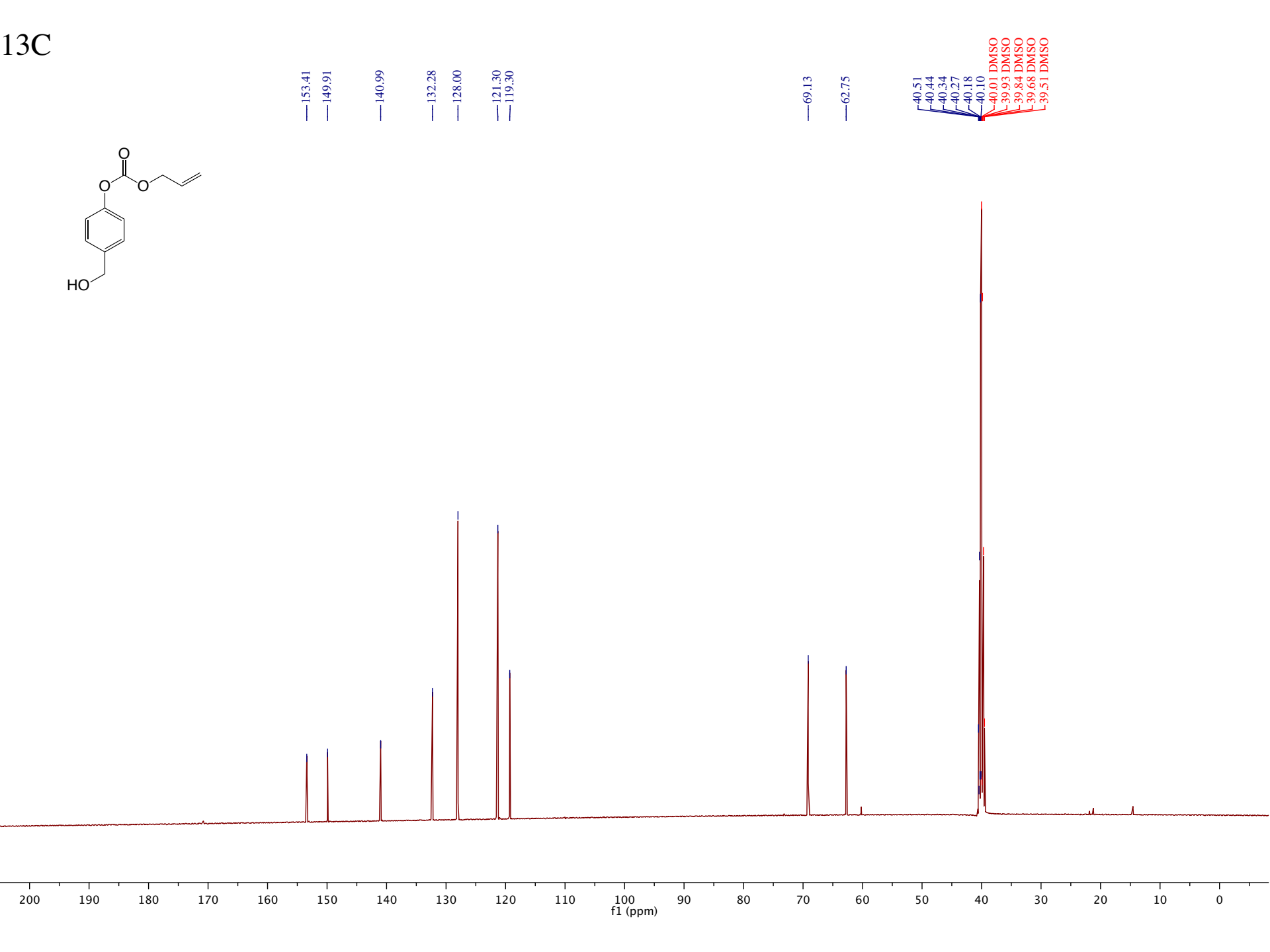
153.41
149.91
140.99
132.28
128.00
121.30
119.30
69.13
62.75
40.51
40.44
40.34
40.27
40.18
40.10
40.01 DMSO
39.93 DMSO
39.84 DMSO
39.68 DMSO
39.51 DMSO
O
O
O
HO
200
190
180
170
160
150
140
130
120
110
100
90
80
70
60
50
40
30
20
10
0
f1 (ppm)

D:\Data\Service\Data\siQEx2192 03/04/16 15:34:47 Sample: RC16
Client: Pavlovic (+)-HR-ESI-MS Solvent: MeOH

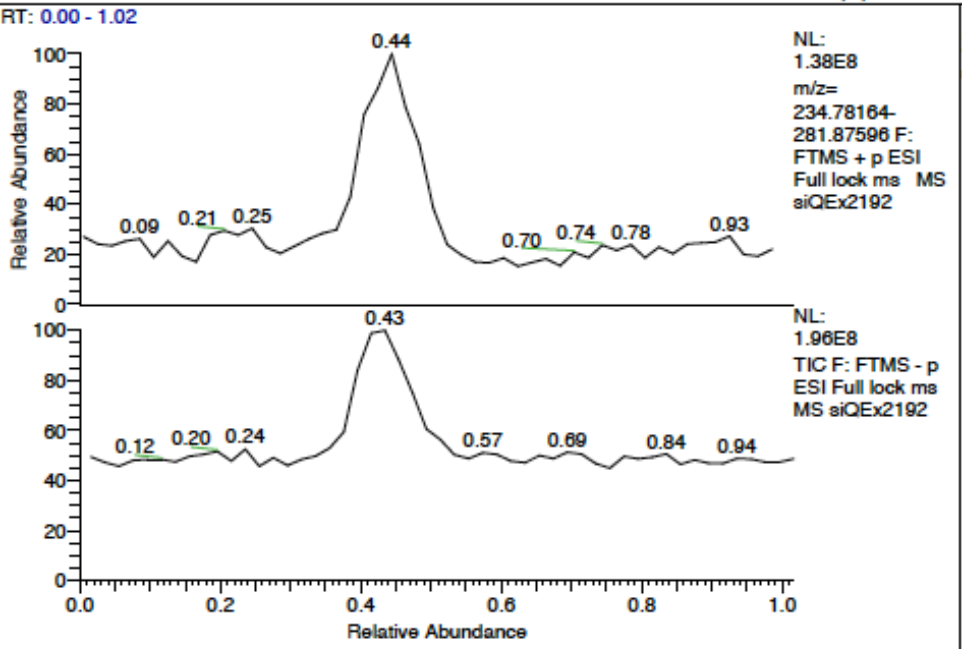

siQEx2192#37-49 RT: 0.37-0.48 AV: 7
SB: 25 0.07-0.29 , 0.71-0.98
T: FTMS + p ESI Full lock ms [50.00-750.00]
m/z= 230.76270-231.47077

m/z	Intensity	Relative	Theo. Mass	Delta (ppm)	RDB equiv.	Composition
231.06284	477287072.0	100.00	231.06276	0.26	5.5	$C_{11}H_{12}O_4Na$

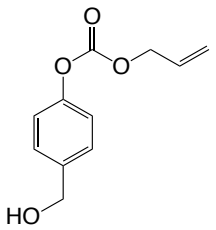

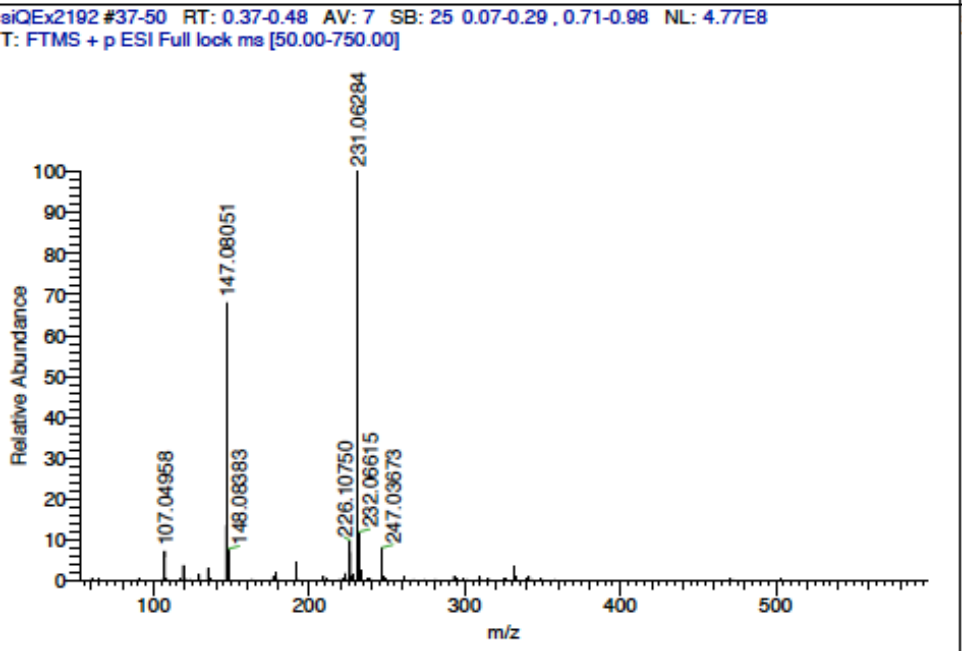

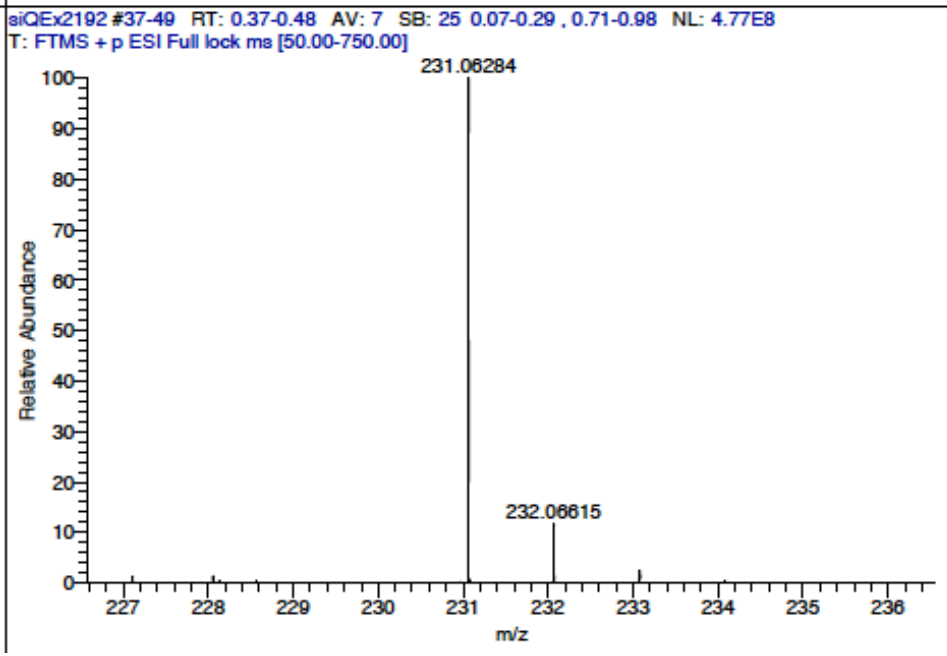

1H

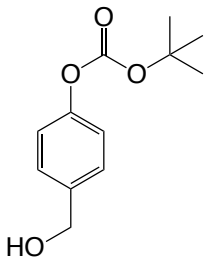

7.39
7.37
7.18
7.17
4.69
1.76
1.58

B (d)
7.18
A (d)
7.38
C (s)
4.69
D (s)
1.76
E (s)
1.58

2.01
2.00
2.01
0.96
9.22

8.5 8.0 7.5 7.0 6.5 6.0 5.5 5.0 4.5 4.0 3.5 3.0 2.5 2.0 1.5 1.0 0.5 0.0 -0.5

f1 (ppm)

13C

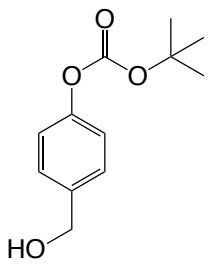

151.86
150.55
138.39
127.96
121.33
83.52
77.25 CDCl3
77.20
77.00 CDCl3
76.74 CDCl3
64.71
60.35
27.70
14.17

200 190 180 170 160 150 140 130 120 110 100 90 80 70 60 50 40 30 20 10 0

f1 (ppm)

D:\Data\Service\Data\jeQEx2128 02/24/16 10:33:12 Sample: ah6.043fc-01
Client: Hofer (+)-HR-ESI-MS Solvent: MeOH

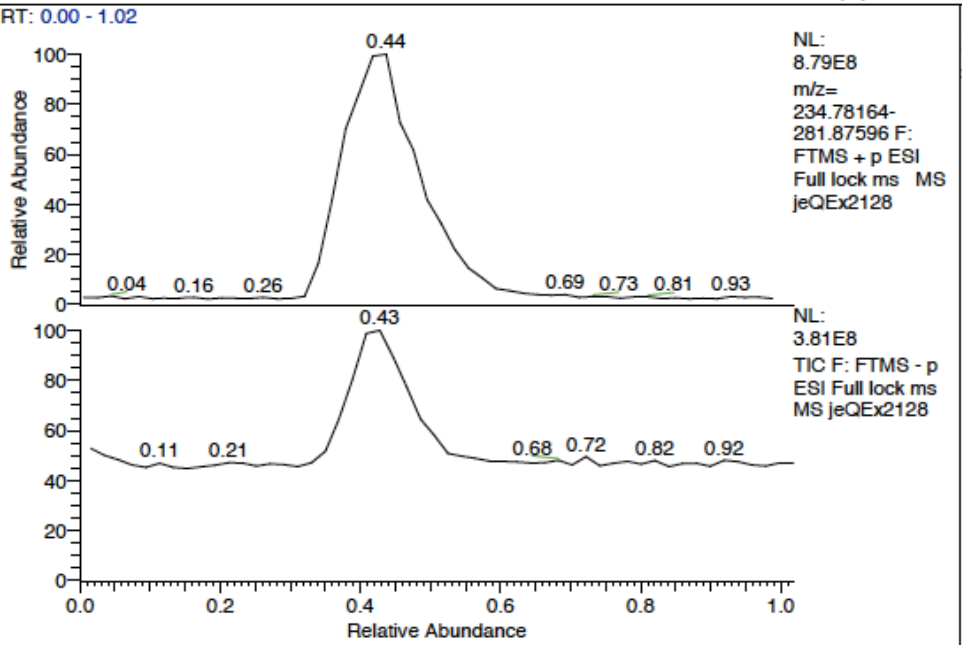

jeQEx2128#39-51 RT: 0.38-0.50 AV: 7
SB: 25 0.07-0.29 , 0.71-0.98
T: FTMS + p ESI Full lock ms [50.00-750.00]
m/z- 246.40962-248.03999

m/z	Intensity	Relative	Theo. Mass	Delta (ppm)	RDB equiv.	Composition
247.09407	410779392.0	100.00	247.09408	-0.02	4.5	C12 H16 O4 Na

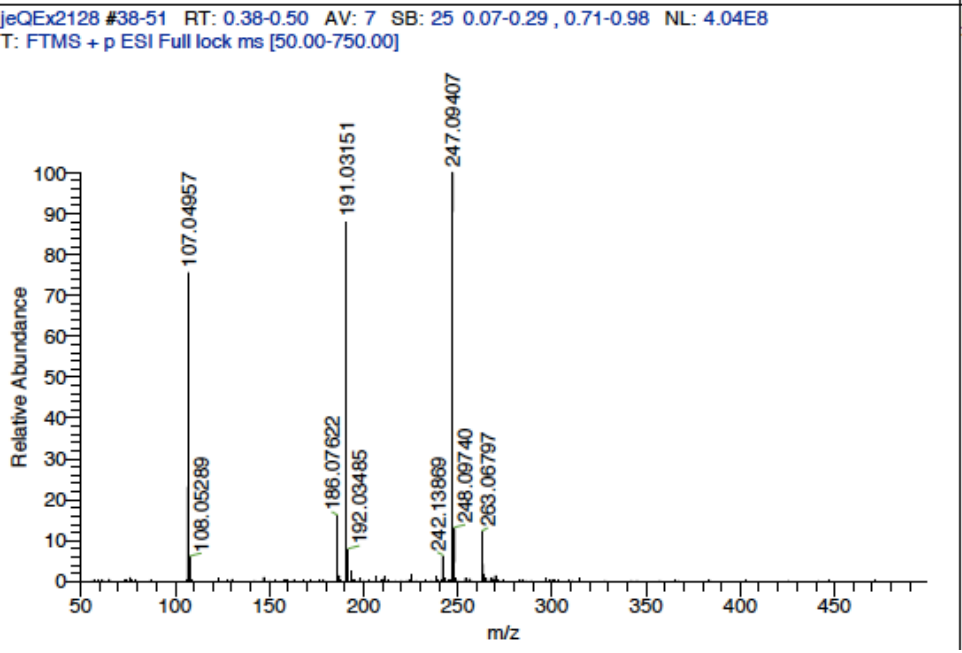

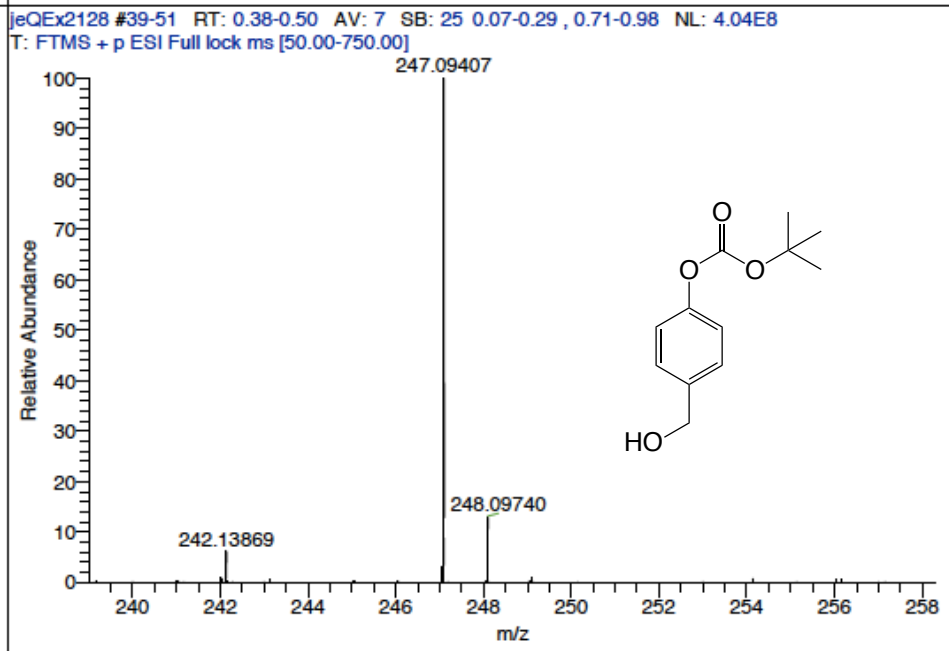

31P, 1H decoupled

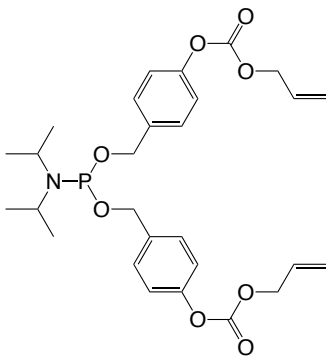

31P, 1H coupled

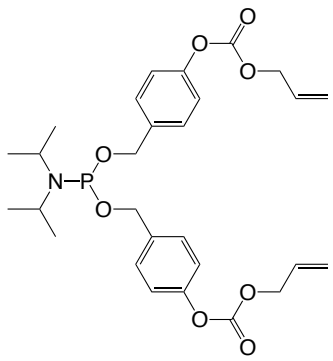

1H

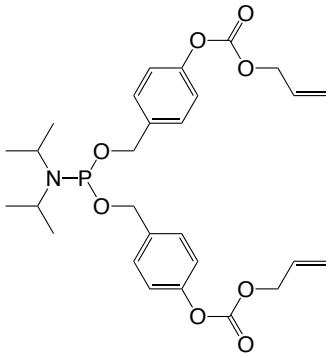

D (d) 7.12
C (d) 7.33
G (ddt) 5.98
F (dd) 5.41
E (dd) 5.31
I (s) 4.68
H (m) 4.71
J (s) 4.66
B (m) 3.67
A (d) 1.18

4.00 3.97 2.11 2.16 2.16 5.84 0.70 0.63 1.88 13.51

f1 (ppm)

13C

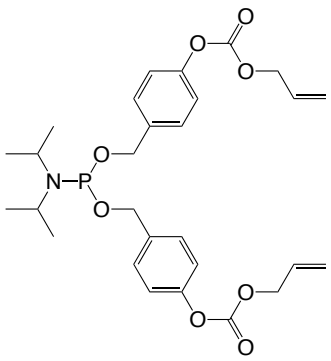

153.70
150.48
137.60
131.37
128.25
121.55
121.02
119.68
110.21
77.54 CDCl3
77.42 CDCl3
77.22 CDCl3
76.90 CDCl3
69.33
66.05
65.09
64.90
43.43
43.31
24.89
24.82
15.49

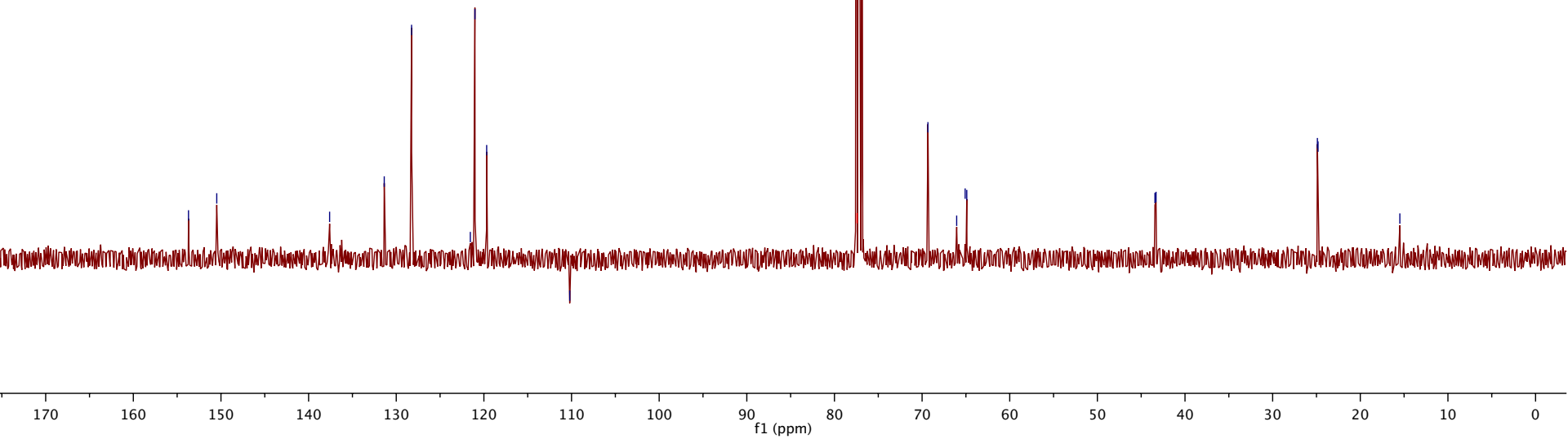

170 160 150 140 130 120 110 100 90 80 70 60 50 40 30 20 10 0

f1 (ppm)

HR-ESI-MS (Bruker maXis)

Analysis Info

Analysis Name	D:\Data\Service\8511sihres.d	Acquisition Date	3/10/2016 12:59:02 PM
Method	tune_low_modified_09_01_14_pos_TuneMix.m	Operator	ust
Sample Name	RC17	Instrument	maXis 255552.00033
Comment	Solvent: MeCN + NaI Client: Pavlovic		

Acquisition Parameter

Source Type	ESI	Ion Polarity	Positive	Set Nebulizer	0.5 Bar
Scan Begin	50 m/z	Set Capillary	2000 V	Set Dry Heater	180 °C
Scan End	3000 m/z	Set End Plate Offset	-500 V	Set Dry Gas	4.0 l/min

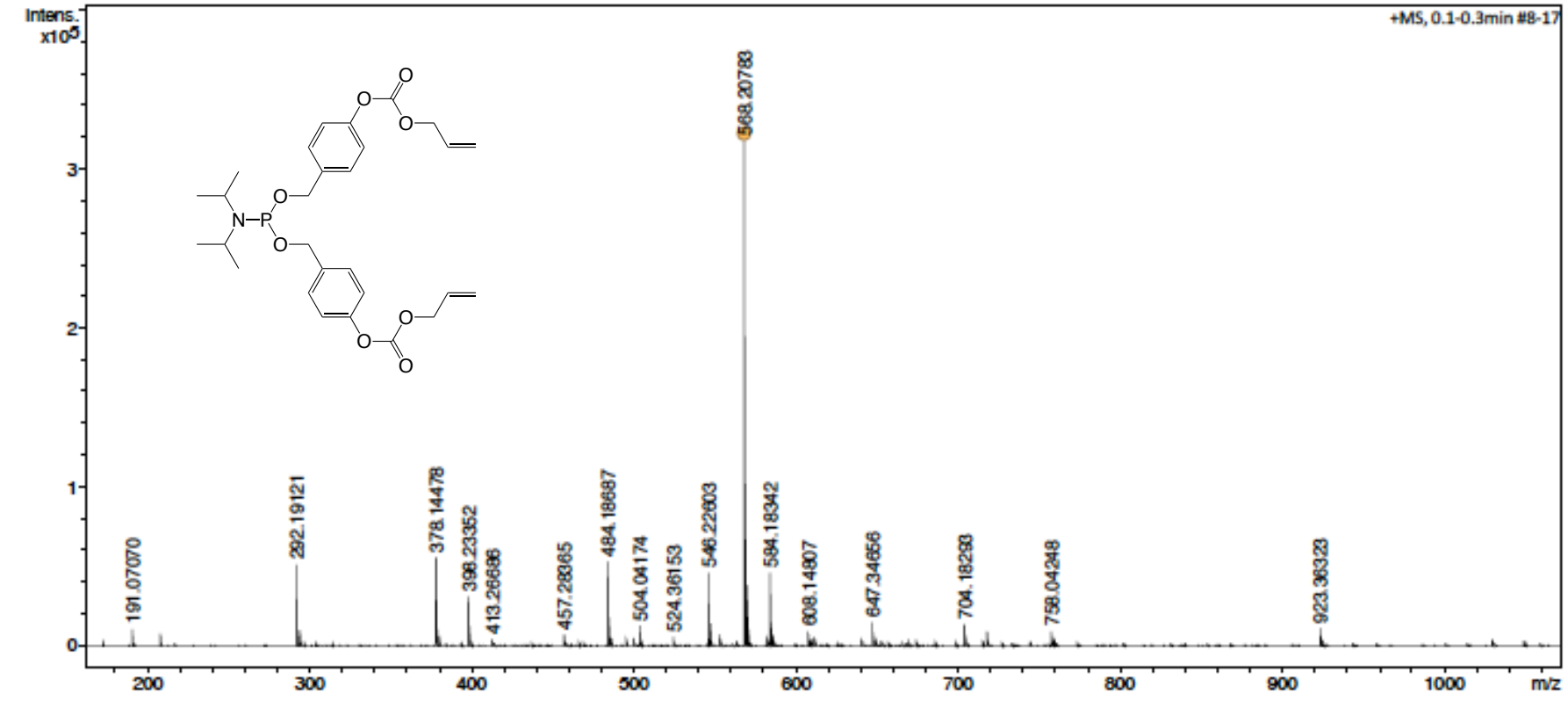

31P

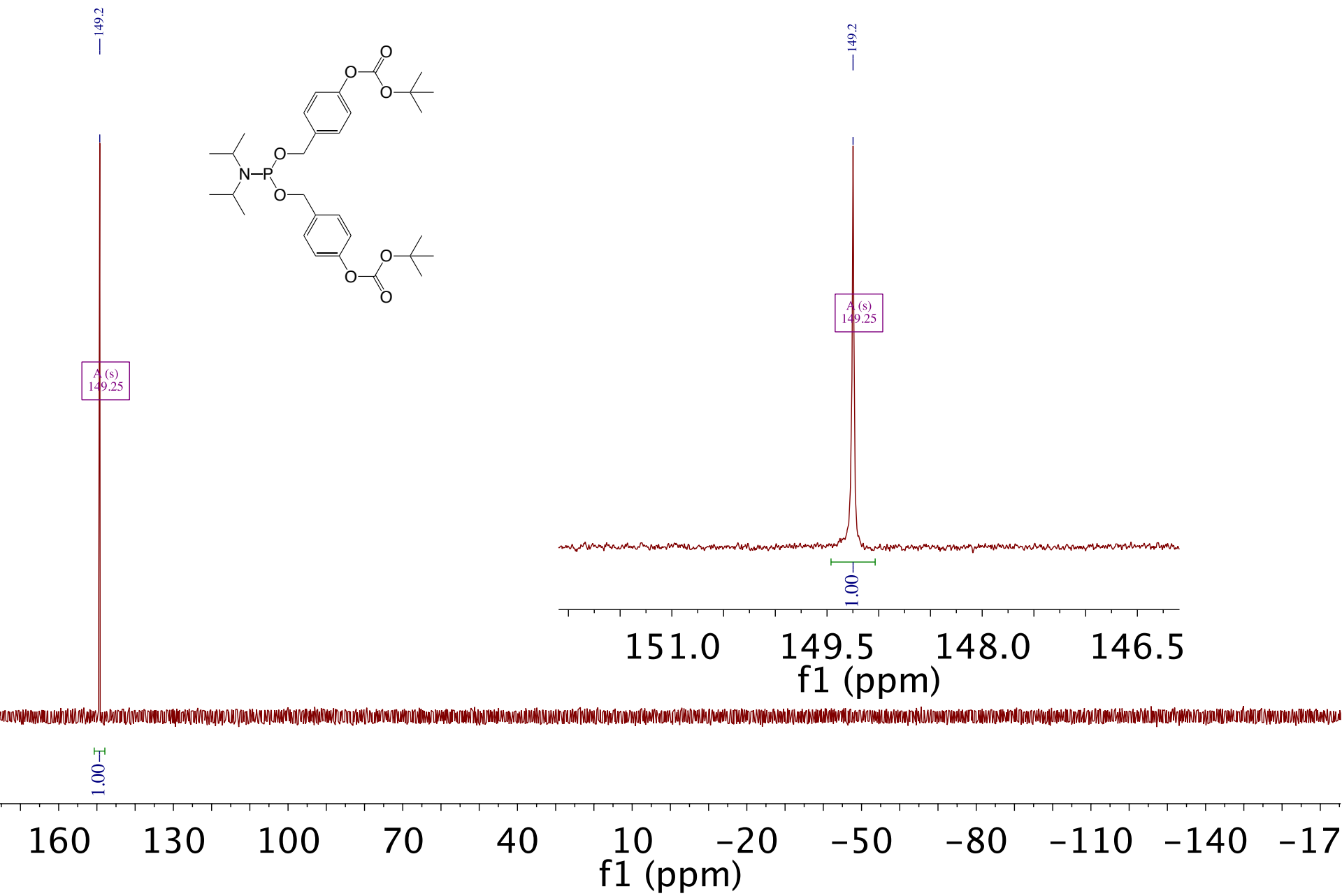
149.2
A (s)
149.25
1.00
149.2
A (s)
149.25
1.00
151.0
149.5
148.0
146.5
f1 (ppm)
160
130
100
70
40
10
-20
-50
-80
-110
-140
-17
f1 (ppm)

31P 1H coupled

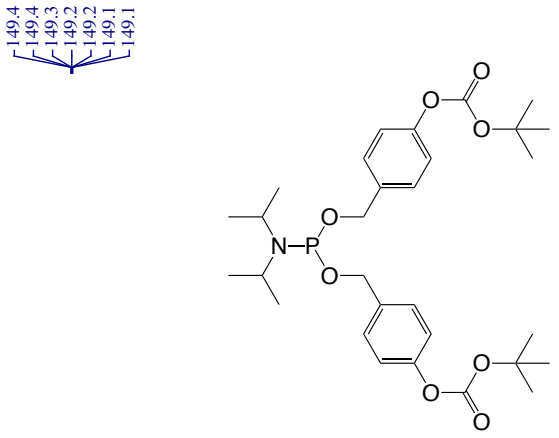

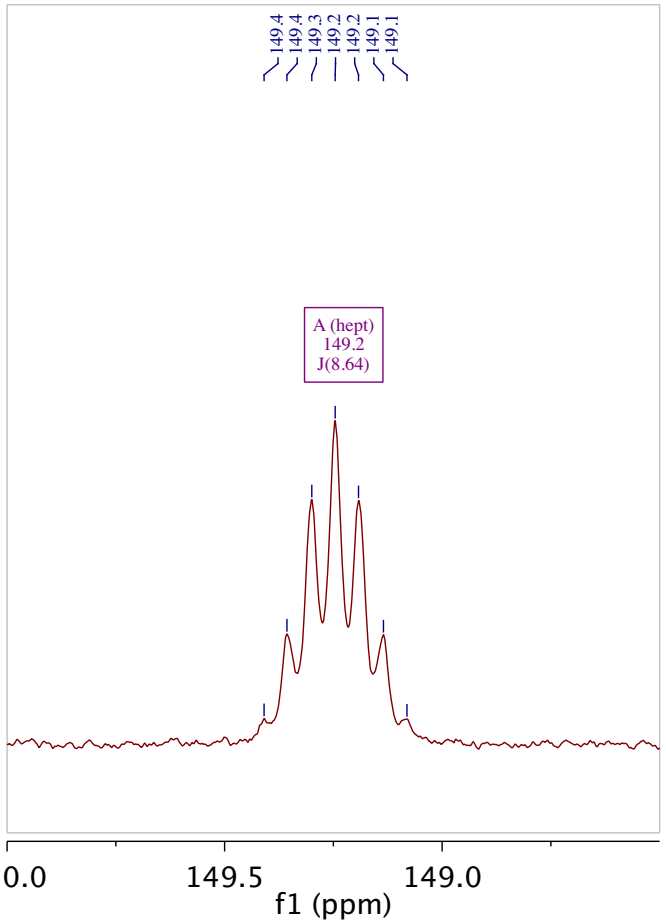

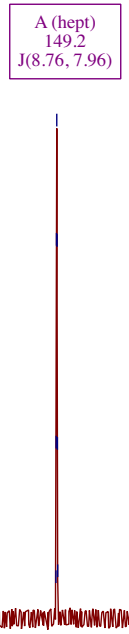

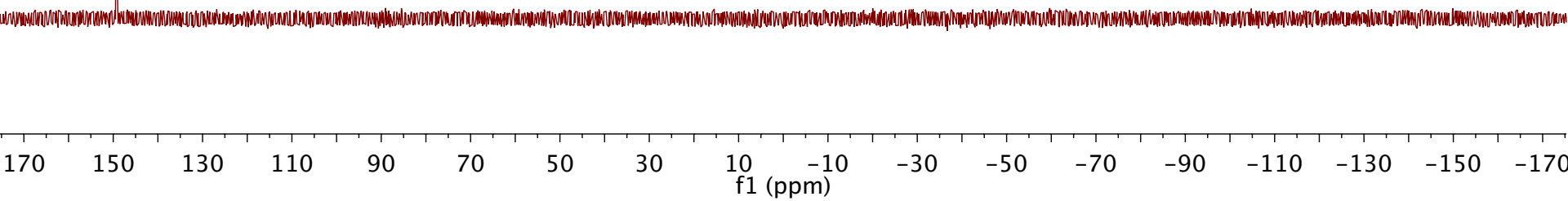

1H

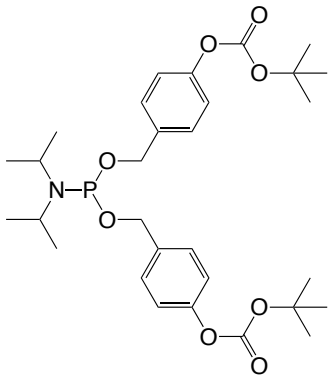

B (d)
7.4
J(8.37)

A (d)
7.2
J(8.45)

C (m)
4.7

D (m)
3.7

F (s)
1.6

E (d)
1.2
J(6.81)

4.00

3.97

4.03

2.04

18.72

12.47

f1 (ppm)

13C

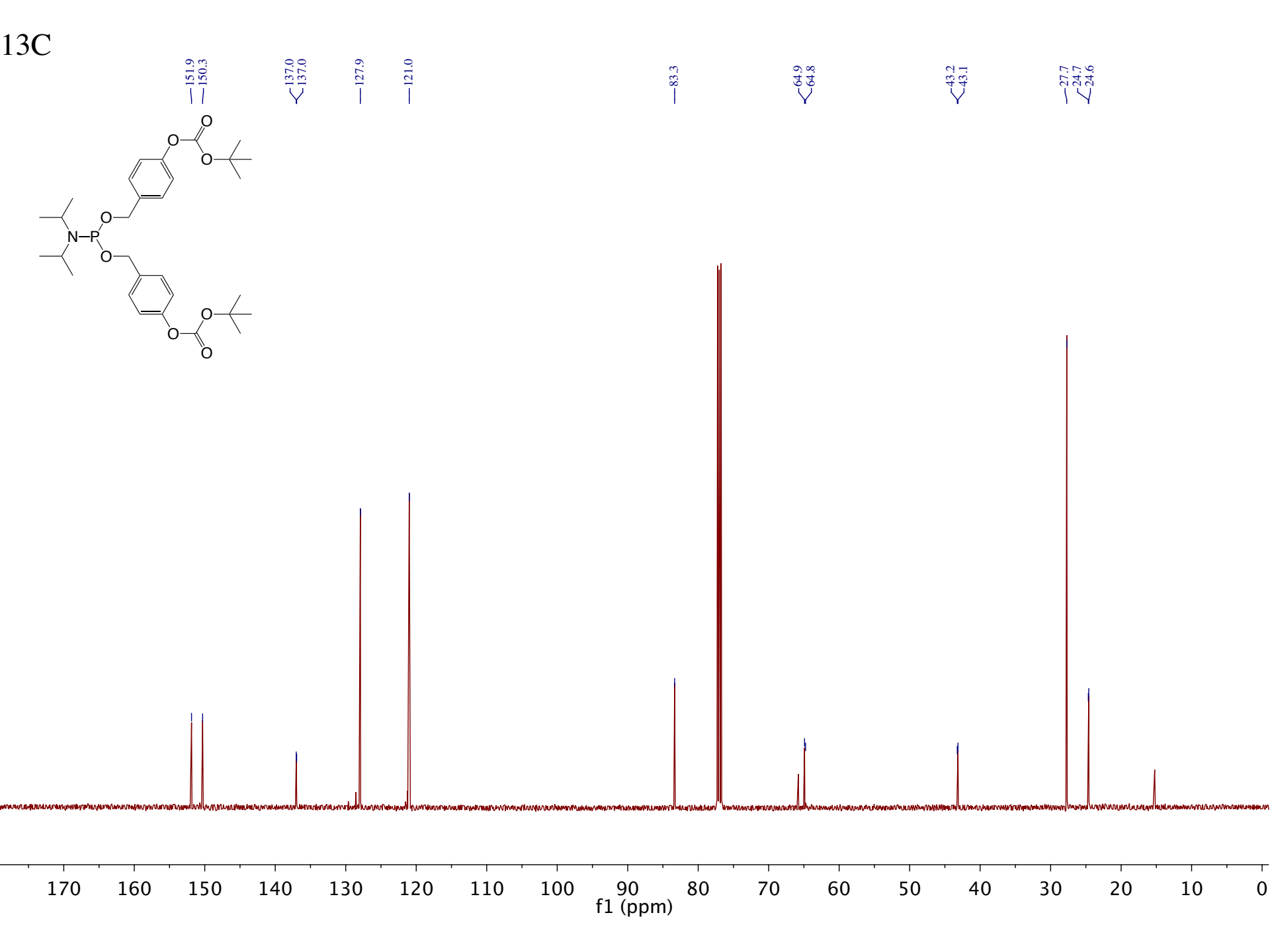
151.9
150.3
137.0
137.0
127.9
121.0
83.3
64.9
64.8
43.2
43.1
27.7
24.7
24.6
O
O
O
O
N
P
O
O
O
O
O
170
160
150
140
130
120
110
100
90
80
70
60
50
40
30
20
10
0
f1 (ppm)

HR-ESI-MS (Bruker maXis)

Analysis Info

Analysis Name	D:\Data\Service\8501jehres.d	Acquisition Date	2/29/2016 9:52:36 AM
Method	tune_low_modified_09_01_14_pos_TuneMix.m	Operator	ust
Sample Name	ah6.044f-04	Instrument	maXis 255552.00033
Comment	Solvent: MeCN + NaI Client: Hofer		

Acquisition Parameter

Source Type	ESI	Ion Polarity	Positive	Set Nebulizer	2.0 Bar
Scan Begin	50 m/z	Set Capillary	4000 V	Set Dry Heater	180 °C
Scan End	3000 m/z	Set End Plate Offset	-500 V	Set Dry Gas	4.0 l/min

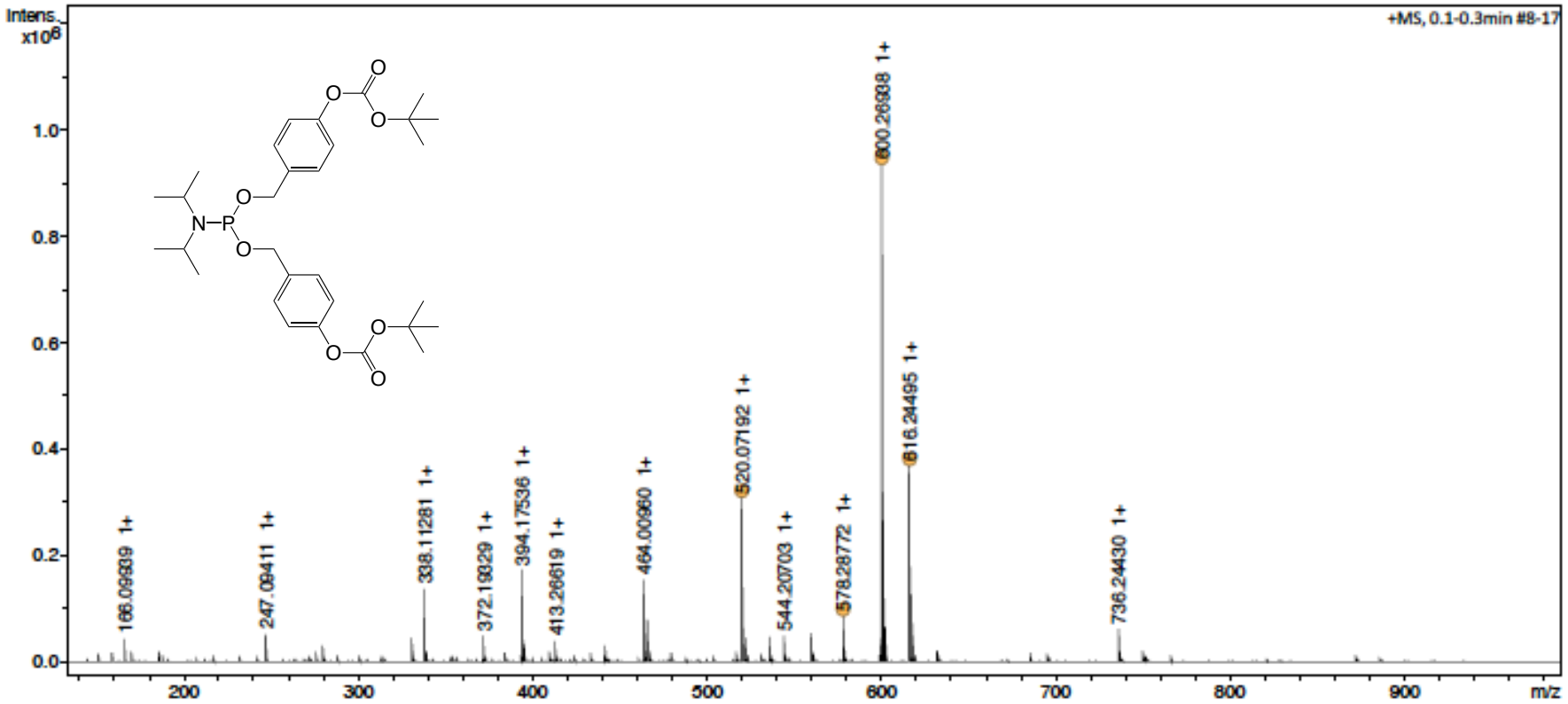

31P, 1H decoupled

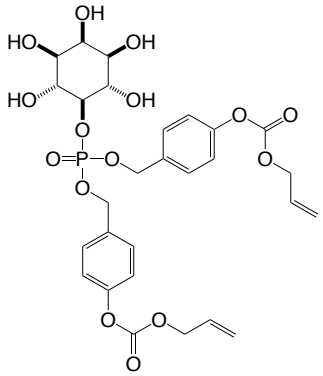

31P, 1H coupled

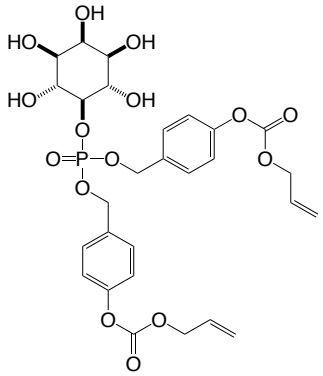

1H

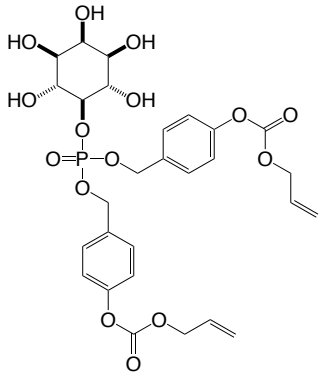

A (d) 7.46
B (d) 7.24
C (ddt) 6.01
D (dt) 5.41
E (d) 5.32
F (d) 5.12
G (d) 4.74
H (dd) 3.26
I (d) 3.75
J (q) 4.03
K (t) 3.65
L (m) 5.02

3.99 4.00 1.99 2.09 2.09 3.69 0.92 4.66 1.14 1.32 2.30 2.76

f1 (ppm)

13C

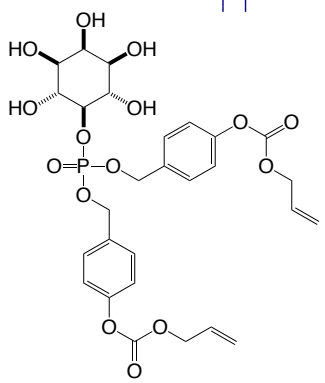

152.73
150.38
134.72
134.66
131.72
129.08
121.14
118.87
83.41
83.35
72.41
71.50
71.32
71.29
68.72
67.44
67.40
30.92
28.45
22.03
13.93

A (d)
134.69

B (d)
83.38

D (d)
71.31

C (d)
67.42

180 170 160 150 140 130 120 110 100 90 80 70 60 50 40 30 20 10 0 -10

f1 (ppm)

D:\Data\Service\Data\siQEx2636 05/09/16 11:35:51 Sample: IP-11-26T1
Client: Pavlovic (+)-HR-ESI-MS Solvent: MeOH

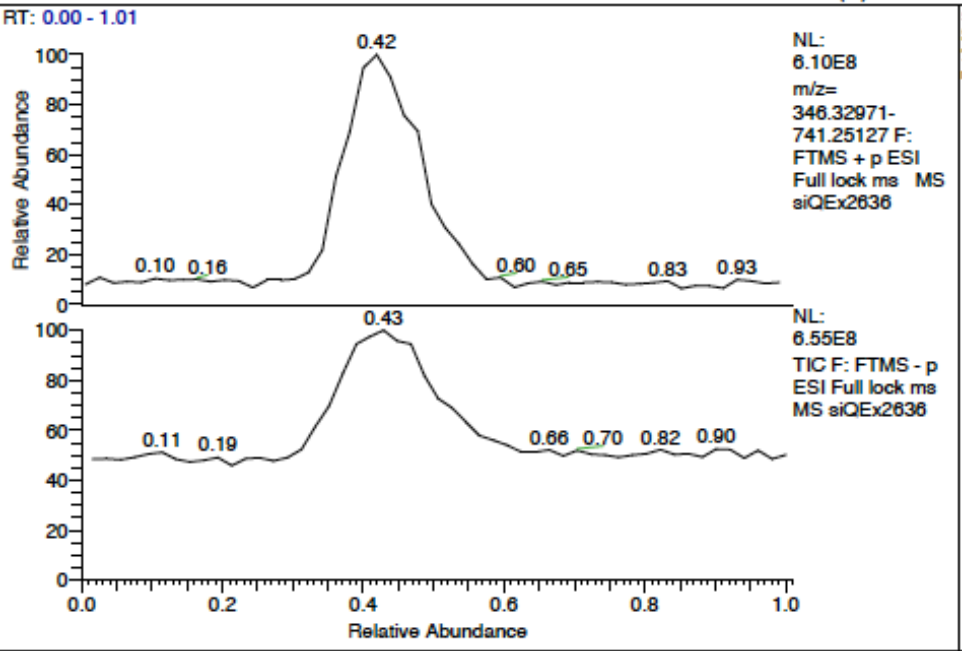

siQEx2636#37-55 RT: 0.36-0.54 AV: 10
SB: 26 0.07-0.29 , 0.71-0.98
T: FTMS + p ESI Full lock ms [100.00-1500.00]
m/z= 640.22810-664.05926

m/z	Intensity	Relative	Theo. Mass	Delta (ppm)	RDB equiv.	Composition
641.16350	15766276.0	25.92	641.16346	0.07	6.0	$C_{19}H_{32}O_{18}N_3Na$
			641.16326	0.38	14.0	$C_{29}H_{33}O_{12}NNaP$
			641.16401	-0.80	22.0	$C_{33}H_{27}O_{11}N_3$
			641.16298	0.81	12.5	$C_{26}H_{34}O_{15}P$
			641.16295	0.86	16.5	$C_{33}H_{30}O_{12}Na$
663.14527	60912268.0	100.00	663.14493	0.51	12.5	$C_{28}H_{33}O_{15}NaP$
			663.14568	-0.62	20.5	$C_{32}H_{27}O_{14}N_2$
			663.14595	-1.03	22.0	$C_{33}H_{26}O_{11}N_3Na$
			663.14599	-1.09	16.0	$C_{28}H_{30}O_{14}N_3P$
			663.14434	1.41	21.0	$C_{30}H_{25}O_{13}Ns$

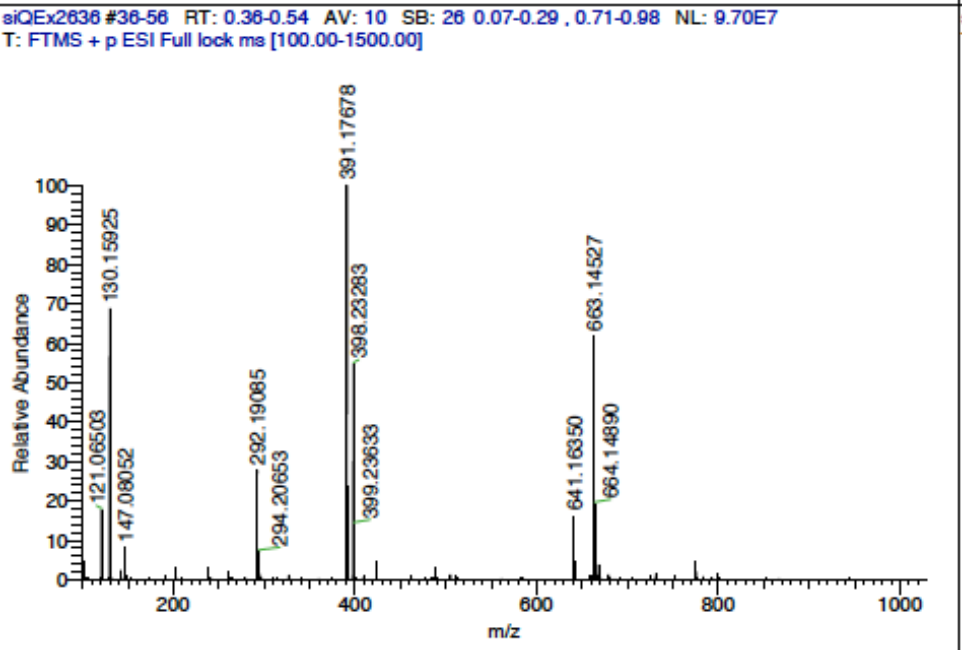

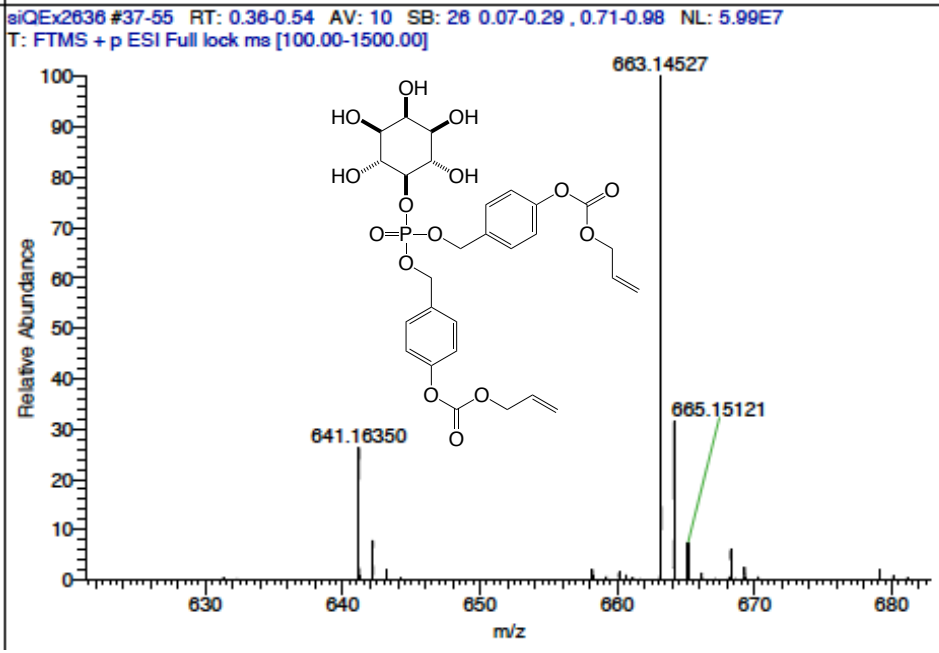

31P 1H decoupled

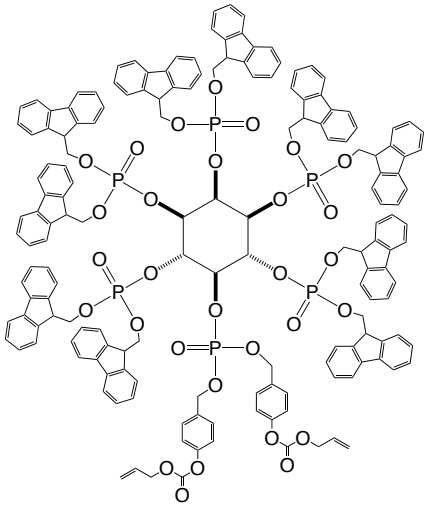

31P, 1H coupled

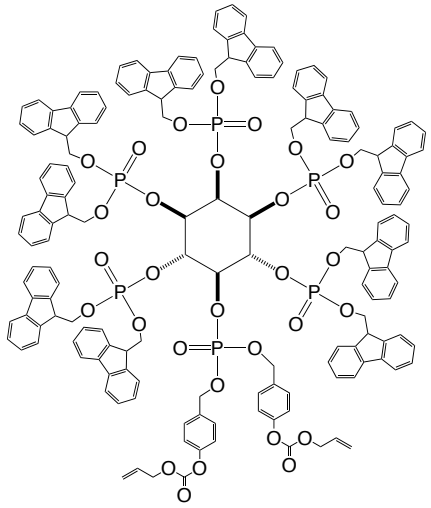

1H

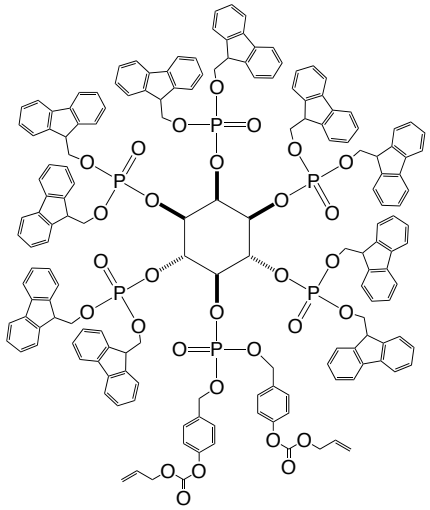

S (m) 7.30
W (s) 6.86
O (s) 7.84
R (s) 7.37
V (m) 6.96
N (s) 7.96
Q (m) 7.49
U (s) 7.09
P (m) 7.66
T (m) 7.19
M (ddt) 5.94
K (dd) 5.38
I (m) 4.92
E (m) 4.39
C (m) 3.94
L (d) 5.76
H (m) 5.19
G (q) 4.68
D (m) 4.29
B (m) 3.76
A (dd) 2.88
J (dd) 5.28
F (m) 4.58

3.27 3.28 1.47 13.25 11.10 4.66 5.34 10.64 11.69 4.00 20.31 3.55 1.51 0.73 1.60 1.60 1.98 1.73 5.74 3.25 2.06 8.37 6.81 3.54 0.98

11.0 10.5 10.0 9.5 9.0 8.5 8.0 7.5 7.0 6.5 6.0 5.5 5.0 4.5 4.0 3.5 3.0 2.5 2.0 1.5 1.0 0.5 0.0 -0.5 -1.0

f1 (ppm)

13C

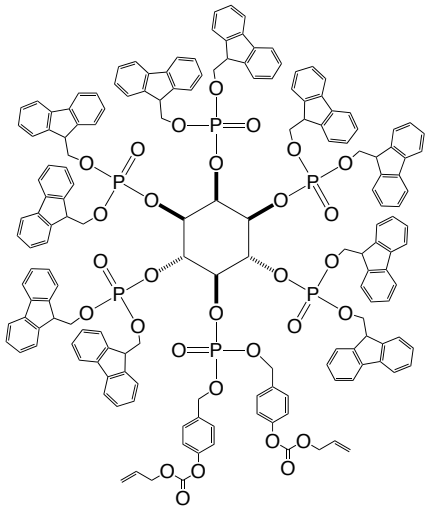

169.24
151.53
143.80
143.65
143.58
143.50
143.32
143.24
141.86
141.82
141.77
141.71
141.63
134.98
133.74
132.22
131.68
130.59
130.17
129.83
128.68
128.16
128.10
127.64
127.54
127.42
126.19
125.95
125.85
125.76
121.46
120.38
120.26
120.21
119.98
73.96
70.66
69.64
48.35
22.92

200 190 180 170 160 150 140 130 120 110 100 90 80 70 60 50 40 30 20 10 0 -10 -20

f1 (ppm)

HR-ESI-MS (Bruker maXis)

Analysis Info

Analysis Name	D:\Data\Service\8579sihres.d	Acquisition Date	5/17/2016 3:03:43 PM
Method	tune_low_modified_09_01_14_pos_TuneMix.m	Operator	ust
Sample Name	IP-11-28T1	Instrument	maXis 255552.00033
Comment	Solvent: MeOH/CHCl3 3:2 + NaI Client: Pavlovic		

Acquisition Parameter

Source Type	ESI	Ion Polarity	Positive	Set Nebulizer	0.5 Bar
Scan Begin	50 m/z	Set Capillary	5000 V	Set Dry Heater	180 °C
Scan End	3000 m/z	Set End Plate Offset	-500 V	Set Dry Gas	4.0 l/min

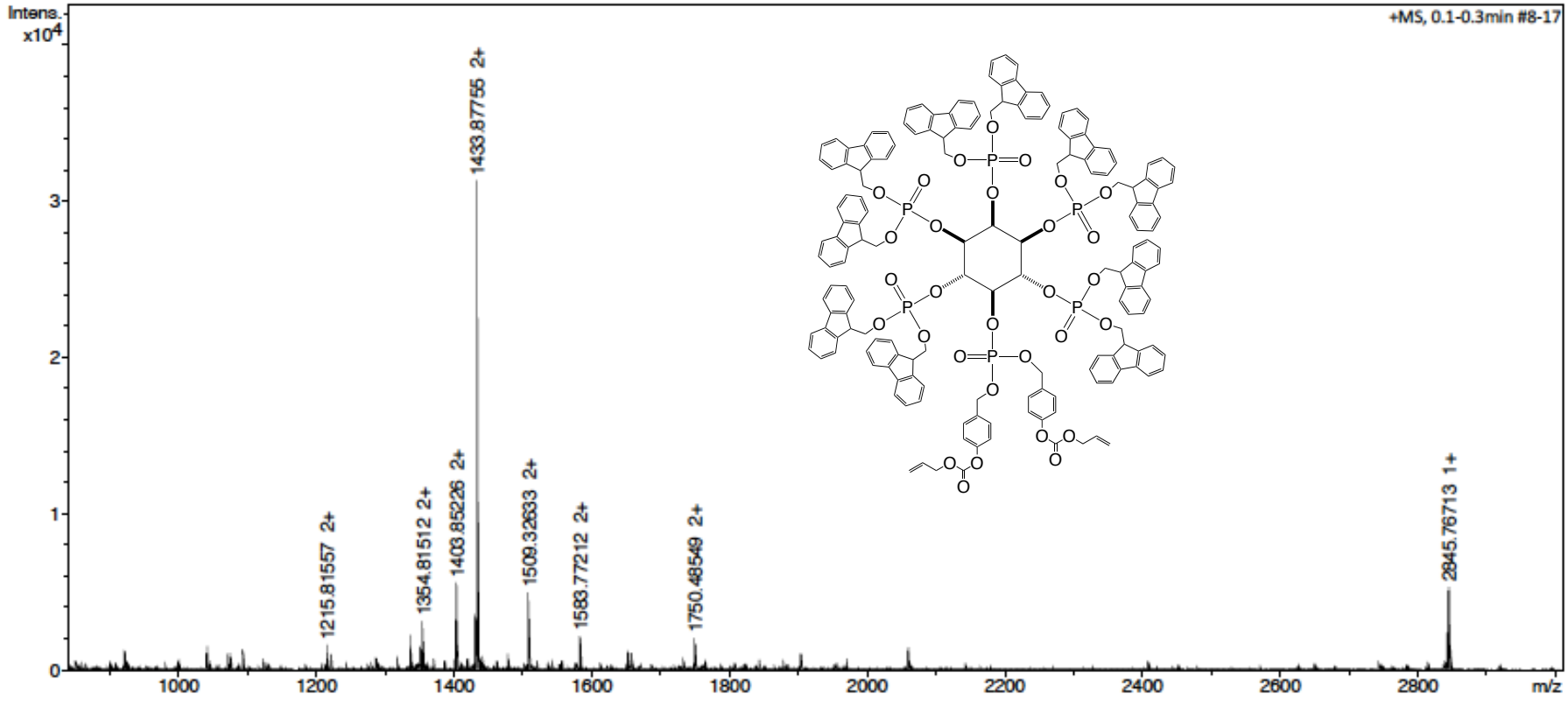

31P 1H decoupled

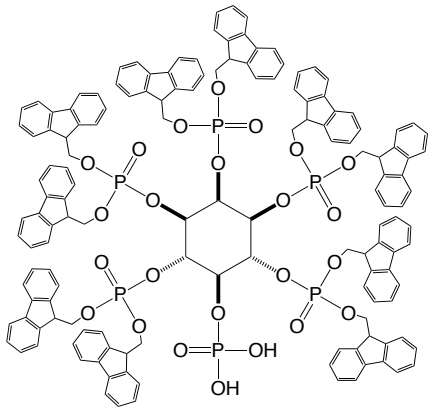

31P, 1H coupled

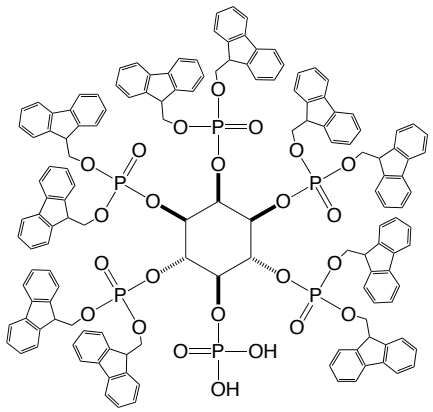

1.77
1.69
1.37
1.43
1.94

1.77
1.69

1.37
1.38
1.43
1.85
1.94
1.95
2.05

A (d)
1.73

B (m)
-1.38

C (m)
-1.91

1.00
4.59
1.26

2.5 1.5 0.5 -0.5 -1.5 -2.5 -3.5
f1 (ppm)

1.00
4.59
1.26

50 130 110 90 70 50 30 10 -10 -30 -50 -70 -90 -110 -130 -150 -170 -190 -210 -230 -25
f1 (ppm)

HR-ESI-MS (Bruker maXis)

Analysis Info

Analysis Name	D:\Data\Service\8673sihres.d			Acquisition Date	7/8/2016 9:47:48 AM
Method	tune_low_neg_Aug2014_TuneMix.m			Operator	ust
Sample Name	IP-11-82P1			Instrument	maXis 255552.00033
Comment	Solvent: MeOH/CHCl3 3:2 Client: Pavlovic				

Acquisition Parameter

Source Type	ESI	Ion Polarity	Negative	Set Nebulizer	0.5 Bar
Scan Begin	50 m/z	Set Capillary	6000 V	Set Dry Heater	180 °C
Scan End	4000 m/z	Set End Plate Offset	-500 V	Set Dry Gas	4.0 l/min

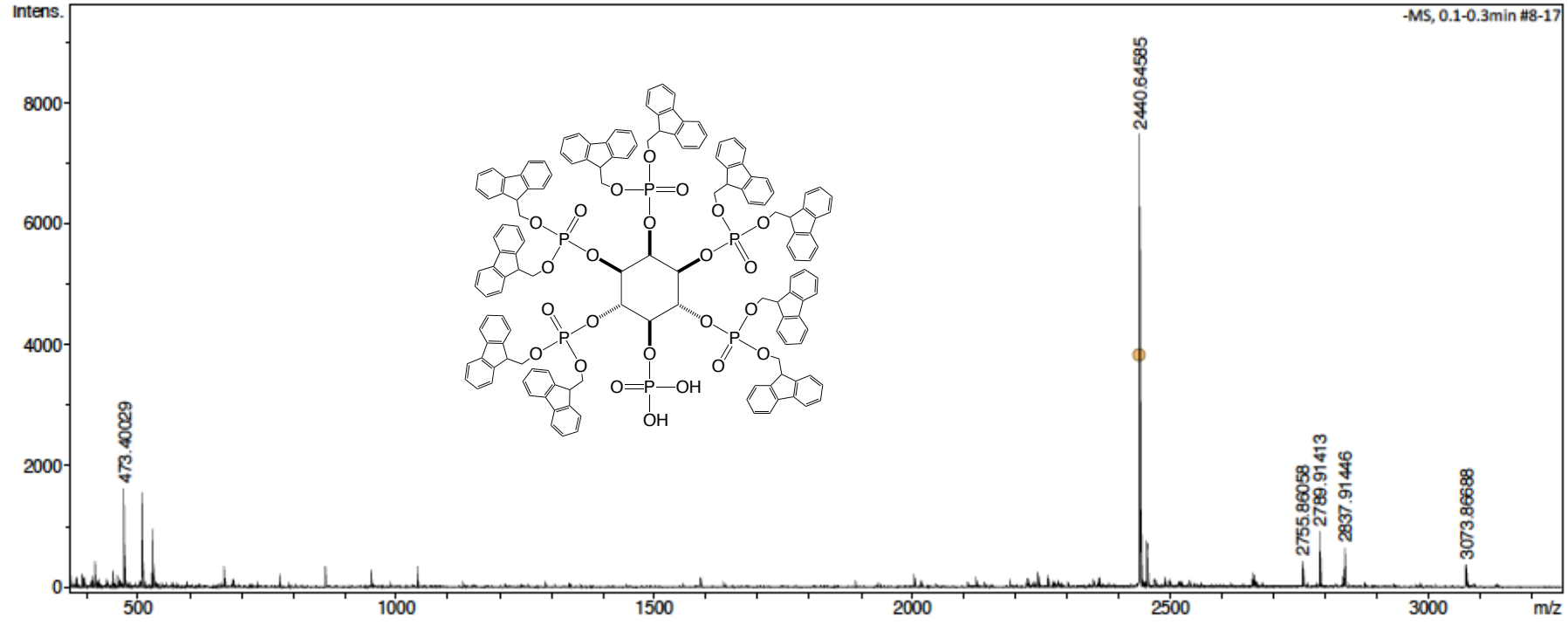

31P 1H decoupled

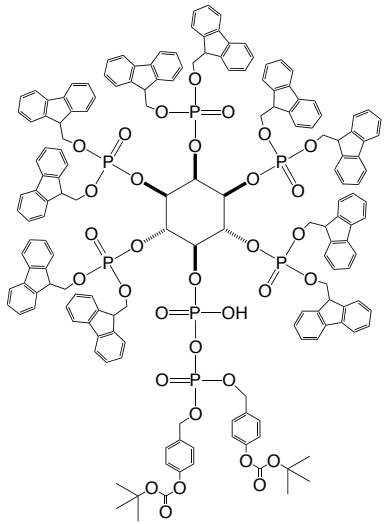

31P, 1H coupled

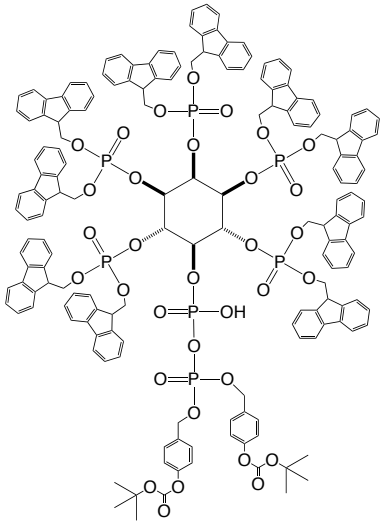

1H

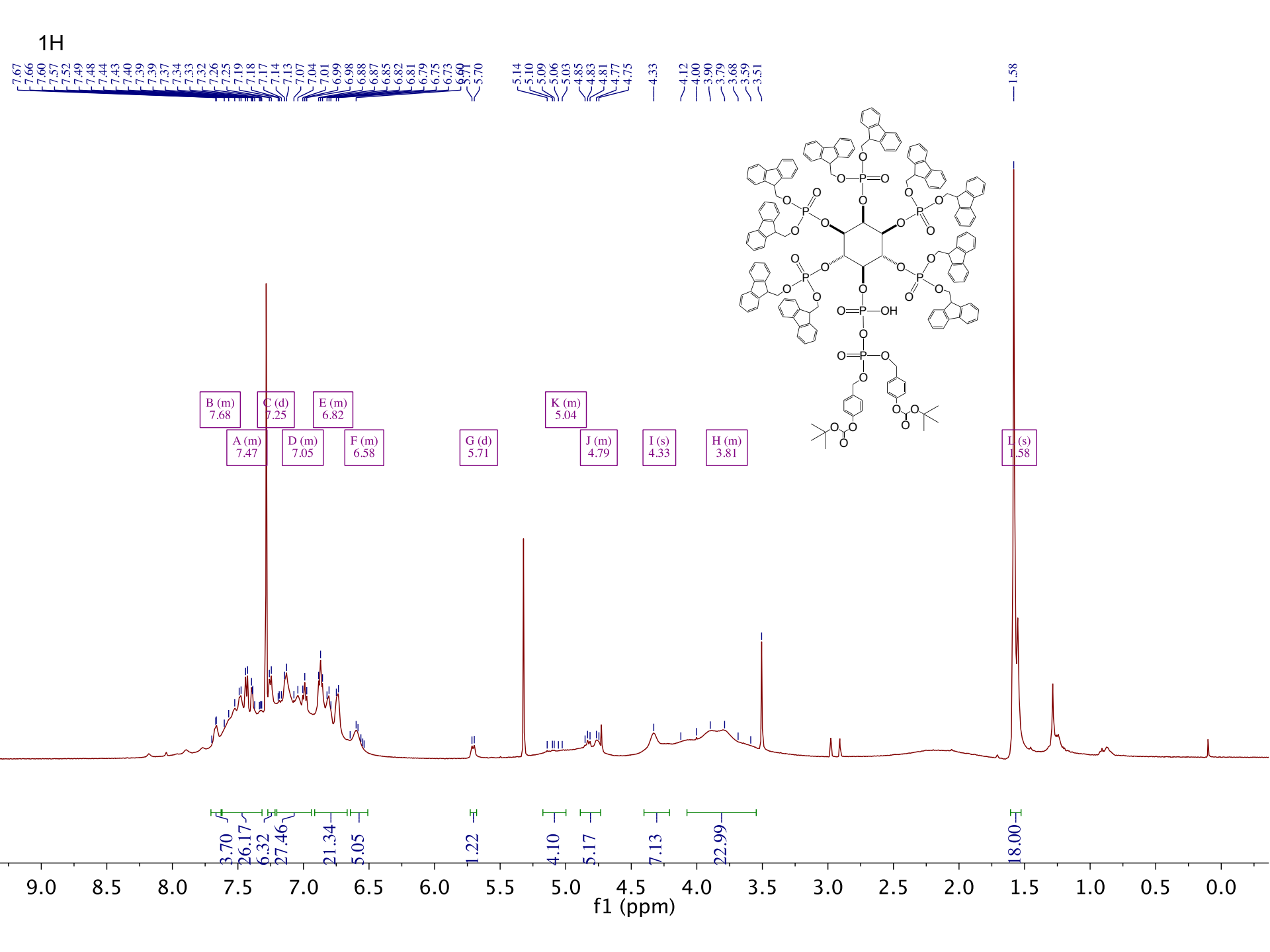
7.67
7.66
7.60
7.57
7.52
7.49
7.48
7.44
7.43
7.40
7.39
7.39
7.37
7.34
7.33
7.32
7.26
7.25
7.19
7.18
7.17
7.14
7.13
7.07
7.04
7.01
6.99
6.98
6.88
6.87
6.85
6.82
6.81
6.79
6.75
6.73
6.60
5.71
5.70
5.14
5.10
5.09
5.06
5.03
4.85
4.83
4.81
4.77
4.75
4.33
4.12
4.00
3.90
3.79
3.68
3.59
3.51
1.58
B (m) 7.68
C (d) 7.25
E (m) 6.82
K (m) 5.04
A (m) 7.47
D (m) 7.05
F (m) 6.58
G (d) 5.71
J (m) 4.79
I (s) 4.33
H (m) 3.81
L (s) 1.58
3.70
26.17
6.32
27.46
21.34
5.05
1.22
4.10
5.17
7.13
22.99
18.00
9.0
8.5
8.0
7.5
7.0
6.5
6.0
5.5
5.0
4.5
4.0
3.5
3.0
2.5
2.0
1.5
1.0
0.5
0.0
f1 (ppm)

13C

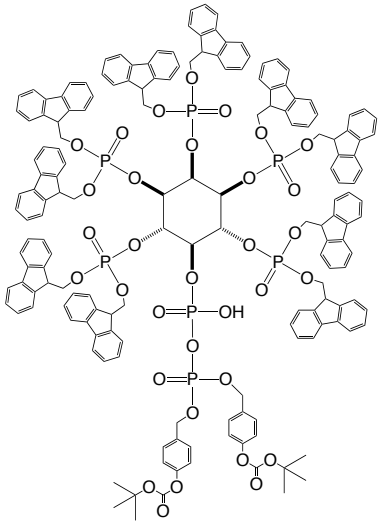

151.37
150.67
143.21
142.79
141.25
141.00
132.21
128.57
127.72
127.56
127.06
126.99
126.87
126.70
125.46
125.19
120.87
83.07
77.26 CDCl3
77.21 CDCl3
77.01 CDCl3
76.75
75.88
73.24
69.66
69.23
53.41
50.86
47.53
29.71
27.74
27.70
170
160
150
140
130
120
110
100
90
80
70
60
50
40
30
20
10
f1 (ppm)

HR-ESI-MS (Bruker maXis)

Analysis Info

Analysis Name	D:\Data\Service\8672sihres.d	Acquisition Date	7/8/2016 9:19:16 AM	
Method	tune_low_neg_Aug2014_TuneMix.m	Operator	ust	
Sample Name	IP-11-87P1	Instrument	maXis	255552.00033
Comment	Solvent: MeOH/CHCl3 3:2 Client: Pavlovic			

Acquisition Parameter

Source Type	ESI	Ion Polarity	Negative	Set Nebulizer	0.5 Bar
Scan Begin	50 m/z	Set Capillary	6000 V	Set Dry Heater	180 °C
Scan End	4000 m/z	Set End Plate Offset	-500 V	Set Dry Gas	4.0 l/min

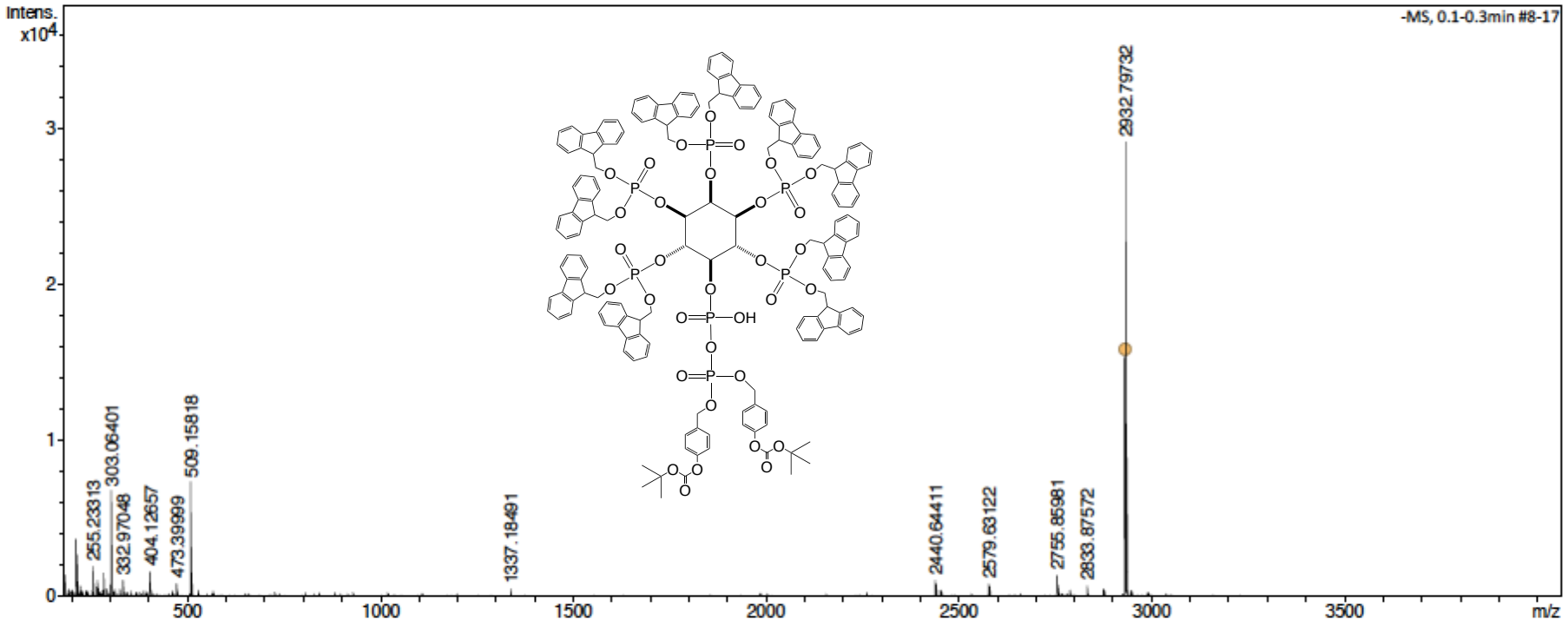

31P, 1H decoupled

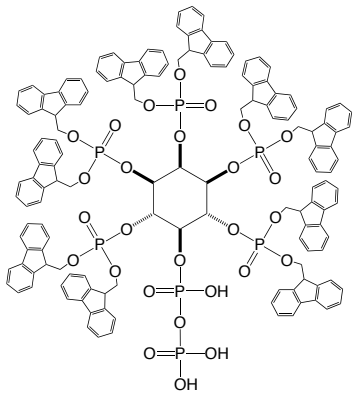

-1.62
-2.03
-2.85
-9.13
-11.74

D (s)
-1.62

C (s)
-2.85

B (s)
-9.13

A (s)
-11.74

5.26
2.25
1.00
1.11

16 14 12 10 8 6 4 2 0 -2 -4 -6 -8 -10 -12 -14 -16 -18 -20 -22 -24 -26 -28 -30 -32

f1 (ppm)

31P, 1H coupled

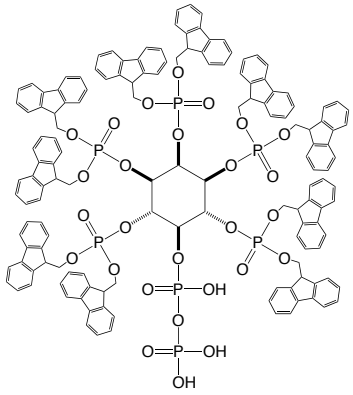

-1.62
-2.92
-9.47
-11.44

D (m) -1.62
C (m) -2.92
A (m) -9.47
B (m) -11.44

7.31
1.50
1.00
1.10

20 18 16 14 12 10 8 6 4 2 0 -2 -4 -6 -8 -10 -12 -14 -16 -18 -20 -22 -24 -26 -28 -30 -32 -34

f1 (ppm)

HR-ESI-MS (Bruker maXis)

Analysis Info

Analysis Name	D:\Data\Service\8036jehres.d	Acquisition Date	6/19/2015 4:37:24 PM
Method	tune_low_neg_Aug2014.m	Operator	ust
Sample Name	IP-8-59P1	Instrument	maXis 255552.00033
Comment	Solvent: MeOH/CHCl3 3:2 Client: Pavlovic		

Acquisition Parameter

Source Type	ESI	Ion Polarity	Negative	Set Nebulizer	1.0 Bar
Scan Begin	50 m/z	Set Capillary	6000 V	Set Dry Heater	180 °C
Scan End	3500 m/z	Set End Plate Offset	-500 V	Set Dry Gas	4.0 l/min

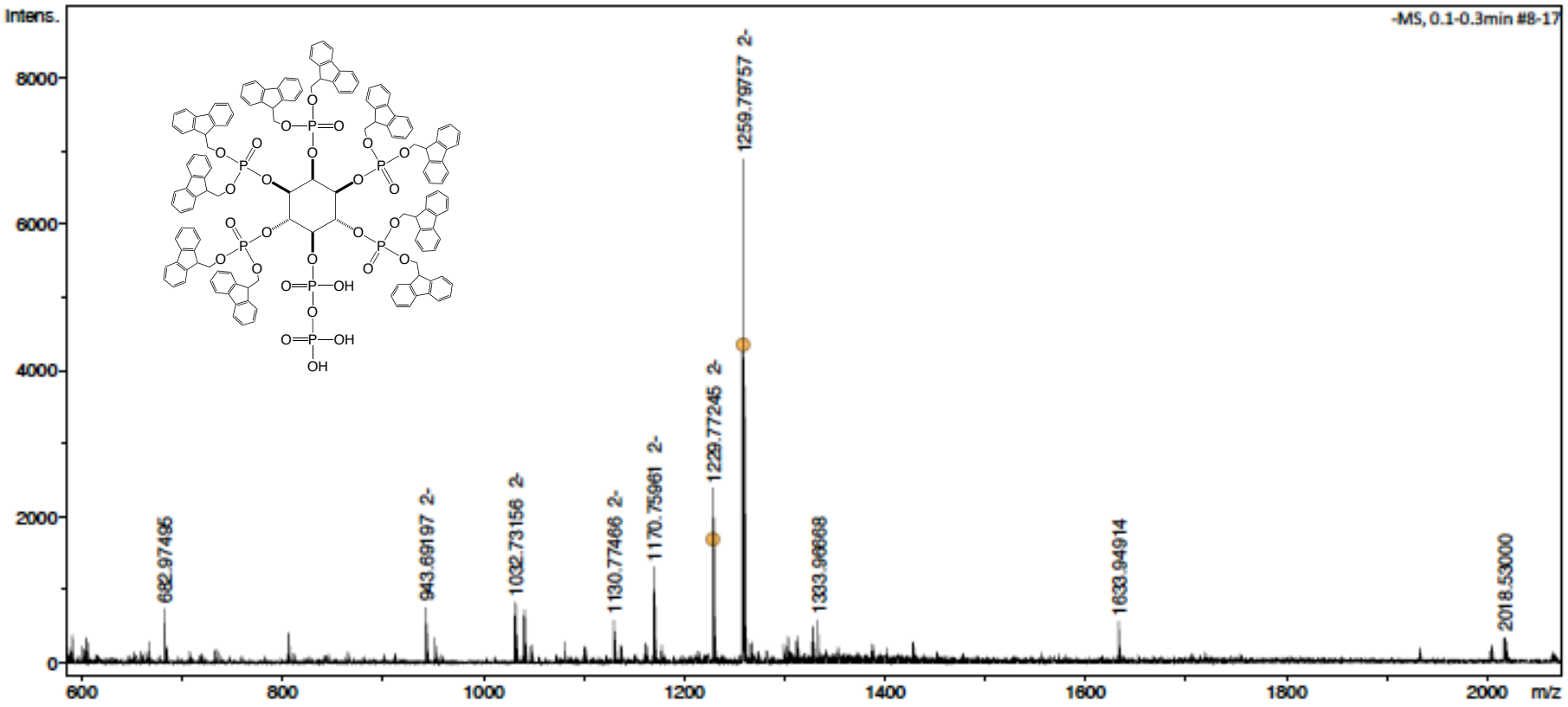

31P, 1H decoupled

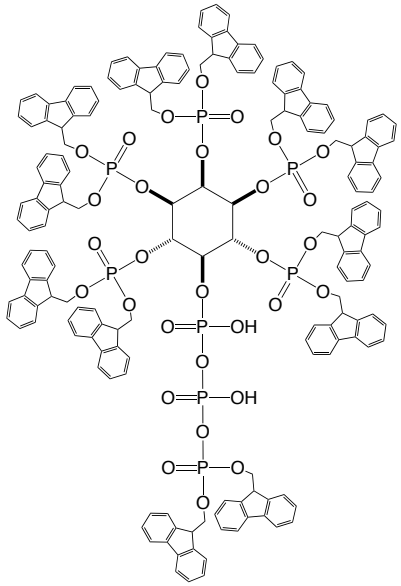

31P, 1H coupled

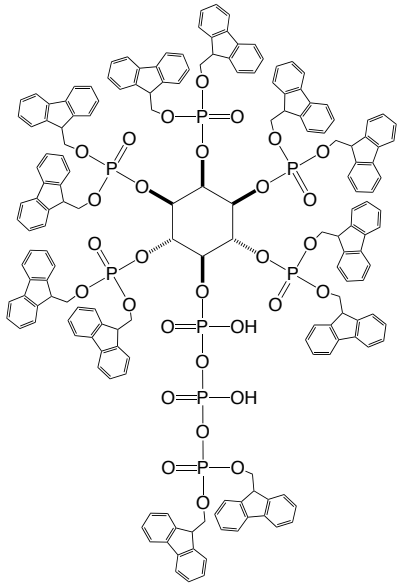

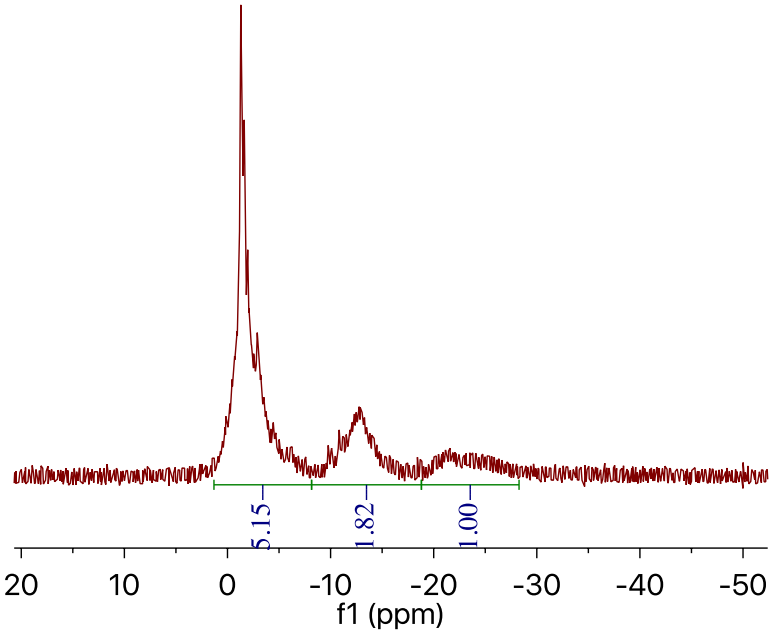

1H

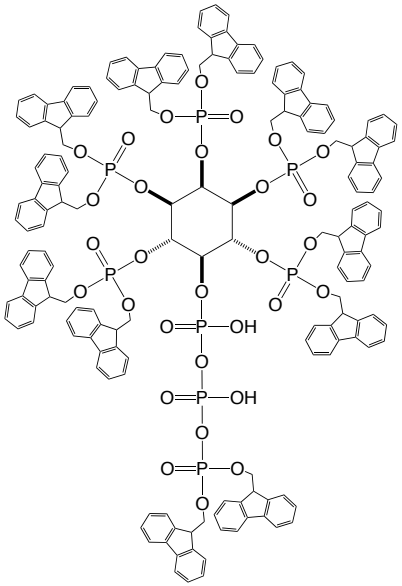

A (m) 7.53

B (m) 7.11

C (m) 4.13

42.00

54.46

42.30

f1 (ppm)

13C

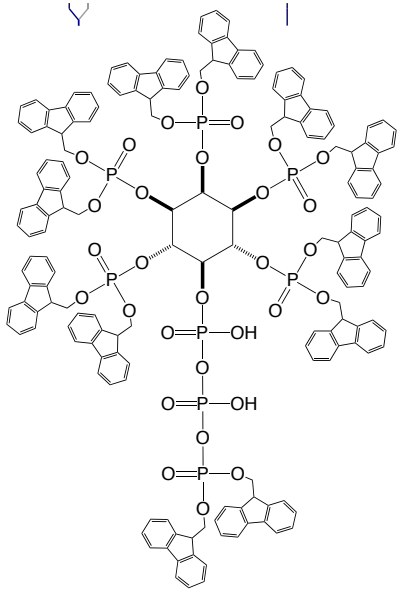

162.55
162.55
141.13
127.59
127.08
126.96
125.30
119.97
119.68
92.90
80.83
80.83
77.27 CDCl3
77.22
77.02 CDCl3
76.77 CDCl3
74.51
73.86
69.87
50.84
50.84
47.69
36.49
36.49
31.45
31.45
29.71
29.68
25.77
19.10
1.03
1.03

180 170 160 150 140 130 120 110 100 90 80 70 60 50 40 30 20 10 0

f1 (ppm)

D:\Data\ASamp_Service\siQEx0422 05/18/15 11:08:43 Sample: IP-8-51A1

Client: Pavlovic (+)-HR-ESI-MS Solvent: MeOH

RT: 0.00 - 1.02

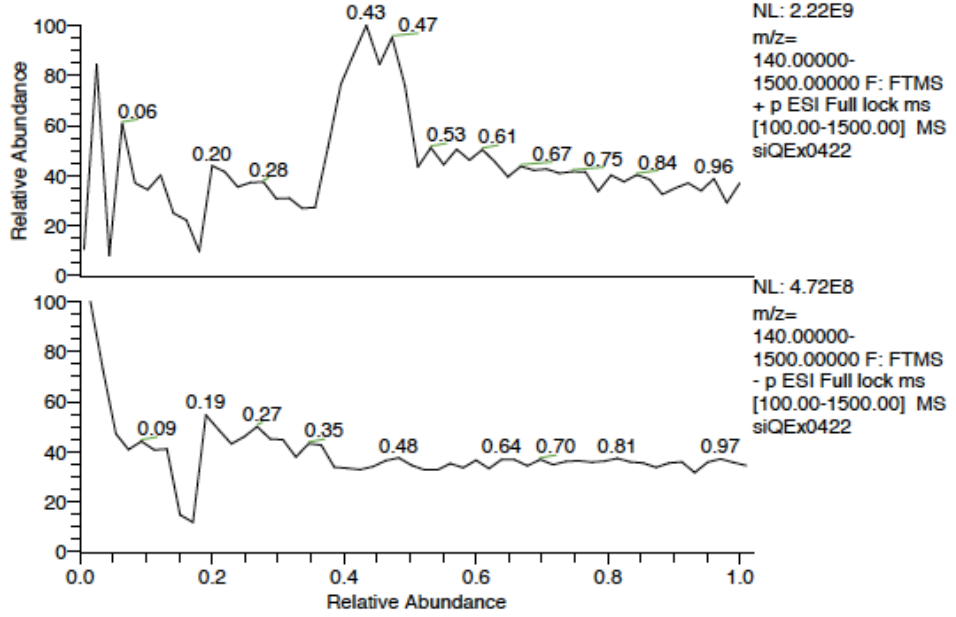

siQEx0422#42-62 RT: 0.40-0.60 AV: 11
SB: 10 0.06-0.25
T: FTMS - p ESI Full lock ms [100.00-1500.00]
m/z- 1477.05724-1477.58406

m/z	Intensity	Relative	Theo. Mass	Delta (ppm)	RDB equiv.	Composition
1477.36121	220429.8	100.00	1477.36125	-0.03	119.5	$C_{178}H_{132}O_{23}N_5P_8$
			1477.36151	-0.20	101.5	$C_{165}H_{140}O_{34}N_3P_8$
			1477.36087	0.23	177.5	$C_{176}H_{11}O_{33}N_4P_8$
			1477.36154	-0.23	177.0	$C_{178}H_{13}O_{34}NP_8$
			1477.36058	0.42	114.5	$C_{177}H_{136}O_{27}NP_8$
			1477.36192	-0.48	119.0	$C_{180}H_{134}O_{24}N_2P_8$
			1477.36218	-0.66	101.0	$C_{167}H_{142}O_{35}P_8$
			1477.36221	-0.68	182.0	$C_{179}H_9O_{30}N_5P_8$
			1477.35991	0.88	115.0	$C_{175}H_{134}O_{26}N_4P_8$
			1477.36285	-1.11	106.0	$C_{168}H_{138}O_{31}N_4P_8$
			1477.35924	1.33	110.0	$C_{174}H_{138}O_{30}P_8$
			1477.36352	-1.56	105.5	$C_{170}H_{140}O_{32}NP_8$
			1477.35857	1.78	110.5	$C_{172}H_{136}O_{29}N_3P_8$
			1477.36419	-2.02	110.5	$C_{171}H_{136}O_{28}N_5P_8$
			1477.36486	-2.47	110.0	$C_{173}H_{138}O_{29}N_2P_8$

siQEx0422 #42-62 RT: 0.40-0.60 AV: 11 SB: 10 0.06-0.25 NL: 4.14E5
T: FTMS - p ESI Full lock ms [100.00-1500.00]

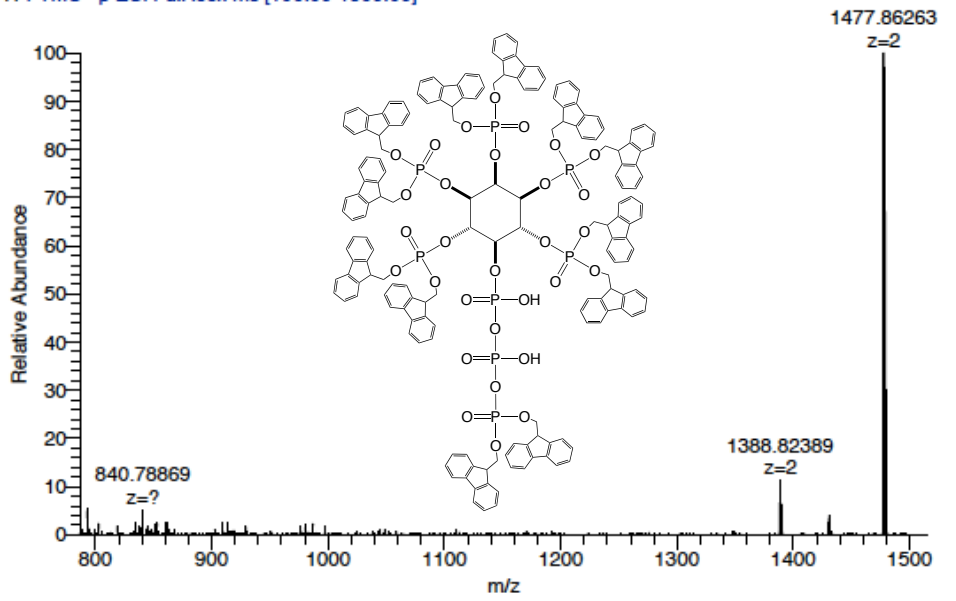

siQEx0422 #42-62 RT: 0.40-0.60 AV: 11 SB: 10 0.06-0.25 NL: 4.14E5
T: FTMS - p ESI Full lock ms [100.00-1500.00]

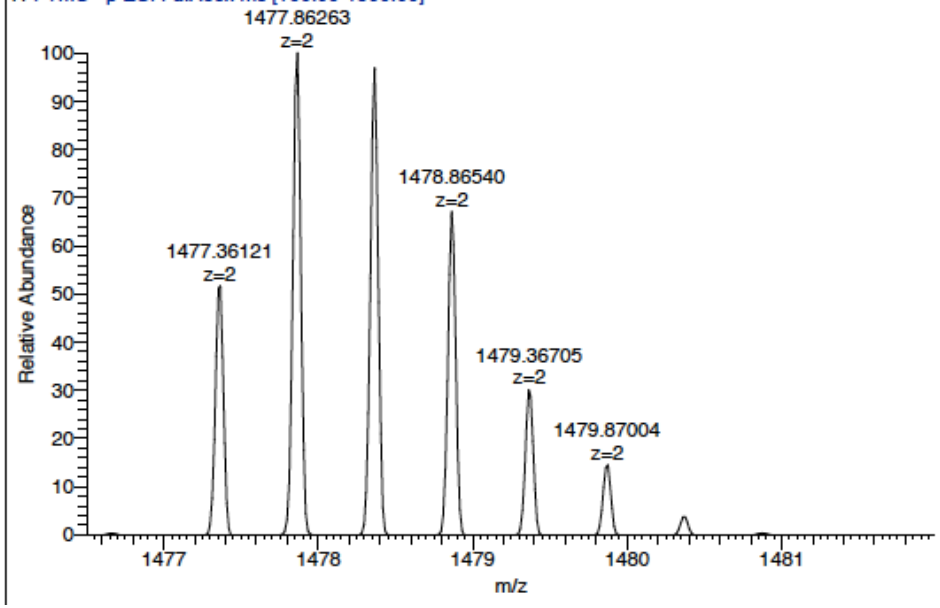

siQEx0422 #42-62 RT: 0.40-0.60 AV: 11 SB: 10 0.06-0.25 NL: 4.14E5
T: FTMS - p ESI Full lock ms [100.00-1500.00]

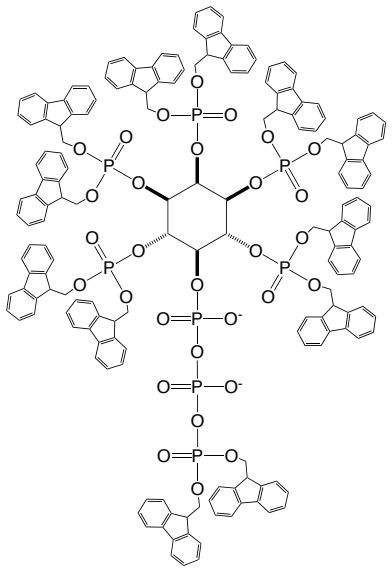

31P, 1H decoupled

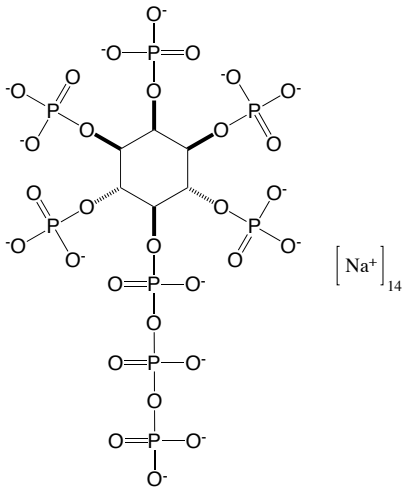

1.72
0.29
0.17
0.02
-5.40
-10.30
-10.51
-18.91

B (m)
0.16
B (s)
-10.30
C (s)
-5.40
A (m)
-18.91
D (m)
1.72

2.81
3.72
0.93
1.15
1.00

f1 (ppm)

1.72
0.29
0.17
0.02
-5.40
-10.30
-10.51
-18.91

2.81
3.72
0.93
1.15
1.00

f1 (ppm)

31P, 1H coupled

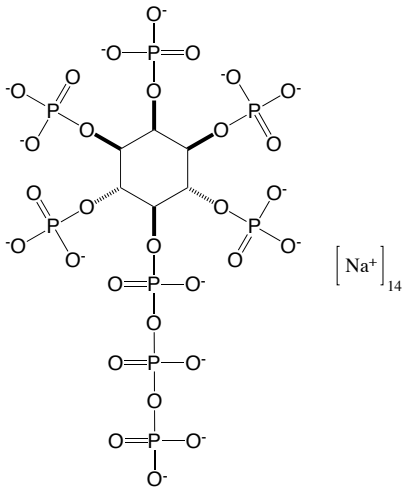

1H

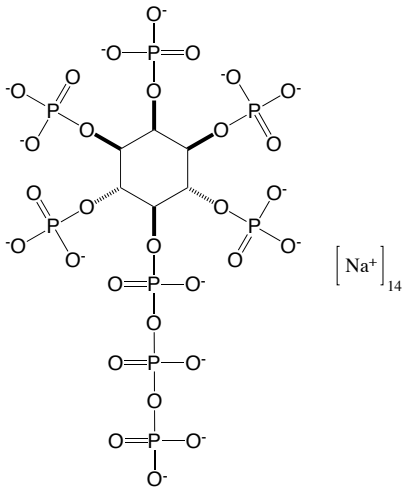

4.88
4.85
4.83
4.83
4.56
4.54
4.52
4.49
4.37
4.34
4.32
4.30
4.24
4.22
4.21
4.19

B (dd)
4.33

D (dd)
4.85

A (dd)
4.22

C (dd)
4.53

Piperidine

0.27
0.12
0.17
1.25
1.96
1.00
1.87
2.82
2.78
1.58

9.5 9.0 8.5 8.0 7.5 7.0 6.5 6.0 5.5 5.0 4.5 4.0 3.5 3.0 2.5 2.0 1.5 1.0 0.5 0.0 -0.5
f1 (ppm)

5.4 5.2 5.0 4.8 4.6 4.4 4.2 4.0 3.8
f1 (ppm)

13C

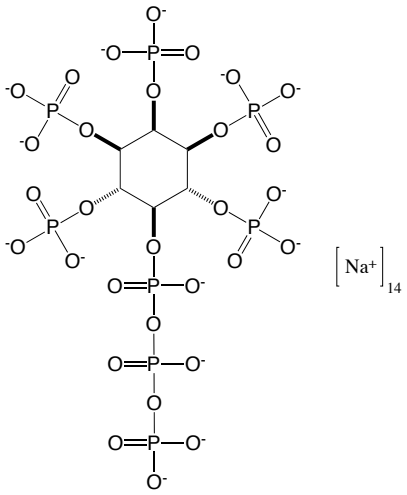

77.57
75.98
75.66
73.26
66.00
48.86
44.52
36.90
31.38
22.22
21.50
14.07

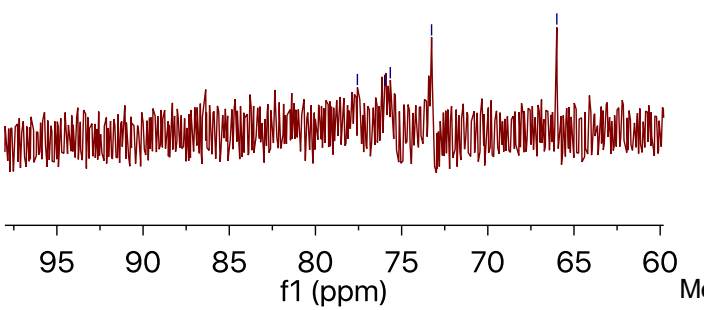

Piperidine

MeOH

160 150 140 130 120 110 100 90 80 70 60 50 40 30 20 10 0

f1 (ppm)

HR-ESI-MS (Bruker maXis)

Analysis Info

Analysis Name	D:\Data\Service\8666sihres.d			Acquisition Date	6/30/2016 4:54:41 PM
Method	tune_low_neg_Aug2014_TuneMix.m			Operator	ust
Sample Name	IP-11-86P1			Instrument	maXis 255552.00033
Comment	Solvent: H2O Client: Pavlovic				

Acquisition Parameter

Source Type	ESI	Ion Polarity	Negative	Set Nebulizer	0.6 Bar
Scan Begin	50 m/z	Set Capillary	6000 V	Set Dry Heater	180 °C
Scan End	3000 m/z	Set End Plate Offset	-800 V	Set Dry Gas	4.0 l/min